Turun yliopisto
University of Turku

COVALENT CONJUGATES OF THERAPEUTIC OLIGONUCLEOTIDES FOR *IN VIVO* TARGETING

Satish Jadhav

University of Turku

Faculty of Mathematics and Natural Sciences
Department of Chemistry

Supervised by

Professor Harri Lönnberg
Department of Chemistry
University of Turku, Turku, Finland

Professor Pasi Virta
Department of Chemistry
University of Turku, Turku, Finland

Dr. Päivi Poijärvi-Virta
Department of Chemistry
University of Turku, Turku, Finland

Reviewed by

Professor Jesper Wengel
Nucleic Acid Center
Department of Physics and Chemistry
University of Southern Denmark
Odense, Denmark

Professor Jørgen Kjems
Interdisciplinary Nanoscience Center
Aarhus University
Aarhus, Denmark

Custos

Professor Pasi Virta
Department of Chemistry
University of Turku, Turku, Finland

Opponent

Dr. Malgorzata Honcharenko
Department of Bioscience and Nutrition
Karolinska Institute
Stockholm, Sweden

ABSTRACT

UNIVERSITY OF TURKU
Department of Chemistry/Faculty of Mathematics and Natural Sciences

JADHAV, SATISH GANPAT: Covalent conjugates of therapeutic oligonucleotides for *in vivo* targeting

Doctoral thesis, 115 P.
Laboratory of Organic Chemistry and Chemical Biology
September 2016

Over last few years, the development of oligonucleotide based therapeutics (antisense, siRNA, antagomirs) have received much interest as a novel class of drugs for the treatment of many diseases. Cell/organ specific targeting of oligonucleotides by covalent conjugation has become a promising approach for developing therapeutic RNAs. The major obstacle in the use of therapeutic RNAs is the cell/organ specific targeting and internalization of the large anionic oligonucleotides across the plasma membrane of the cells.

This thesis focuses on the synthesis of different receptor specific ligand conjugates of oligonucleotides. The oligonucleotides are conjugated with different targeting ligands such as i) Galactose cluster, ii) Hyaluronic acid hexamer, and iii) Bisphosphonate derivative. Multi-galactose-conjugated 2'-*O*-methyl oligoribonucleotides showed remarkable galactose-dependent liver targeting of the conjugates monitored by *in vivo* positron emission tomography (PET) imaging in healthy rats. Hyaluronic acid hexasaccharide oligonucleotide were conjugated efficiently by using copper free click reaction (SPAAC conjugation approach) and also studied by *in vivo* PET imaging in myocardial infarction rat models. Bone targeting bisphosphonate oligonucleotide conjugates were prepared by SPAAC conjugation approach and *in vivo* PET imaging exhibited enriched radioactivity accumulation to bones in healthy rats. Additionally, a straightforward method was described for the synthesis of solid supported porphyrin biomolecule conjugates. The whole-body distribution of the conjugates in rats was monitored by PET. These oligonucleotide conjugates were efficiently labeled by complexing ^{68}Ga, with a 3´-terminal 1,4,7-triazacyclononane-1,4,7-triyl)triacetic acid (NOTA) ligand. This allowed *in vivo* quantification of oligonucleotide pharmacokinetics and bio-distribution data in rats.

Key words: Galactose cluster, Hyaluronic acid, Bis(phosphonate), ^{68}Ga-labeled oligonucleotides, *in vivo* PET imaging.

PREFACE

This thesis is based on the experimental work carried out at the Laboratory of Organic Chemistry, Department of Chemistry at University of Turku, Finland, during September 2011 to March 2016. The financial support from Erasmus Mundus Action II (EXPERTS Program), Finnish Cultural Foundation, and Physical and Chemical Sciences Graduate School, University of Turku are gratefully acknowledged.

I am deeply grateful to Professor Harri Lönnberg for giving me an opportunity to pursue PhD studies under his guidance in the bioorganic chemistry research group. I admire his wide knowledge and experience in the field of nucleic acid chemistry. I thank him for his patience and encouragement. I am also very much grateful to my supervisor Professor Pasi Virta. His knowledge of synthetic organic chemistry and thoughtful suggestions in the laboratory experiments were very helpful. I thank him for his guidance, support and patience during the years. In addition I thank Dr. Päivi Poijärvi-Virta for kind help in all stages of my PhD studies and especially teaching me solid phase synthesis techniques.

I would like to thank our collaborators from PET center. I am grateful to Professor Anne Roivainen and her research group: Meeri Käkela, Dr. Tiina Laitala-Leinonen, Jussi Mäkilä, and Mathieu Bourgery, this work would not have been possible without this collaboration. I am grateful to Professor Jesper Wengel and Professor Jørgen Kjems for their reviewing of my thesis. I thank to Dr. Malgorzata Honcharenko for accepting to act as my opponent.

My gratitude goes to all present and former co-workers in the bioorganic chemistry research group for creating easy and a nice working environment. I wish to thank: Dr. Alejandro Gimenez Molina, Dr. Luigi Lain, Ville Tähtinen, Lotta Granqvist, Dr. Tuomas Karskela, Marika Karskela, Dr. Anu Kiviniemi, Dr. Oleg Golubev, Tiina Buss, Dr. Kaisa Ketomäki, Dr. Emilia Kiuru, Dr. Heidi Korhonen, Vyacheslav Kungurtsev, Dr. Anna Leisvuori, Dr. Tuomas Lönnberg, Dr. Satu Mikkola, Dr. Helmi Neuvonen, Dr. Teija Niittymäki, Dr. Mikko Ora, Dr. Sharmin Taherpour and Dr. Sajal Maity. Personnel from Instrument Center and Arcanum, Dr. Jari Sinkkonen, Dr. Maarit Karonen, Jaakko Hellman, Kirsi Laaksonen, Kari Loikas and Mauri Nauma are also thanked.

I would like to thank all my friends, especially Dr. Shyam Disale, Dr. Rajiv Sawant and Dr. Anant Ghumare. Finally, I owe my deepest gratitude to my parents, Kamal, and Ganpat, brother Prakash, sister-in-law Seema, and my nephew Jayant, and niece Gita.

Satish Jadhav   Turku, September 2016

CONTENTS

LIST OF ORIGINAL PUBLICATIONS

This thesis is based on the following publications:

I   Mäkilä, J., Jadhav, S., Kiviniemi, A., Käkelä, M., Liljenbäck, H., Poijärvi-Virta, P., Laitala-Leinonen, T., Lönnberg, H., Roivainen, A., Virta. P. Synthesis of multi-galactose-conjugated 2'-O-methyl oligoribonucleotides and their in vivo imaging with positron emission tomography. *Bioorg. Med. Chem* **2014**, *22*, 6806–6813.

II   Jadhav, S., Käkelä, M., Mäkila, J., Kiugel, M., Liljenbäck, H., Virta, J., Poijärvi-Virta, P., Laitala-Leinonen, T., Kytö, V., Jalkanen, S., Saraste, A., Roivainen, A., Lönnberg, H., Virta. P. Synthesis and In Vivo PET Imaging of Hyaluronan Conjugates of Oligonucleotides. *Bioconjugate. Chem*. **2016**, *27*, 391–403.

III Jadhav, S., Käkelä, M., Burgery, M., Rimpilä, K., Liljenbäck, H., Siitonen, R., Mäkila, J., Laitala-Leinonen, T., Poijärvi-Virta, P., Roivainen, A., Lönnberg, H., Virta. P. In Vivo Bone-Targeting of Bis(phosphonate)-Conjugated Double Helical RNA Monitored by Positron Emission Tomography. *Mol. Pharm*. **2016**, *13*, 2588–2595.

IV   Jadhav, S., Yim, C-B., Rajander, J., Grönroos, T., Solin, O., Virta, P. Solid-Supported Porphyrins Useful for the Synthesis of Conjugates with Oligomeric Biomolecules. *Bioconjugate Chem*. **2016**, *27*, 1023-1029.

ABBREVIATIONS

A	adenosine
Ac	acetyl
AcOH	acetic acid
ASO	antisense oligonucleotide
ASGPR	asialoglycoprotein receptor
BAIB	(diacetoxyiodo)benzene
BP	bisphosphonate
Bz	benzoyl
Bn	benzyl
C	cytidine
CPG	controlled pore glass
CPP	cell-penetrating peptides
DBU	1,8-diazabicyclo[5.4.0]undec-7-ene
DCA	dichloroacetic acid
DCC	*N,N′*-dicyclohexylcarbodiimide
CD44	cluster of differentiation 44
DMAP	4-dimethylaminopyridine
DMF	*N,N*-dimethylformamide
DMSO	dimethyl sulfoxide
DMTr	4,4′-dimethoxytrityl
dsRNA	double-stranded RNA
DNA	deoxyribonucleic acid
ESI-MS	electrospray ionization mass spectroscopy
FDA	Food and Drug Administration (U. S. A)
G	guanosine
Gal	galactose
GalNAc	*N*-acetylgalactosamine
HA	hyaluronic acid
HPLC	high-performance liquid chromatography
LNA	locked nucleic acid
MeCN	acetonitrile
mRNA	messenger RNA
miRNA	microRNA
NMR	nuclear magnetic resonance
NOTA	1,4,7-triazacyclononane-1,4,7-triyl)triacetic acid

ON	oligonucleotide
PET	positron emission tomography
PEG	polyethylene glycol
PMO	phosphorodiamidate morpholino oligomer
PNA	peptide nucleic acid
RISC	RNA-induced silencing complex
RNA	ribonucleic acid
RNAi	RNA interference
RNase	ribonuclease
RP	reversed phase
siRNA	small interfering RNA
T	thymidine
*T*m	melting temperature
TBDMS	*tert*-butyldimethylsilyl
TEMPO	2,2,6,6-tetramethyl-1-piperidinyloxy
TEA	triethylamine
TEAA	triethylammonium acetate
TCA	trichloroacetyl
TFA	trifluoroacetic acid
THF	tetrahydrofuran
UV	ultraviolet

1.   INTRODUCTION

1.1   RNA as drug target

1.1.1   Structure of RNA

RNA, as DNA, consists of a long polynucleotide chain linked via phosphodiester bonds (Fig. 1). The structure of the sugar moiety is, however, different, RNA chain contains β-D-ribofuranosyl residues instead of *2′*-deoxy-β-D-*erythro*-pentofuranosyl groups of DNA. RNA contains adenine, cytosine and guanine bases, like DNA, but thymine base of DNA is replaced by uracil. Unlike DNA, RNA is more often found in nature as a single stranded molecule, and it may fold onto itself and form hairpin loops via intramolecular hydrogen bonding between complementary bases. However, RNA can also form RNA/DNA hybrid duplex via Watson-Crick base-pairing.
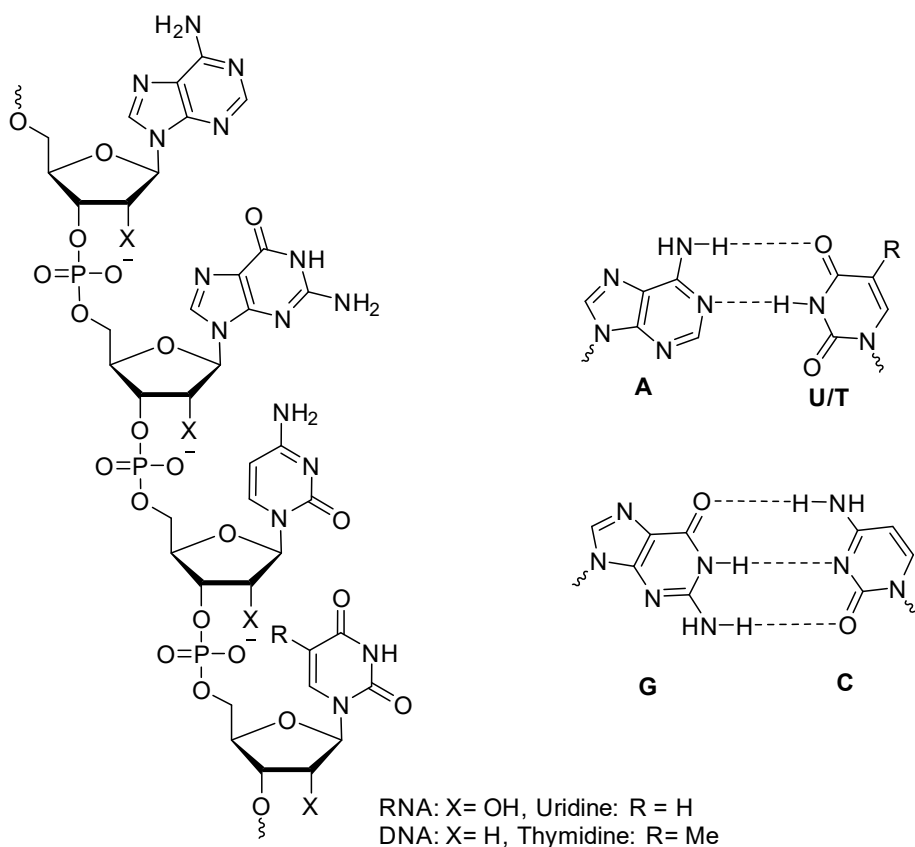

Figure 1. The structure of RNA and DNA and Watson-Crick base pairing.

1.1.2 **Biological functions of RNA (drug target)**

RNAs has long been dominated by central dogma view in molecular biology.[1, 2] In general, messenger RNAs (mRNAs) transcript instructions from DNA in the form of specific base sequences, and mediate the information to ribosomes, nucleoprotein complexes where the protein synthesis takes place. Two other RNAs, viz. ribosomal RNAs (rRNAs) forming the core structural framework of this protein synthesis machine, and transfer RNAs (tRNAs) carrying amino acids to this machinery, participate in the process. In fact the primary transcript of mRNA, called pre-mRNA, is longer than the mature mRNA containing non-coding sequences, introns, between the coding regions, exons. The non-coding introns are removed and exons relegated by splicing reactions catalyzed by spliceosome, a protein complex of short RNA-oligonucleotides.

The RNAs that are used for other purposes than protein synthesis are called as noncoding RNAs. Numerous noncoding RNAs are responsible for regulation of gene expression,[3, 4] *i. e.* protein production from coding genes, which is the foundation of cellular structure and physiology. In prokaryotic cells (*e.g.* bacteria), small antisense RNAs regulate the gene activities by binding to target mRNA. In addition, the so-called riboswitches also function as regulatory domains in longer mRNAs, via binding to small molecule nucleotides or amino acids.[5] In eukaryotic cells, large number of small RNAs exert interfering properties as well. Among those, miRNAs are the most studied regulatory noncoding RNAs.[6] Generally, double stranded miRNAs of about 22 nucleotide long sequences are produced from long single stranded miRNA precursor which contains hairpin structures. Double stranded miRNAs incorporate into proteins of Argonaut family, bind complementary mRNAs and inhibit stability or translation. First one of the strands is cleaved by Argonaut 2, and the remaining one recognizes mRNA. Several hundreds of miRNAs, present in animals and plants can regulate the activity of up to one third of coding genes. Another well studied noncoding RNA is the small interfering RNA (siRNA).[7,8] SiRNAs are similar to miRNAs in terms of length and also association with Argonaut protein. Essentially, siRNAs can be produced from any copied region of the genome and it acts directly upon that particular location, hence siRNAs are found in those cells where self-regulatory process by RNAi is underway. A major function of some of the noncoding RNAs is to protect cells against viruses, and transposons. In response to viral infections, cells produce complementary siRNAs to viral mRNAs and also inhibits transposons and repeat sequences in similar manner. Similarly, in animals the genome stability is protected by Piwi-associated RNAs (piRNAs).[9]

1.2 **Therapeutic oligonucleotides**

Eventually, the question arose can we stop the protein synthesis at the level of mRNA? Indeed, in 1978 Zamecnik and Stephenson[10] studied inhibition of Rous sarcoma virus

replication by using specific oligonucleotides (ONs). Later, there has been numerous studies that evidenced ONs to target mRNA in a highly selective manner. In principle, any 17 nucleotides sequence occurs only once in human genome (10^9-10^{10}). Accordingly, any mRNA can in principle be entirely selectively arrested by a complementary 17-mer ON.[11] This prevents the hybridization with rRNA and stops disease causing protein being synthesized. Strategies that target mRNA include the use of single stranded antisense ONs, double stranded ONs (siRNA,) (Fig. 2), and nucleic acid enzymes (ribozymes and DNAzymes). In general, antisense ON mechanisms can be based on two main ways: (i) interfering in RNA's function without promoting RNA's degradation and (ii) promoting RNA's degradation. In addition, 70% of the human genes undergoes alternative splicing, and splicing errors because of mutations are responsible for about 50% of gene causing diseases. Antisense ON has emerged as a tool for intervention of these processes. [12]
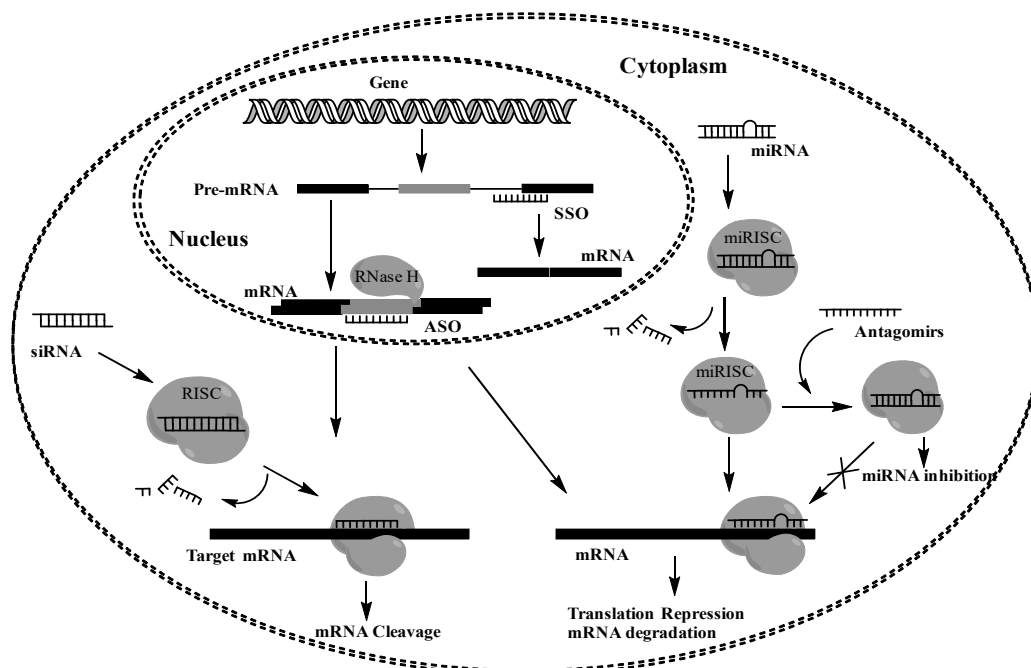
Figure 2. Therapeutic ONs mechanism of actions[13]: 1) antisense ONs, and splice switching ONs, 2) siRNA, and 3) antagomirs.

1.2.1 Antisense oligonucleotides (ASO)

Chemically modified antisense ONs comprise 12-25 nucleotides long single stranded DNA analog chains, designed to be complementary to target mRNA. An antisense ON imparts specific binding to mRNA by Watson-Crick base-pairing .[14, 15, 16, 17] Unlike small molecule drugs, which act as antagonists and alter biological processes by binding to target proteins, receptors and enzymes, antisense ONs bind complementary to the

specific sequences of nucleotides of the target mRNAs. There are two cellular mechanisms that antisense ONs utilize: activation of RNase H by the antisense ON leading to degradation of target mRNA and steric blocking of mRNAs by hybridized antisense ON. Formation of DNA-RNA hybrid duplex recruits the RNase H enzyme present in mammalian cells, which recognizes hybrid duplex substrate and cleaves at the center of target mRNA, retaining DNA intact.[18] Antisense ONs drug can work in both the nucleus and cytosol, due to presence of RNase H enzymes in both cellular compartments.

Antisense ONs that do not activate RNase H mediated mRNA degradation, but can act as steric blocks to mRNAs/pre-mRNAs without its degradation, also can be able to induce modulation of genes.[19] Steric-blocking ON drug can modulate splicing of target pre-mRNA, and also it can block the translation of mRNA. Particularly, splice switching oligos (SSOs) have been emerging in clinical studies against rare genetic diseases such as Duchenne muscular dystrophy and spinal muscular atropy.[12] SSOs can block the spliceosome at the splice site on targeted pre-mRNA and modulate pre-mRNA. In addition, it can also be used to correct defective pre-mRNA by exon skipping and restore the synthesis of beneficial protein.

1.2.2   Small interfering RNAs (siRNA)

RNA interference (RNAi) was evidenced very first in *Caenorhabditis elegans* nematode.[20] The long double stranded RNAs were exogenously delivered. These outcome very efficient and specific silencing of expression of a gene by prompting cleavage of target mRNA. Usually, siRNAs are of about 21-23 nucleotides long, duplexes, with two base 3'-overhang and 5'-phsophate group. In the cytoplasm of cells, siRNAs incorporate into an Argonaut 2 (Ago2) protein complex, the RNA-induced-silencing complex (RISC). Because of the asymmetry in thermodynamic stabilities (predicted) of the two termini of the siRNA duplex, RISC machinery component selects the antisense strand (guide strand), and cleaves the sense strand (non-guide strand). The antisense stand serves as a template for mRNA recognition and binds complementary to target mRNA. In later step, siRNA-mRNA duplex is cleaved between 10 and 11 nucleotides from the 5'-end of antisense strand by the same Ago2.[21]

1.2.3   Antagomirs (anti-miRs)

It has been found that dysregulation of miRNAs has been responsible for variety of disorders, such as myocardial diseases,[22] neurological disorders,[23] different types of cancers,[24] and viral infections.[25] Antagomir is an antisense ON targeted towards miRNA to overcome the inhibition of protein synthesis by miRNA.[26] Hence, antagomirs have been emerging as a promising approach for treatment of diseases caused by dysregulation of miRNA expression. The miRNA biogenesis encompasses transcription

of miRNA genes in nucleus by RNA polymerase II (Pol II), giving primary miRNA transcripts (primiRNAs) that are then cleaved in nucleus by a complex of Drosha and DGCR8. The resulting precursor miRNA hairpin (pre-miRNA) is exported into cytosol through Exportin-5 and further processed by the RNase Dicer to an intermediate miRNA duplex. The leading strand is then loaded into the (mi)RNA-induced silencing complex (mi)RISC, whereas the second strand is subjected to degradation. The strand selection depends on the thermodynamic characteristics of the miRNA duplex. The (mi)RISC complex is guided to target mRNAs sequences that are located within the 3′ untranslated regions (3′UTRs) of the mRNA. Following these reactions, the mRNA is targeted by translational repression and/or degradation. Unlike siRNAs pathway, which requires perfect complementarity to target mRNA, miRNA can bind with mismatches. In general, chemically modified antagomirs are designed to be as steric blocking ONs, it binds fully complementary to seed region of the target miRNA instead of mRNA. Hence, loading of miRNA in to RISC complex and subsequent binding to mRNA can be prevented, resulting in blocking of miRNA functions. [27]

1.3   Stability

Internucleotide phosphodiester linkages in native DNA and RNA are too unstable in serum and in mammalian cells due to phosphodiester cleavage by exo- and endonucleases. Chemical modifications are required to improve their nuclease stability. One obvious way is to modify the internucleosidic phosphodiester linkage. The oldest and most extensively studied modification is substitution of one of the non-bridging oxygen atoms with sulfur, giving phosphorothioates that are sufficiently stable against nucleases (Fig 3). [28] In addition to phosphorothioates, boranophosphate, methylphosphonate, and phosphoramidate, linkages also enhance nuclease resistance. [29] Boranophosphate modification is even more stabilizing than phosphorothioate, [30] unfortunately, their chemical synthesis is difficult. Two heavily modified uncharged DNA analogs, peptide nucleic acid (PNA) and morpholino oligonucleotides (PMO) deserve special attention. PNA has a peptide-like backbone composed of neutral *N*-(2-aminoethyl)glycin units. [31] PMO is, in turn, composed of 6-hydroxymethylmorpholine units that bear a nucleobase at C2 and are linked to each other via phosphoamidate bonds. [32] Both oligomers show excellent nuclease stability. [33,34] Moderate, but not necessarily sufficient, nuclease stability is also achieved by sugar moiety modifications, such as 2′-*O*-methyl (2′-*O*-Me-RNA), [35] 2′-*O*-(2-methoxyethyl) (2′-*O*-MOE-RNA), [36] 2′-deoxy-2′-fluoro (2′-F-RNA), [34] 4′-*C*-aminomethyl-2′-*O*-methyl [37] and 4′-thio (4′-S-RNA) [38] modifications of ribonucleosides, and 2′-fluoro substitution of arabinonucleosides (2′-F-ANA) (Fig. 4). [39] Furthermore, 2'-4' bridged analogs, LNA, ENA and their congeners, are reasonably stable towards nucleases. [40] Besides these 5-membered ring mimics,

expanded ring system containing cyclohexene nucleic acid (CeNA), and oxepane nucleic acids (ONA) also show enhanced nuclease resistance.[41,42]
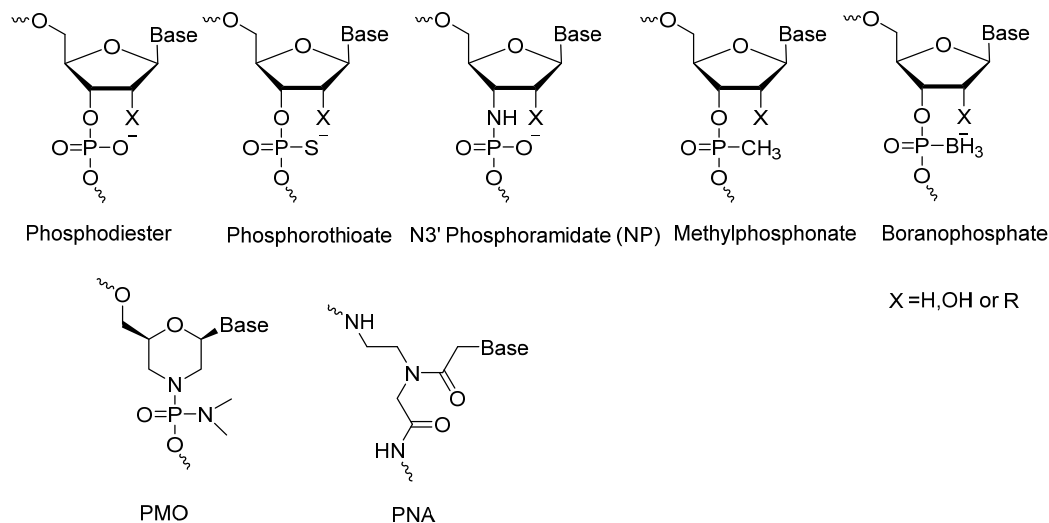

Figure 3. Chemical modifications of backbone linkages

1.4 Affinity & turnover

Phosphorothioate ONs exhibit besides good nuclease stability another useful characteristic; they activate RNase H.[28] RNaseH enzymes present in mammalian cells, recognize DNA-RNA hybrid duplex and cleave only RNA, retaining DNA intact.[43] Accordingly, the action of phosphorothioate ONs is catalytic and, hence, their somewhat less efficient hybridization compared to native DNA ONs is not detrimental. Only few antisense ON candidates have the same property. Boranophosphate ONs, 2´-F-ANA, CeNA and ONA have been shown to activate RNase H.[29, 30, 40] Although most antisense ON candidates do not activate RNase H, they still may be serious drug candidates, providing the affinity to RNA is high. These include PNA, PMO and 3´-phosphoamidate ONs. Similarly, sugar 2'-*O* modifications such as 2'-*O*-Me, 2'-F, and 2'-MOE that prefer the C3'-endo ring-puckering and, hence, enhances binding to RNA,[44,45,36] While, 2'F-ANA analog is structurally a DNA mimic, it still exhibits increased hybridization affinity (1.2°C per insert) to complementary RNA. This together with the ability to activate RNase H.[46] makes it a promising antisense ON candidate.
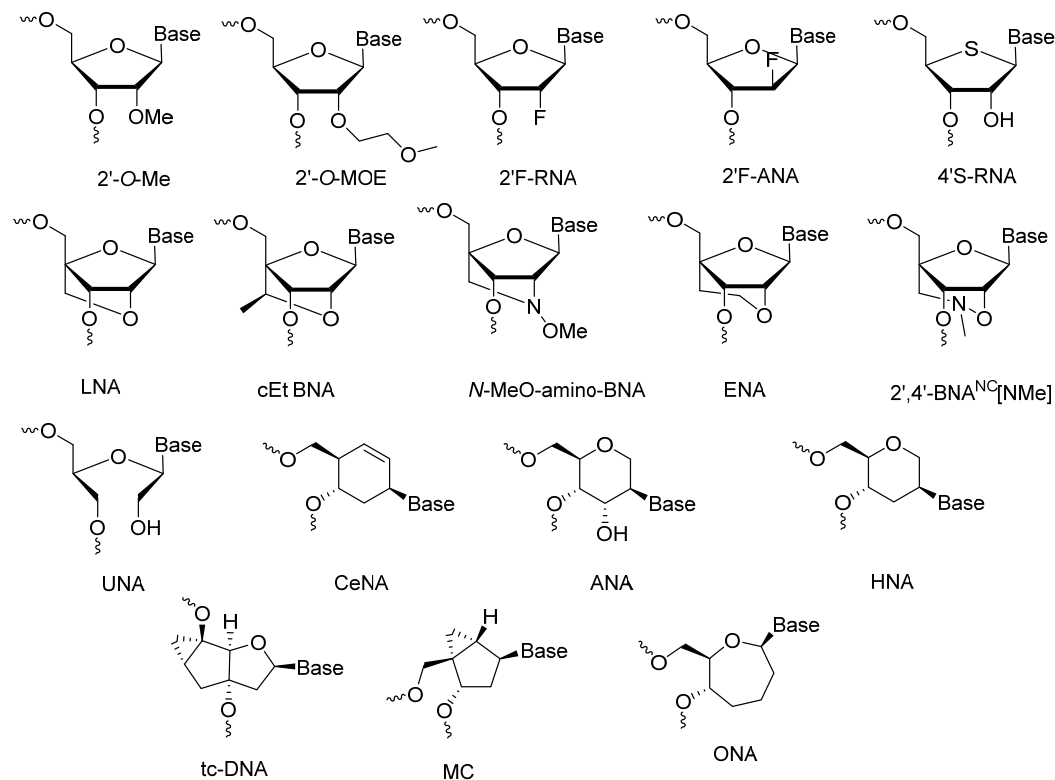
Figure 4. Chemical modifications of sugar units

LNA and its congeners, although unable to activate RNaseH, also deserves special attention, owing to excellent hybridization properties. LNA , units having a rigid N-type conformation impressively enhances the affinity to RNA, ~5.6ºC per insert.[47,48,49], Numerous bicyclic 2'-4' bridged analogs of LNA have been synthesized The best known examples include 2'-*O*,4'-*C* constrained ethyl BNA (cEt-BNA),[50] 2′-*O*,4′-*C*-ethylene nucleic acid (ENA),[51] *N*-MeO-amino BNA, 2'-4' BNA[NC] [NMe].[52] Structurally constrained bicyclic and tricyclic analogs, bicyclo[3.1.0]hexane (MC)[53] and Tricyclo-DNA (tc-DNA),[54] modifications also markedly increase the binding affinity to complementary ONs. CeNA,[55] HNA and ANA[56] analogs bind tightly to complementary RNA strand.

1.5 Pharmacokinetics and bio-distribution of oligonucleotide drugs

ON drugs can be administered systemically via two primary routes, either subcutaneous (SC) injection or intravenous (IV) infusion. During systemic SC or IV administration, PS-modified antisense ONs are quickly transferred through blood circulation into tissues (minutes to hour). As ONs drug start to get into tissues (minutes to hour), the plasma

concentration decreases exponentially followed by slower terminal eliminations (half-life about weeks). As compared to IV infusion, peak plasma concentration are about 3- to 10 times lower in case of SC injection, most likely because of time required to absorb ON drugs in to blood circulation from the site of SC injection, and their rapid tissue distribution from blood circulation. However, during SC injection, plasma concentration decreases gradually as compared to IV infusion.[57] Pharmacokinetic properties of antisense ONs has been observed to be alike across species and gender.[58] Unmodified charged ONs (including unmodified siRNA) as well as neutral ONs (PNA, PMOs) possess low binding affinity to cellular proteins in plasma; they are metabolized in blood or rapidly cleared by glomerulus in kidney, and renal excreted, resulting in low or none tissue uptake. By contrast, PS-modified ONs show high binding affinity to plasma proteins, and albumin. This increases *in vivo* circulation time, results in improved tissue bio-distribution and cell uptake. Systemically administered antisense ONs are naturally highly distributed over tissues such as liver, kidney, spleen, bone marrow, adipocytes, and lymph nodes.[59] In general, across all animal species, antisense ONs distributes broadly into many tissue types, except central nervous system, because of inability to pass blood–brain barrier (BBB). However, central nervous system (CNS) targeting antisense ONs drug has also been administered via intrathecal i.e. direct injection in to subarachnoid spaces, where ONs drug can be targeted to brain through cerebrospinal fluid (CSF).[58]

1.6 Cellular Uptake

Delivering systemically therapeutic ONs into cytoplasm of cells is the key hurdle in development of ON therapeutics. Because of the large, hydrophilic, and anionic nature of the ON molecules, penetration across the cell membrane barrier is difficult. It is also worth noting that the cellular uptake cannot be simply increased by using charge neutral modified ONs. Methyl phosphonates and PNA analogues, for instance, do not show enhanced cellular uptake.[60] Usually ON drugs can be internalized into cells through some form of endocytosis,[61] which involves mainly cell surface receptor mediated endocytosis (Fig. 5) ON binds to cell surface receptors and enters by forming vesicles. Some of the vesicles first traffic in to early endosomes, and few of those endosomes recycles receptor–oligo complex back on the cell surface. In other cases, vesicles enter in to low pH late endosomes, which later leads to lysosomes, where the cargo is degraded. However, due to intracellular dynamic processes, tiny amount of ONs leaks in to cytoplasm from disrupting endosomes; this is the only pharmacologically active portion of ONs usually being utilized. Single stranded P-S modified ONs are internalized more efficiently into hepatocyte cells most likely binding to surface proteins and endocytosis.[28] In general, transport of ONs drugs through cell membrane and endosomal trapping of nonproductive ONs remains the biggest issue in cellular uptake.
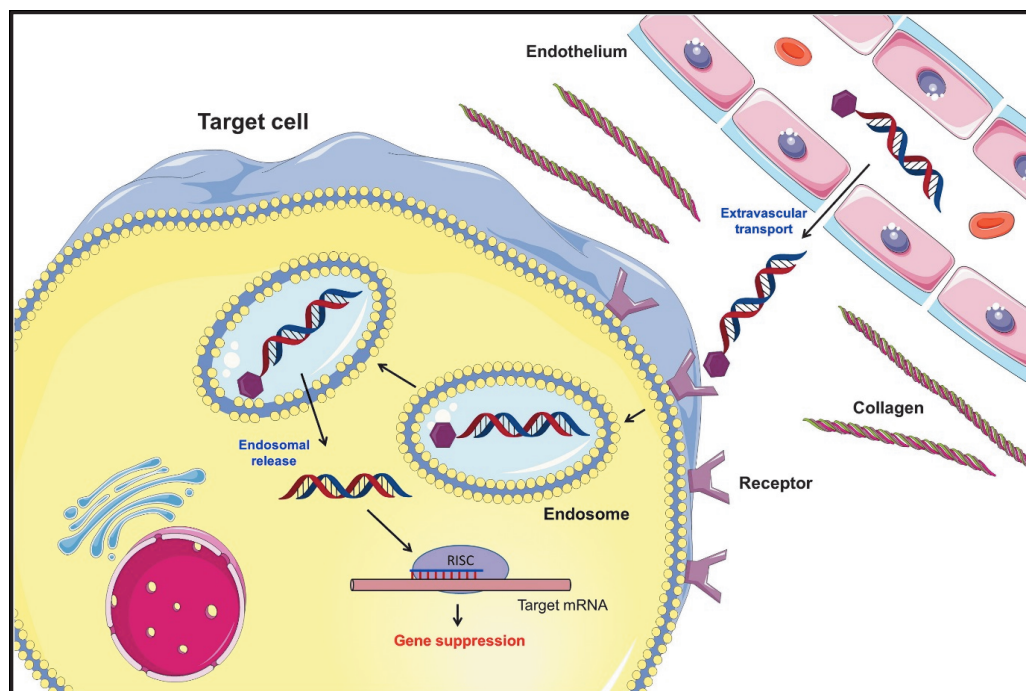
Figure 5. Biological barriers in delivering ON drugs in to cells [67](Adapted from Elsevier with permission)

1.7   Targeting by covalent conjugation

It would naturally be highly desirable to target ON drugs to specific tissues/organs and facilitate cellular uptake for pharmacological activity. There have been two types of strategies being used for delivering ON drugs. Covalently attached ONs and non-covalently bound ONs complexes or different kind of advanced formulation techniques. These non-covalent ONs complexes applications are discussed in more detailed elsewhere. [62, 63, 64, 65]

Recently, many approaches are being developed, based on covalent conjugation of ON with receptor targeting ligands such as lipids, peptides, carbohydrates, small molecules, aptamers and cell penetrating peptides (CPPs).[66, 67, 68]Covalently linked conjugates are molecularly well defined, and often quality of the ON conjugates can be easily monitored and controlled by using standard analytical techniques. In general, covalent ONs conjugates are physically more stable and possess broad tissue distribution space as compared to formulation or nano particles or polymer based delivery techniques. However, inside the cell covalently attached ligands should be inert enough to avoid interference in binding of ONs to target mRNAs, as well as in the post binding events like RNase H or the RNAi machineries. Generally, conjugating small ligand at 3' or 5'-terminus in single stranded ONs is better tolerated than modifications in siRNA.[69]

Inevitably, the 5'-terminus of the antisense strand in siRNA is required to be phosphorylated in order to being recognized by RISC. Hence, ligands cannot be attached to 5'-terminus of antisense strand in siRNA.[70] Commonly used stable irreversible linkages such as, amide, ester, thioether, thiol-maleimide, and triazole has been utilized in synthesis of covalent ON conjugates. However, bio-reversible linkage such as disulfide may provide additional benefits in pharmacological activity, since after entering conjugates into cell cytoplasm, disulfide bond is potentially reduced by cytosolic environment and may liberate intact ON drugs.[71] In addition, acid labile linkages such as β-thiopropionate have also been used. These are aimed at being cleaved at low pH endosomal conditions.[72]

Essentially, existence of a cell-specific receptor, density of the receptors on the targeted cells, the ligand selectivity/specificity and their binding affinity are crucial for cell specific ONs delivery. Intrinsic affinity of P-S modified ONs and phosphodiester linked ONs to certain cell surface receptors may alter the targeting properties, and cellular uptake.[67]

1.7.1 Lipid-oligonucleotide conjugates

Lipid molecules are hydrophobic in nature, they constitute structural component of cell membrane as a hydrophobic interior of the phospholipid bilayers. Conjugates of lipids with ONs do not only minimize the charge repulsion effect but they also bind sufficiently to lipoproteins, which may increase *in vivo* circulation time and possibly lead to desired tissue distribution and enhanced cellular uptake. Very first example of using systemic administration route is the cholesterol-siRNA conjugates that showed efficient targeting of apolipoprotein B mRNA via RNAi by intravenous injection in mice (Fig. 6).[73, 74] These conjugates interact and bind with different lipoprotein particles and lipoprotein receptors in blood circulation. Pre-complexed high density lipoproteins with ON conjugates target to liver, kidney, and steroidogenic organs, via SR-BI receptors mediated endocytosis, while low density lipoproteins-ON conjugate complex facilitates uptake predominantly into liver hepatocytes by targeting LDL-receptors mediated endocytosis.[75]

In addition, by intrathecal administration, *i.e.* direct infusion of cholesterol-siRNA conjugate into central nervous system (CNS), targeting of CNS disorders such as Huntington disease has been achieved and inhibition of the neurodegenerative disease causing gene via RNAi has been demonstrated.[76] Since, LDR receptors are present in brain cells, cholesterol-siRNA conjugates become internalized via receptor mediated endocytosis. In most of the CNS targeting ON conjugates, cholesterol has been tethered covalently to 3' terminus of the passenger strand of siRNA via the hydroxy prolinol strategy. Interestingly, use of a cleavable disulfide linker showed two times higher efficiency in silencing of CNPase (2′, 3′-cyclic nucleotide 3′-phosphodiesterase) mRNA in oligodendrocytes.[77] Similarly, cholesterol-antagomir conjugates also have been

utilized in miRNAs based targeting approach. Covalent adding of cholesterol unit to the 3'-end of anti-miR-122 (2'-*O*-Me) has been utilized for liver specific inhibition of miR-122 in mice.[78] In another study, cholesterol -anti-miR-10b conjugate has been demonstrated for targeting the breast cancer metastasis in mouse mammary tumor models, resulting in efficient silencing of miR-10b *in vivo*.[79] In addition, cholesterol conjugation has been utilized in antisense ONs; hepatitis C virus (HCV) RNA targeting 17-mer (2'-*O*-Me) antisense-ONs were prepared by conjugating cholesterol and octadecanol to the 3' end of ONs by click chemistry and both cholesterol-ONs and octadecanol-ONs, when tested in cultured human hepatic cells, exhibited dose dependent reduction of HCV translation.[80] Furthermore, 5'-palmitic acid conjugates of a 13-mer 3'-thiophosphoramidate bind to the active site of human telomerase. This has been under evaluation for clinical trial II as an anticancer agent. [81]
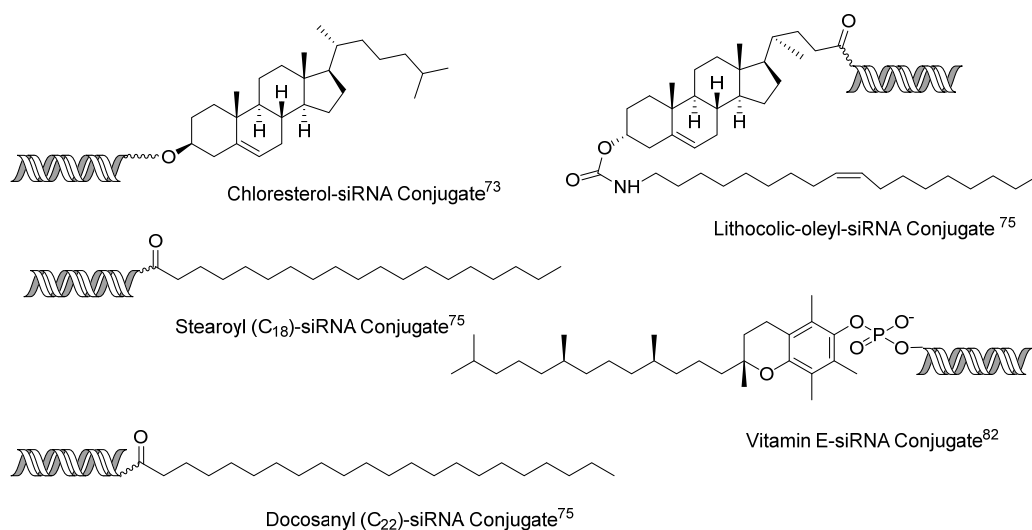

Chloresterol-siRNA Conjugate[73]

Lithocolic-oleyl-siRNA Conjugate [75]

Stearoyl (C$_{18}$)-siRNA Conjugate[75]

Vitamin E-siRNA Conjugate[82]

Docosanyl (C$_{22}$)-siRNA Conjugate[75]

Figure 6. siRNA conjugates with (i) cholesterol, (ii) fatty acids, (iii) vitamins, and (iv) bile acid

Besides cholesterol, other lipophilic moieties such as long chain fatty acids and bile acid have been conjugated to 3'-end passenger strand of siRNA. These studies reveal that conjugates with longer alkyl chain (C18) possess high binding affinity to lipoprotein particles and result in efficient gene silencing compared to shorter alkyl chains.[75] The fat-soluble hydrophobic vitamins, such as α-tocopherol, have their own physiological pathway to most of the organs. α-Tocopherol conjugated to 5'-end of the guide strand of siRNA has been used for silencing apoB. After entering cells, α-tocopherol moiety was cleaved by Dicer, liberating active siRNA and resulting in efficient gene inhibition in liver without triggering immune response.[82] Complexing of high density lipoprotein (HDL) with α-tocopherol-siRNA conjugate facilitates uptake into brain, as demonstrated via intracerebroventricular (ICV) infusion.[83] Other studies demonstrate that the vitamin A (retinol)-liposomes facilitate the siRNA uptake into hepatic stellate cells.[84] Vitamin A

most likely binds to retinol-binding proteins and mediates receptor mediated internalization into these cells.

1.7.2 Small molecule–oligonucleotide conjugates

Small molecule-ON conjugates also have been recently explored for targeted receptor-specific delivery approach. Trivalent anisamide conjugate of a splice switching antisense oligonucleotide (SSO), which target a sigma receptor, when tested by their ability to modify splicing of a reporter gene (luciferase) in tumor cells in culture, displayed enhanced cellular uptake and was markedly more effective than an unconjugated SSO or the monovalent conjugate (Fig. 7).[85] Another example is offered by folic acid that binds to folate receptors overexpressed in many human cancer tumors. Conjugates of folic acid with siRNA and also with other therapeutic biomolecules have been targeted via receptor mediated endocytosis to enhance cellular uptake and pharmacological effect.[86] In another study, folic acid-PEG-siRNA conjugate in cell culture showed to be internalized into folic acid receptor expressing cells, but it did not silence the reporter genes. However, transfection along with a structurally defined polycation resulted in specific gene silencing.[87] By a similar approach, neuronal and immune cells have recently been targeted by anandamide (arachidonoylethanolamin)-siRNA conjugates.[88] Anandamide (*cis*-configuration) is a ligand for cannabinoid receptors present on neuronal and immune cells. Anandamide-siRNA conjugates are most likely taken up via receptor mediated endocytosis and they show similar silencing effect as standard cationic transfection reagents. In addition, dendritic siRNA nanostructures were covalently conjugated with anandamide moiety by copper catalyzed click reaction.[89] Interestingly, single anandamide moiety was able to internalize about nine siRNA duplexes and elicited efficient RNAi in neural stem cells and also exhibited suppression of viral titer of the rabies virus (RABV) in neurons.
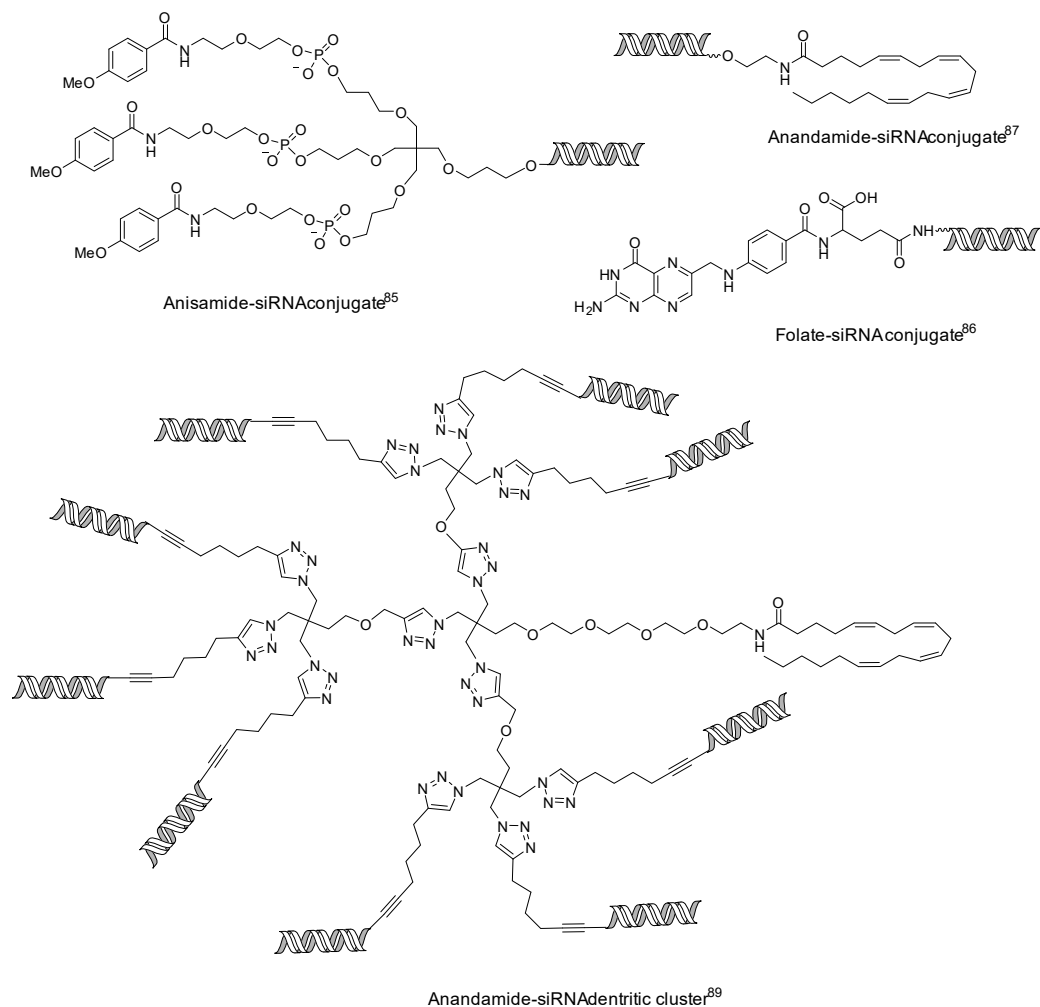
Figure 7. Small molecule-siRNA conjugates

1.7.3 Peptide-oligonucleotide conjugates

Two types of peptides, cell penetrating peptides (CPP) and receptor targeting peptides, have been used for delivery of ON drugs into cells (Fig. 8). Numerous *in vitro* studies on peptide conjugates of ONs and PNAs are available, the *in vivo* data still is scarce.[90] Cell penetrating peptides are typically 10-30 residues long, positively charged peptides that contain highly basic amino acids. When conjugated with neutral ONs, such as PNA and PMO, they efficiently enhanced transport across the cellular membrane, most likely via receptor mediated endocytosis, although precise mechanism is still an open question. In an early study, a conjugate of 21-mer PNA and transportan (a 27 amino acid-long CPP) downregulated galanin type 1 receptor in the rat spinal cord when administered intrathecally.[91] Most promising results were obtained with Duchenne muscular

dystrophy (DMD) disease on using PNA or morpholino (neutral) antisense oligomers for splice-switching (correcting out-of-frame mutations).[92]
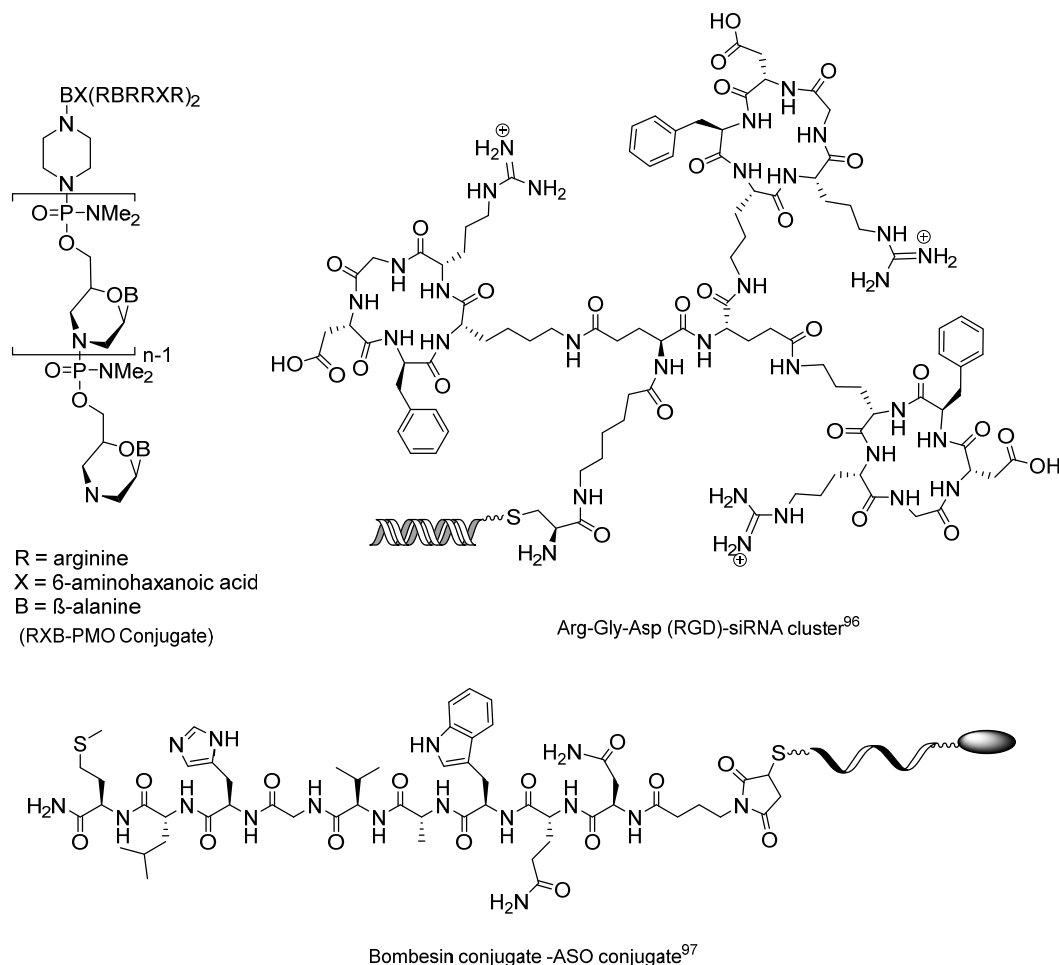

R = arginine
X = 6-aminohaxanoic acid
B = ß-alanine
(RXB-PMO Conjugate)

Arg-Gly-Asp (RGD)-siRNA cluster[96]

Bombesin conjugate -ASO conjugate[97]

Figure 8. Cell penetrating petide conjugates and receptor targeting peptide conjugates.

Systemic delivery of a conjugate of morpholino oligomer (PMO) and a CPP targeted towards a mutated dystrophin exon restored dystrophin to almost normal levels in the cardiac and skeletal muscles in dystrophic mdx mouse, utrophin-dystrophin double-knockout mice, and CXMD dogs, as well as in DMD patients in clinical trials.[93] Another study showed that addition of a muscular-targeting heptapeptide in the construct enhanced the efficiency. The conjugate restored uniform dystrophin protein expression in multiple peripheral muscle groups, yielding functional correction and improvement of the mdx dystrophic mice phenotype.[94] By peptide sequence optimization a peptide-PMO conjugate was obtained that showed highly efficient exon skipping and dystrophin production in mdx mice, leading to >50% of the normal level of dystrophin in heart. The

enhanced activity was partly explained by more efficient nuclear delivery.[95] As an example of usefulness of targeting peptides, integrin receptors have been targeted by Arg-Gly-Asp (RGD) conjugates, but so far only cell culture results are available. Mono- and multi-valent versions of the cyclic RGD peptide that binds selectively to the αvβ3 integrin that is over-expressed in angiogenic vasculature and in certain tumors, have been prepared and receptor-mediated uptake demonstrated in cell lines.[96] Although cellular uptake level seemed equal for bi-, tri-, and tetravalent –RGD-siRNA conjugates, tri- or tetra-valent cluster was necessary for significant pharmacological activity. Similarly, gastrin-releasing peptide receptor (GRPR), a member of the G protein-coupled receptor superfamily, has been targeted in a cell culture by a bombesin conjugate of splice-shifting 2′-*O*-Me phosphorothioate ON and receptor-mediated uptake.[97]

1.7.4 Aptamer- CpG- oligonucleotide conjugates

Aptamers are single stranded tertiary structures of ONs that possess binding properties to specific target receptors. These ONs are selected from screening pools of ONs via Systemic Evolution of Ligands by Exponential Enrichment (SELEX) method.[98] In addition to binding as inhibitors, aptamers can mediate receptor mediated endocytic delivery of ONs drugs.[99] One of the promising targets has been targeting of prostate-specific membrane antigen (PSMA), which is overexpressed in prostate cancer cells.[98] Aptamer conjugated with siRNA, has been tested in cells expressing PSMA. The conjugate was selectively taken up into cells and processed by Dicer, as demonstrated by inhibition of target mRNA and consequent cell death. These conjugates specifically inhibit tumor growth and mediate tumor regression in a xenograft model of prostate cancer.[100] Furthermore, the structurally optimized aptamer-siRNA conjugates employed via systemic administration exhibit prominent regression of PSMA-expressing tumors. Interestingly, introducing polyethylene glycol moiety showed enhancement in anti-tumor activity, which most likely results from increased circulation half-life in blood.[101] Similarly, there has been development of anti-HIV gp120 aptamer mediated siRNA delivery. An aptamer with high binding affinity to the HIV-1 envelope (gp120) protein and virus neutralization, when attached to siRNA showed that siRNA triggers sequence-specific degradation of HIV RNAs. The aptamer-siRNA conjugate resulted in more prominent inhibition and promising antiviral activity as compared to the aptamer alone.[102]

Toll like receptors also has been targeted for (TLR9) agonist– mediated delivery of ONs drugs.[103] siRNA linked to a CpG ON agonist of toll-like receptor (TLR)9 was shown to target and silence genes in TLR9+ myeloid cells and B cells.[104] Conjugates of siRNA-TLR9 agonist, targeting immune suppressor gene *Stat3*, demonstrated internalization in tumor-associated dendritic cells, macrophages and B cells. In general, silencing of *Stat3* activates tumor-associated immune cells and as a result antitumor immune responses.

1.7.5 Carbohydrates-oligonucleotide conjugates

Carbohydrates play numerous pivotal roles in cellular processes via carbohydrate-protein and carbohydrate-carbohydrate interactions.[105,106] Lectins are the cell surface carbohydrate binding proteins present in most of the living organisms. Although carbohydrates lectin binding on the cell surface usually is specific for a certain monosaccharide, the interactions with monomeric sugars are low affinity interactions (at millimolar level). To ensure high affinity binding, carbohydrate epitopes and lectins are *in vivo* oriented in such a manner that multiple binding events can occur simultaneously (Fig. 9). In other words, the lack of strength of an individual interaction is compensated via multivalency. Most of naturally occurring glycoconjugates and their synthetic analogues show enhancement in affinity per a mole of saccharide compared to the corresponding monovalent ligand. This phenomenon is known as *'Cluster glycoside Effect'*.[107]
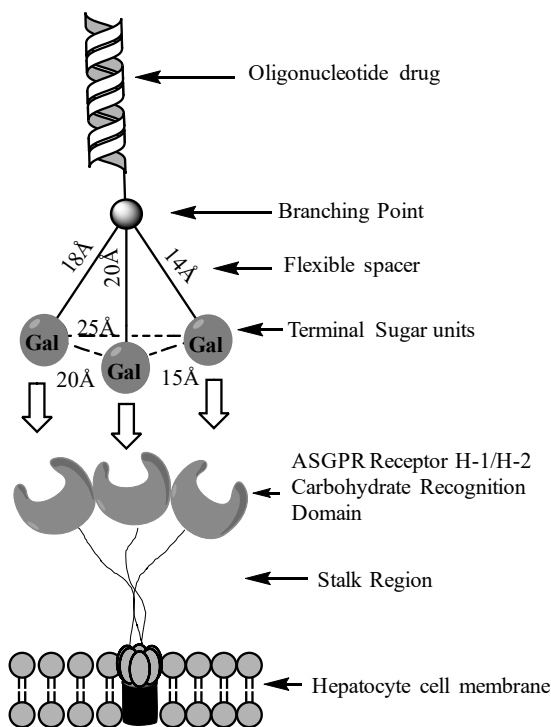

Figure 9. Design of multivalent ASGPR receptor specific Galactose/GalNAc ligands.[108]

A most successful emerging approach is targeting of asialoglycoprotein receptors (ASGPR) in liver.[109] ASGPR is abundantly expressed only by parenchymal hepatocytes (~500 000 copies/cell). It is a type II transmembrane glycoprotein (~40 KD) regulating the homeostasis of serum glycoprotein levels by binding and uptake of galactose terminated glycoprotein. The human ASGPR consists of two subunits, H1 and H2, with

the H1 subunit mediating Ca^{2+} dependent galactose or *N*-acetylgalactosamine (GalNAc) recognition (Fig. **9**). ASGPR mediates the endocytosis of bound ligands, such as galactose or GalNAc, by internalization via clathrin-coated pits endocytosis. In case the ligand becomes released into endosomal compartments, the lectin receptor is recycled to cell surface. There has been wide interest in development of carbohydrate-ON conjugates for tissue specific targeted delivery and to facilitate the cellular uptake through receptor mediated endocytosis.[110, 111]

Trivalent GalNAc cluster was in early studies covalently conjugated with methylphosphonate and phosphorothioate ODN via a neoglycopeptide linker. These conjugates were tested in rats for *in vivo* biodistribution and metabolism. The results showed 70% improved liver uptake of the conjugates.[112,113] Similarly, Biessen *et al*. demonstrated that the galactose tetrantennary lysine-based cluster conjugated to a 20-mer ^{32}P-ODN showed *in vivo* four-fold increase in parenchymal liver cells uptake compared to unconjugated ODN.[114,115] Monogalactosylated-PEG-33P-ODN conjugates with an acid labile ester linkage of β-thiopropionate also has been shown to enhance uptake by hepatocytes.[116] In a very similar approach, siRNA has been conjugated at the 3'-end of the sense strand with mono galactose or mannose-6-phosphate unit with the aid of a PEG linker containing a cleavable disulfide linkage (Fig. 10). The siRNA conjugates were studied for targeted delivery and gene silencing *in vitro*, in hepatocytes and hepatic stellate cell.[117] In another study, GalNAc[118] and galactosylated[119] peptide nucleic acid (PNA) conjugates have also been efficiently targeted to rat liver.

Scope of GalNAc cluster-ONs conjugates has not only remained limited to academic research but also has been of interest for pharmaceutical industries. Alnylam Inc. (MA, USA) has been developing siRNA based drugs. On support synthesis for a triantennary GalNAc cluster tethered to the 3'-terminus of the sense strand of the siRNA has been developed, and the conjugate has been applied to targeting to hepatocytes and shown to elicit efficient gene silencing *in vitro* and *in vivo*. Furthermore, these GalNAc-siRNA conjugates have been advanced for subcutaneous (SC) injection; preclinical trials showed significant improvement in tissue-specific delivery and efficacy compared to intravenous (IV) administration.[112] Transthyretin (TTR) mRNA targeting GalNAc-siRNA conjugate has been observed to decrease of the level of TTR protein in blood in early human samples for the treatment of amyloidosis.[120] Furthermore, GalNAc-siRNA conjugates also have been tested against hemophilia A and B for an RNAi mediated silencing of antithrombin III, a hemostasis regulatory protein.[121]
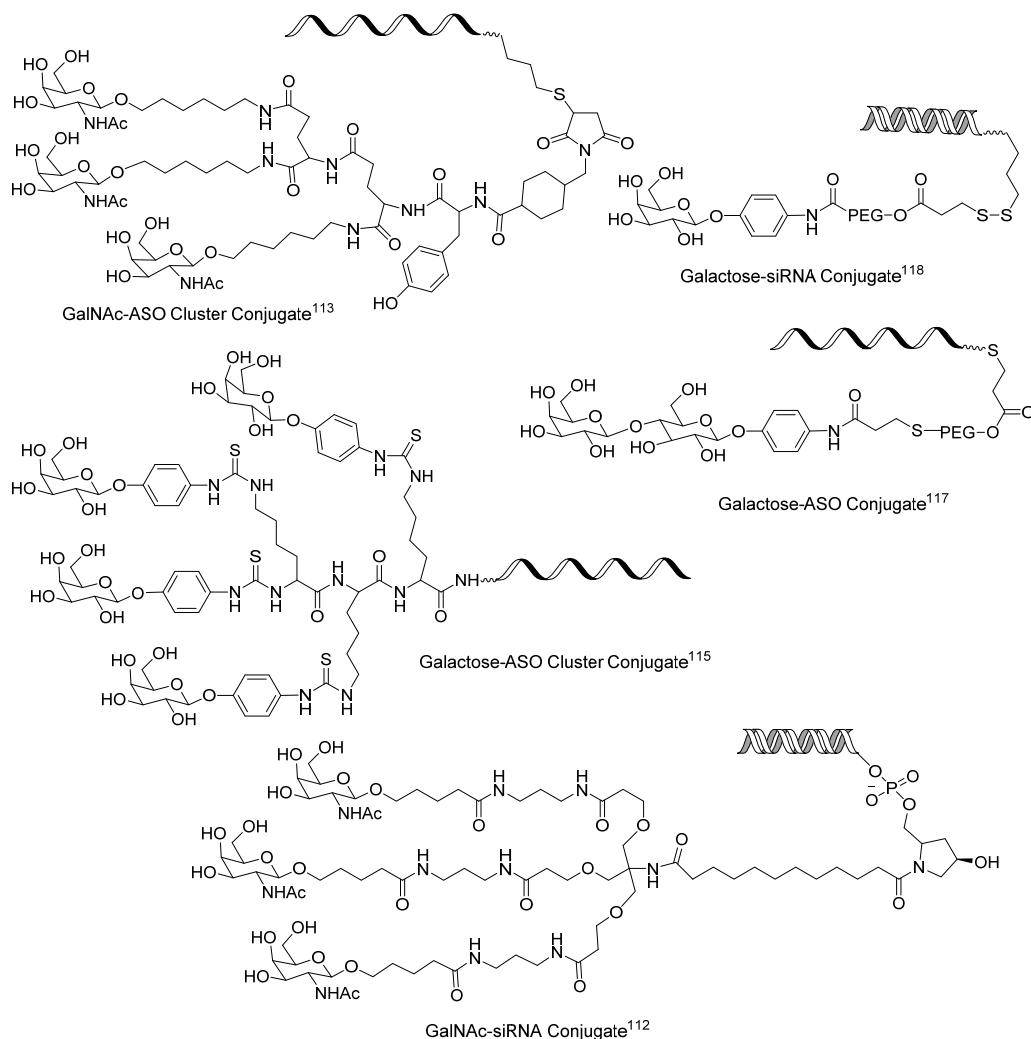
Figure 10. Galactose/GalNAc ON clusters

IONIS Inc. (formerly known as ISIS Inc. CA, USA) has also been involved in developing antisense ON drugs, utilizing GalNAc-ASOs conjugate strategy. Recent results on 5'-terminus conjugated GalNAc-ASOs showed 10 fold enhancement in silencing potency of second-generation gapmer ASOs in mouse liver.[122] Furthermore, 5'–tethered GalNAc-ASO conjugates showed more potent in cell studies and animal studies as compared to 3'–tethered GalNAc-ASO conjugates. In case of 5'–GalNAc-ASOs cluster, the carbohydrate moieties were metabolized more rapidly and cleanly than 3'-conjugate, liberating active ASO in cytosol of hepatocytes.[123] Very recently, extensive Structure Activity Relationship (SAR) study of GalNAc-ASO clusters has been published.[124] In addition, Arrowhead Research Corporation (CA, USA) has been developing the GalNAc-endosomolytic polymer-siRNA conjugates targeting to the hepatocytes by dynamic polyconjugates siRNA delivery; siRNA is tethered to the polybutyl aminovinyl

ether polymer, which is masked with PEG chains, and GalNAc attached by a dialkylmaleic acid linker provides productive endosomal escape properties.[125]

There has been high demand for finding new strategies for targeting and delivering ONs drug beyond the liver (ASGPR) target. For example, some of the cancer cell types overexpress receptors, which could be targeted specifically by either oligomeric or multivalent glyconjugate with ONs drugs. Recent studies on labelled glucose-ONs conjugates has demonstrated cell surface absorption and internalization via GLUT receptor mediated endocytosis (Fig. 11).[126,127] Glucose molecule is very vital in cell metabolism and it is transported by glucose transporter proteins present in wide range of mammalian cells. In this study it has been noticed that longer spacer (15 to 18 atoms) were taken up more efficiently in cells than shorter ones (4 atoms) and surprisingly, tetravalent glucose ON conjugates did not facilitate cell uptake.

Finally, PNA conjugates of 6-aminoglucosamine ring (ring II) of aminoglycoside antibiotic neomycin B was efficiently internalized in human cells and well distributed in cytosol and nucleus without trapping into nonproductive endosomes.[128] Internalized PNA conjugates exhibited very high specificity towards target and resulted *in vitro* robust inhibition of Tat mediated transactivation of HIV-1 LTR transcription.
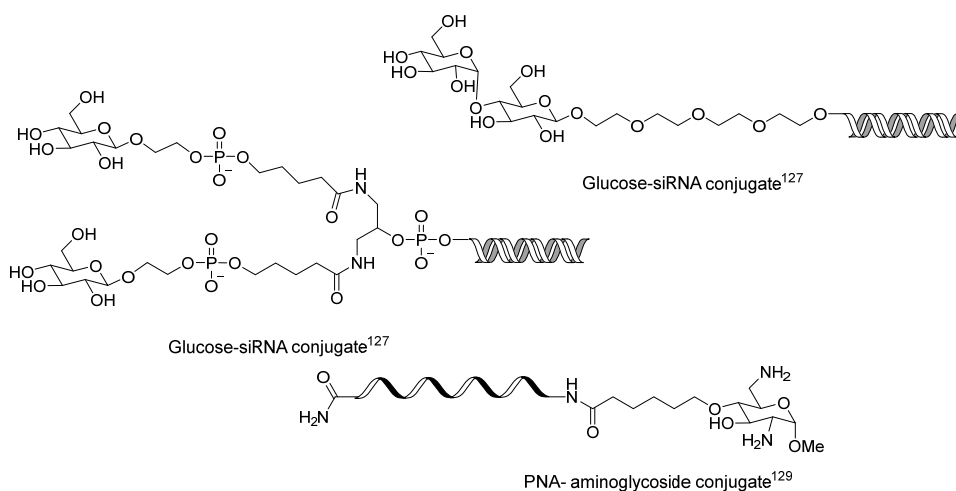

Glucose-siRNA conjugate[127]

Glucose-siRNA conjugate[127]

PNA- aminoglycoside conjugate[129]

Figure 11. Glucose-ON Conjugates and PNA- aminoglycoside conjugate

1.8 Oligonucleotide conjugation strategies

Synthesis of ON chain is classically performed on a controlled pore glass resin (CPG) solid support, using an automated DNA/RNA synthesizer and standard phosphoramidite coupling protocols.[129] Sequences are typically assembled 3'→ 5'direction, and hence the 5'-terminus is the obvious choice for conjugation. Different types of functionalities can

be attached to the 5'-hydroxyl group. 3'-End is another accessible site, but the chain assembly is then usually accomplished on a modified solid support bearing the desired conjugate group. It is also possible to assemble ON sequence in reverse manner, so that 5'-terminus is attached to solid support and chain is grown in 5'→ 3' direction. Intrachain conjugation can be achieved, by making use of exposable hydroxyl groups of pre-fabricated building blocks.[130,131] Therefore, various cell targeting ligands/moieties can be tethered to different sites on ON chains, as long as they do not too severely affect base pairing, biophysical properties and pharmacological activity.

Strategies for synthesis of ON conjugates fall in to two main types: i) Solution phase conjugation of the pre-fabricated and purified ON and conjugate group, each bearing an appropriate functionality required for coupling. In an optimal case, the coupling is so efficient that stoichiometric amount of ON and conjugate group can be used, which markedly simplifies the purification. ii) Solid phase synthesis, in which entire conjugate is assembled on single support. The assembly can be carried out by either using prefabricated building blocks or by stepwise assembling the conjugate group prior to or after the ON synthesis. Solid phase conjugation strategy allows the use of excess amount of reagents for pushing the reaction towards completion and conjugates are easily purified in the end by washing with solvents. However, solution phase conjugation is the method of choice in some cases, for instance when the conjugate moiety is unstable under ammonolytic conditions or it is synthetically so-challenging that usage of an excess amount for conjugation is not reasonable.[111,131,132]

1.8.1 Covalent linkages in oligonucleotide conjugates

Several types of reversible and irreversible linkages have been exploited in ON conjugation chemistry. Recently developed bioorthogonal conjugation approaches have received special attention. These post-synthetic conjugation methods can be efficiently utilized in both - solid supported as well as in solution phase synthesis. Some of the most commonly used covalent linkages are briefly described (Fig. **12**).[131] Naturally, amine groups have been used for amide bond formation by reacting with activated carboxylic group, while thiourea linkage are formed when amine attacks on isocyanate group. Aldehyde having electron deficient carbonyl center reacts quickly with nucleophilic amine, hydrazine, and aminooxy functional groups to produce imines, hydrazone and oxime linkages, respectively.

i) Amide
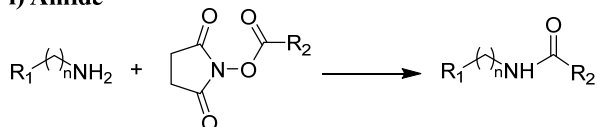
ii) Thiourea
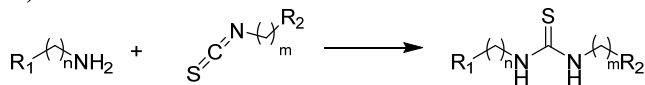
iii) Reductive amination
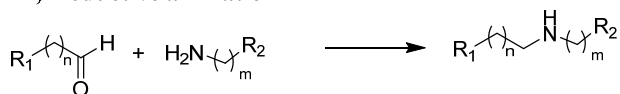
iv) Hydrazone
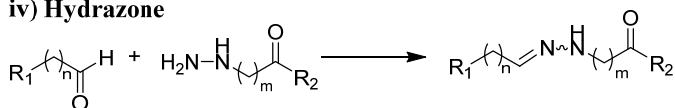
v) Oxime
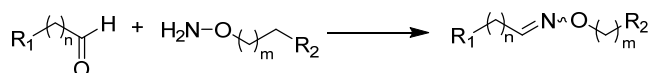
vi) Glyoxylic-oxime
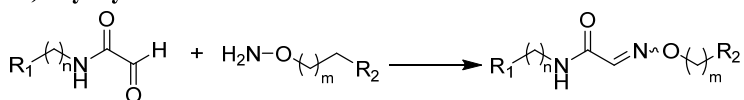
vii) Disulfide
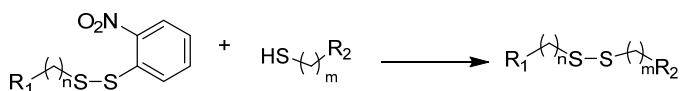
viii) Thioether
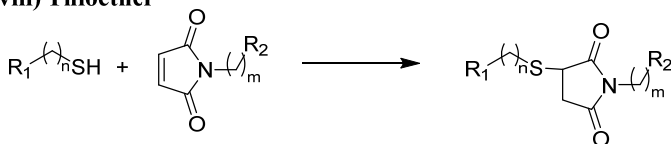
ix) Thiazolidine
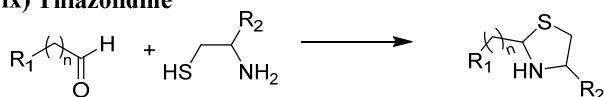
x) Native ligation
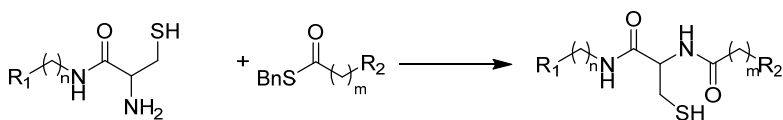
xi) Diels-Alder cycloaddition
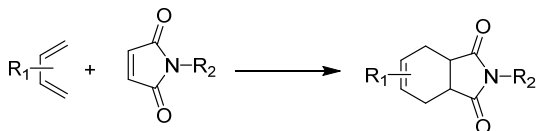
xii) Staudinger ligation
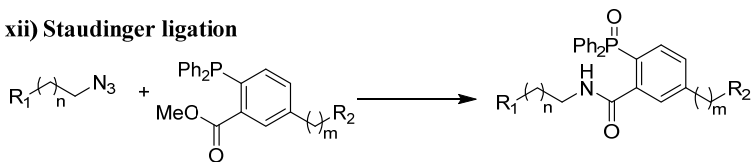
xiii) Huisgen 1,3-dipolar cycloaddition
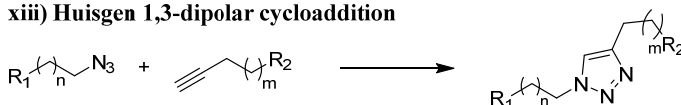
xiv) Strain promoted azide alkyne cycloaddition
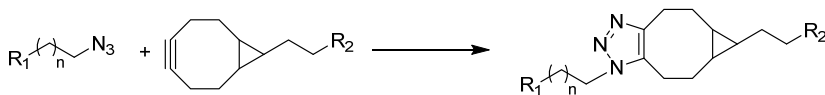
xiv) Strain promoted nitrone alkyne cycloaddition
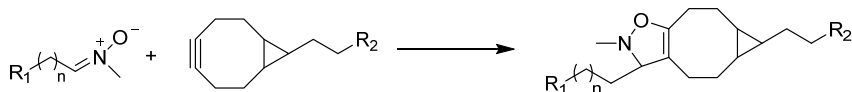
Figure 12. Common linkage types used for ON conjugations.

Among these, amine linkages are obtained from imines by reductive amination. There has been mounting interest for the use of sulfur containing cleavable linkage such as disulfides in ON conjugates.[133] Disulfides are linked to ONs in such manner that under reductive environment in cytosol, it liberates ONs, which may improve the pharmacological properties. Synthesis of disulfide linkages can be obtained by reaction of free thiol group with active thiol. Similarly, thioethers and thiazolidines that undergo cleavage in acidic medium have been utilized in ON conjugation.[71]

Stable trizole linkage is obtained by recently developed click chemistry.[134] Click reaction usually works with high specificity, and efficiency. It is also known as Huisgen 1,3-dipolar cycloaddition,: a Cu(I)-catalyzed azide-alkyne cycloaddition (CuAAC), forms a triazole linkage in aqueous solvents at room temperature. However, removal of copper from the reaction mixture is challenging, traces of copper remained along with conjugates may be cytotoxic in biological assays. As an alternative, recently copper free click reactions have recently been developed by using strained cyclooctyne derivatives, which reacts with azide moiety very efficiently, without any catalyst and the reaction

can be performed in aqueous medium.[135],[136]Similarly, nitrone moiety is reacted with strained cycloocyne derivative to obtain N-alkylated isoxazolines linked ON conjugates.[137] In addition, classical Diels-Alder cycloaddition reaction and Staudinger ligations also has been performed in ON conjugate synthesis.[138],[139] In addition, the length of attached linker is crucial in conjugation reactions and it may influence the pharmacokinetics of ON conjugates. Usually long chain linkers are preferred in preparation of ON conjugates. However alkyl chains are lipophilic in nature, in some instances they are less soluble in aqueous medium, and may forms aggregation. Hence, PEG linkers of about 8 to 10 atoms are used as an alternative.[140]

2. AIMS OF THE THESIS

Over three decades, there has been mounting interest for the applications of potent ONs as a novel class of therapeutics. However, several biological barriers are inevitably required to pass and improve ONs properties more like drugs. A major hurdle, which remains to be overcome, is the efficient delivery of these charged macromolecules into cells across the cell membrane. In general, cellular uptake of naked ONs is inefficient and only a small number of ON molecules actually gain entry to the cell. Traditionally, in cell culture studies, commercially available transfecting agents, a positively charged cationic lipids has been used by forming complexes with negatively charged ONs. However, the successful *in vivo* applications of the single stranded antisense ONs or antigomirs or double stranded siRNAs in the animal models and clinic obviously require improvements in cellular targeting, intracellular delivery and pharmacological properties.

The covalent chemical conjugation approach may possibly alter the *in vivo* bio-distribution and possibly cellular uptake. This expectedly leads to enhanced internalization of the conjugate by receptor-mediated endocytosis to facilitate the cellular uptake directly in cytoplasm for pharmacological effects. This approach in general, is aimed at facilitating targeted cellular uptake of both single stranded antagomirs and double stranded siRNAs.

The whole-body distribution of the conjugates in rats has been followed by positron emission tomography (PET). The ^{68}Ga-labeled ONs conjugated with different receptor targeting moieties were used as imaging agents for PET studies. These studies included clarification of the metabolic fate of ^{68}Ga-ONs in healthy rats and in diseased rat models, which also elucidated the *in vivo* specificity of ONs. The ONs were efficiently labeled by binding ^{68}Ga, a PET tracer, to a 3′-terminal conjugated 1,4,7-Triazacyclononane-1,4,7-triyl)triacetic acid (NOTA) ligand. This offered a powerful tool for determination of pharmacokinetics and tissue distribution of antagomir molecules, and allowed *in vivo* quantification of ON pharmacokinetics and bio-distribution data in rats.

The present thesis is aimed at clarifying the applicability of different receptor-based strategies for cell-specific targeting of ON drugs. The conjugate moieties, in the form of clustered/linear oligomeric carbohydrates and bisphosphonate derivative, may possibly enrich the ON conjugate on the surface of a certain organ/cell-type. i) Galactose cluster ON conjugates have been successfully emerged for *in vivo* targeting of liver.[112,123] Combination of PET technique and galactose cluster ON conjugation approach, may potentially provide rational quantitative data for bio-distribution, which could be an expedient for the development of ON therapeutics. ii) Hyaluronic Acid (HA)-CD44 interactions,[141] may possibly offer CD44 receptors targeting by HA-ON conjugates for

therapeutic applications. Enrichment of HA ligands with conjugated ONs on the CD44 expressing cell surface could lead to enhanced internalization by endocytosis and eventually also to increase concentration in the cytoplasm. iii) Bisphosphonates (BPs) are the attractive moiety for the targeting of bone tissues.[142-144] The efficacy of BPs is based on their remarkable tendency to localize rapidly on the bone surface after being administered.[145,146] Therefore, by linking of an ONs to BPs, selective targeting to bone tissue can be achieved. iv) Porphyrins recently have been emerged as a bifunctional agent in tumor imaging and photo dynamic therapy (PDT).[147] Carbohydrates-conjugated porphyrin based photosensitizers have attracted particular interest, since the sugar moiety may offer selective targeting of cancer cells via host lectin binding.[148] Porphyrin core forms stable chelation with radiometals, which makes porphyrins good probes for (PET) studies.[149] Hence, immobilization of porphyrins to a solid support may allow simple and even automated tailoring of the conjugate part that facilitates, in particular, screening of new photosensitizers and PET-tracers.

The aims of the thesis are summarized as follows:

- Synthesis of ^{68}Ga-labeled galactose cluster ON conjugates and their *in vivo* PET imaging studies in healthy rats.
- Synthesis of hyaluronic acid ON conjugates and their *in vivo* PET imaging studies in healthy and myocardial infarction rats.
- Synthesis of bisphosphonate ON conjugates and their *in vivo* PET imaging studies in healthy rats.
- Preparation of solid supported porphyrins for the straightforward synthesis of porphyrin biomolecules (particularly ONs and oligosaccharides) conjugates.

3. RESULTS AND DISCUSSION

3.1 Therapeutic significance of anti-miR-15b and anti-miR-21

The miR-15, microRNA precursor family comprises small noncoding RNAs such as miR-15a, miR-15b, miR-16-1, miR-16-2, miR-497 and miR-195. It has been suggested that, miR-15b is involved in hepatocyte apoptosis.[150, 151] In addition, silencing of miR-15b protects against cardiac ischemic injury.[152] Therefore, inhibition of miR-15b has emerged as a potential therapeutic target in liver and heart. It was recently found that, many types of cancer and solid tumours showed overexpression of miR-21. Several studies exhibited that overexpression of miR-21 results in suppression of vital tumour suppressing genes, like PTEN, tropomyosin 1 (TPM1), and programmed cell death protein 4 (PDCD4). Hence, inhibition of miR-21 via antagomir approach has emerged as a promising therapeutic approach to combat cancer.[153]

3.2 Positron emission tomography (PET)

PET is a non-invasive nuclear imaging technique, which has been advanced for quantitative visualization of various radiolabeled biomolecules, including ONs with high imaging contrast. Spontaneous decay of radioactive isotope emits high energy gamma ray photons, which are detected during imaging process. Mechanistically, nucleus of radioactive isotope undergoes beta plus (β^+) decay, because of unstable nuclear system. Proton is converted into a neutron, as well as positron, and an electron neutrino. Positron and electron annihilation, produces two gamma ray photons, travelling in (180º) opposite direction. Commonly used radionuclide isotopes in PET imaging includes, ^{18}F ($t_{1/2}$ = 109.8 min), ^{68}Ga ($t_{1/2}$ = 68 min), and ^{64}Cu ($t_{1/2}$ = 12.7 h). For instance, ^{68}Ga radiometal has been complexed with an appropriate ligands like NOTA, or DOTA, which are covalently linked to the ONs.[154,155]

3.3 Synthesis of 3'-NOTA-conjugated oligonucleotides using solid supported chelator strategy (SSCS)

NOTA modified controlled pore glass (CPG) support (**2**) allows preparation of 3'-radiometallated ONs and subsequent derivatization of the 5'-end with a conjugate group. Support **2** was prepared according to a previously reported method. [155] The trimethyl ester precursor of (1,4,7-triazacyclononane-1,4,7-triyl)triacetic acid **1**, bearing a 4,4′-dimethoxytrityl protected 4-(4-hydroxybutoxy)phenyl side arm on one of the acetic acid moieties, was immobilized to a long chain alkyl amine derived LCAA-CPG with the aid of an ester linker (Scheme **1**). A 22-mer 2'-*O*-methyl oligoribonucleotides such as anti-miR-15b (5'-UGU AAA CCA UGA UGU GCU GCU A-3'), anti-miR-21 (5'-AUC

GAA UAG UCU GAC UAC AAC U-3') and T6 sequences were assembled on support **2** by automated RNA-synthesis (1.0 μmol scale) via phosphoramidite chemistry. The ON conjugates were released from the support by two-step cleavage protocol: (i) the supports in micro-centrifuge tubes were first treated with 0.1 mol L^{-1} aq. NaOH for 3 h at 55ºC and the suspensions were neutralized by addition of 1.0 mol L^{-1} aqueous ammonium chloride. (ii) Overnight incubation in concentrated aqueous ammonia at 55ºC was then performed (Scheme **11**). Otherwise, direct global hydrolysis using conc. ammonia may form side products containing amide bond instead of desired free carboxylic acid/salt functions on NOTA chelator. The product was purified by RP HPLC and characterized by ESI-MS.
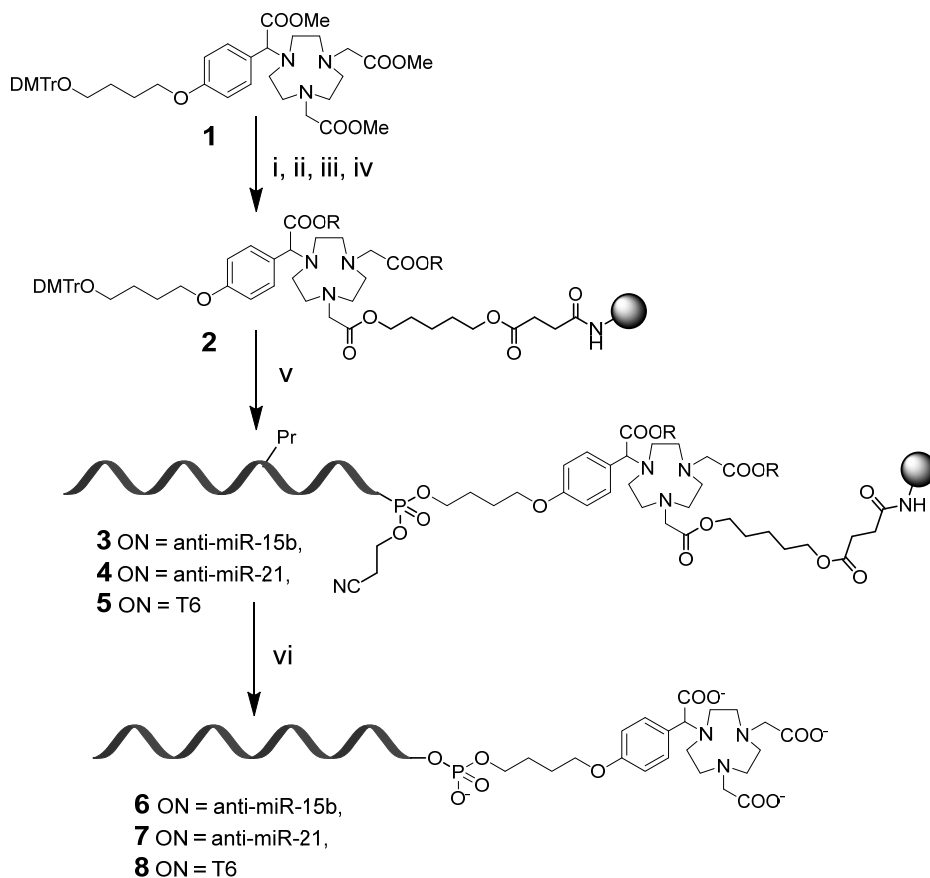
Scheme 1. Reagents and conditions: i) NaO(CH$_2$)$_5$OH, in pentane-1,5-diol, MeCN, ii) succinanhydride, DMAP, pyridine, iii) LCAA-CPG, PyBOP, DMAP, DMF, iv) Ac$_2$O, 2,6-lutidine, *N*-methylimidazol, THF, v) An automated ON synthesis via phosphoramidite chemistry, vi) (1) 0.1 mol L^{-1} aq NaOH, 3h at 55ºC (2) conc. aq NH$_3$, overnight at 55ºC.

3.4 Synthesis of 5'-galactose cluster, 3'-NOTA oligonucleotide-conjugates

Non-nucleosidic phosphoramidite building blocks were attached to the 5'-terminus to allow synthesis of glyco-ON conjugates. 2-Cyanoethyl (methyl 2,3,4-tri-*O*-acetyl-α-D-galactopyranoside-6-*O*-yl)-*N,N*-diisopropyl phosphoramidite **9** was prepared by phosphitylation of methyl 2,3,4-tri-*O*-acetyl-α-D-galactopyranoside with 2-cyanoethyl *N,N*-diisopropylphosphoramidochloridite. On support coupling of **9** to the 5'-terminus of the ON gave support **15**. 3'-NOTA modified ONs bearing three or seven galactose residues were obtained by solid-supported oximation (Scheme **3** and **4**). An aminoxy group is highly nucleophilic towards carbonyl moiety and the oxime linkage resulted is stable over wide pH range. Non-nucleosidic phosphoramidites such as, 2-cyanoethyl-5-(phthaliimidooxy)pent-1-yl-*N,N*-diisopropylphosphoramidite[156] **10** and 2-cyanoethyl-3-(4,4'-dimethoxytrityloxy)-2,2-bis{3-[(phthaliimidooxy)propyl]carbamoyl}propyl-*N,N*-diisopropylphosphoramidite, **11** were synthesized as per previous reports[157] and their coupling to the 5'-terminus of ONs, gave supports **17** and **20**, respectively.
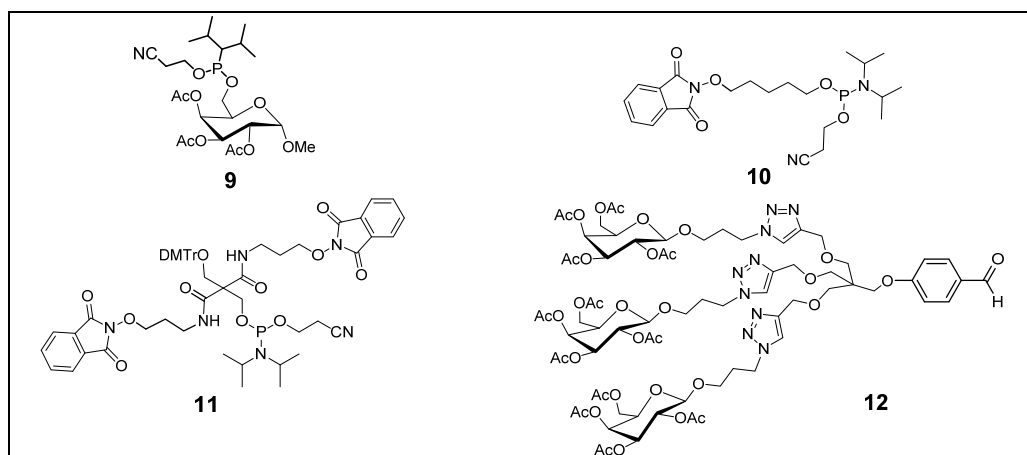
Figure. 13 Structures of Non-nucleosidic phosphoramidite building blocks and trigalactose scaffold.

Trigalactose scaffold **12** bearing a benzaldehyde group was synthesized by Cu(I) promoted click reaction of 3-azidopropyl 2,3,4,6-tetra-*O*-acetyl-β-D-galactopyranoside[158] **13** with previously reported 4-(tri-*O*-propargylpentaerythrityloxy)benzaldehyde[159] **14** (Scheme **2**). Pthaloyl protection on conjugate **17** was removed by treatment with hydrazinium acetate in pyridine. Trigalactose cluster bearing a benzaldehyde group was reacted with the exposed aminoxy group of **17** gave oxime linked on support conjugate **18**. Similarly, to obtain a heptagalactose clustered ON, support **3** was first phosphitylated with **11**, detritylated and subjected to treatment with **9** to get support **20**. The branching unit was capped in this manner in order to avoid cleavage via retro aldol condensation.

Afterward, both pthaloyl groups were removed by hydrazinium acetate treatment in pyridine and the exposed aminoxy units were subjected to oximation with trigalactose cluster **12** to afford support **21**. Finally, all supports **15**, **18**, and **21** were deprotected via previously reported two step protocols.[155] The desired conjugates **16**, **19** and **22** were purified by RP HPLC and characterized by MS (ESI-TOF) (Table **1**). An example of HPLC chromatograms and MS (ESI-TOF) spectra of the products (homogenized hepta-galactose-ON cluster conjugate) is depicted in figure **13**.
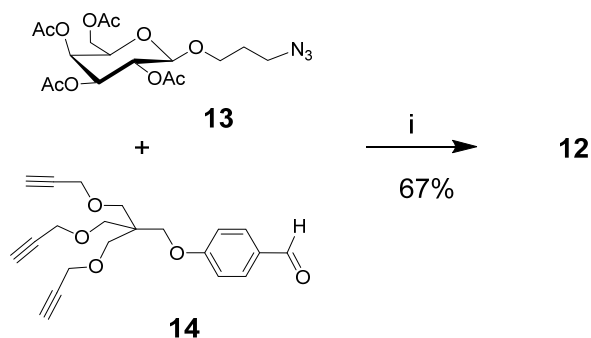
Scheme 2. Synthesis of the trivalent galactose cluster. Conditions: (i) $CuSO_4$, sodium ascorbate, H_2O, dioxane
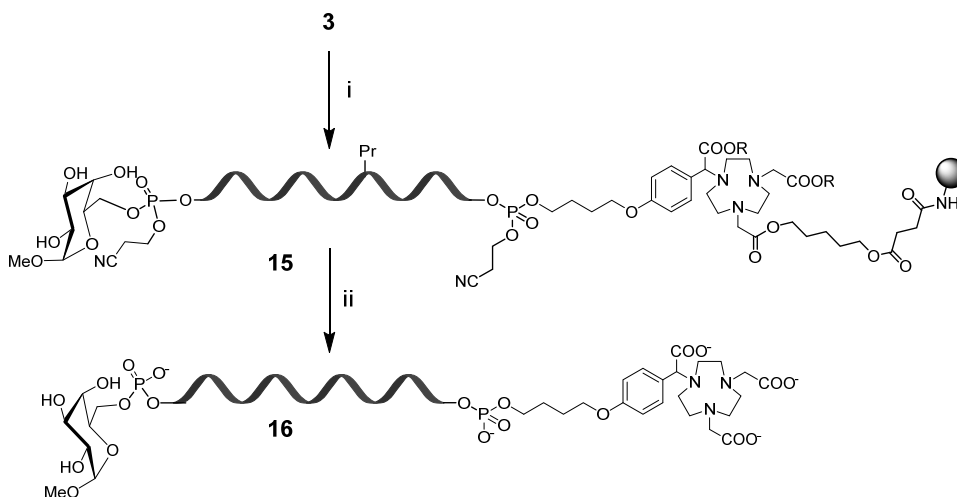
Scheme 1. i) **9**, phosphoramidite coupling, ii) (1) 0.1 mol L^{-1} aq NaOH, 3h at 55ºC (2) conc. aq NH_3, overnight at 55ºC.
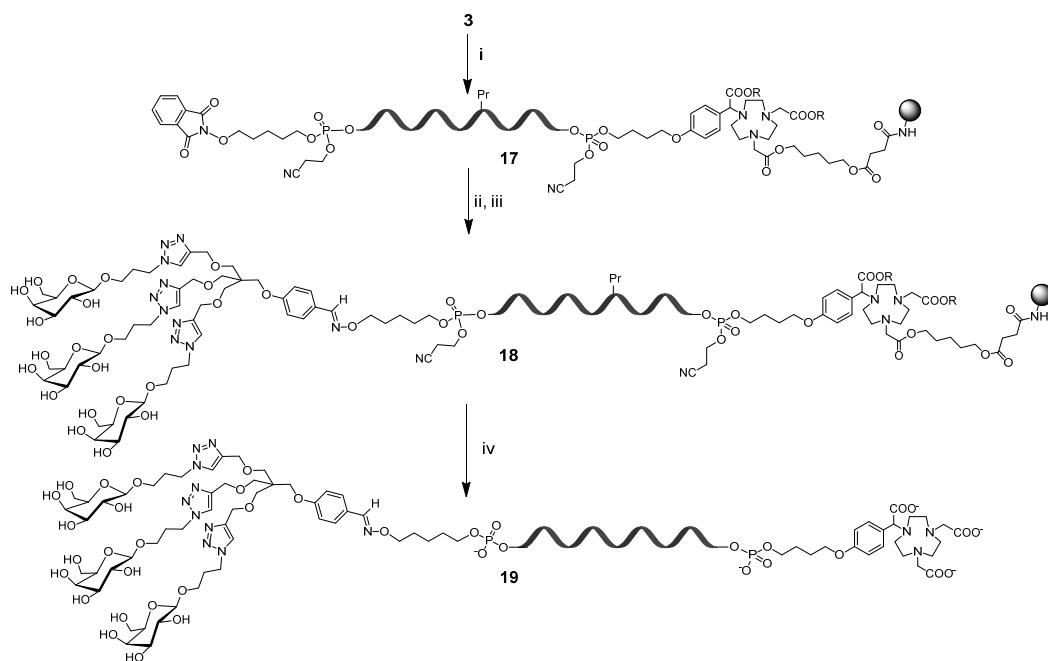
Scheme 3. Reaction and conditions: i) phosphoramidite coupling with **10** on automated ON synthesizer, ii) hydrazinium acetate, AcOH, pyridine, iii) 0.17 mol L^{-1} of **12** in MeCN, overnight at r.t., iv) (1) 0.1 mol L^{-1} aq NaOH, 3h at 55ºC (2) conc. aq NH$_3$, overnight at 55ºC.
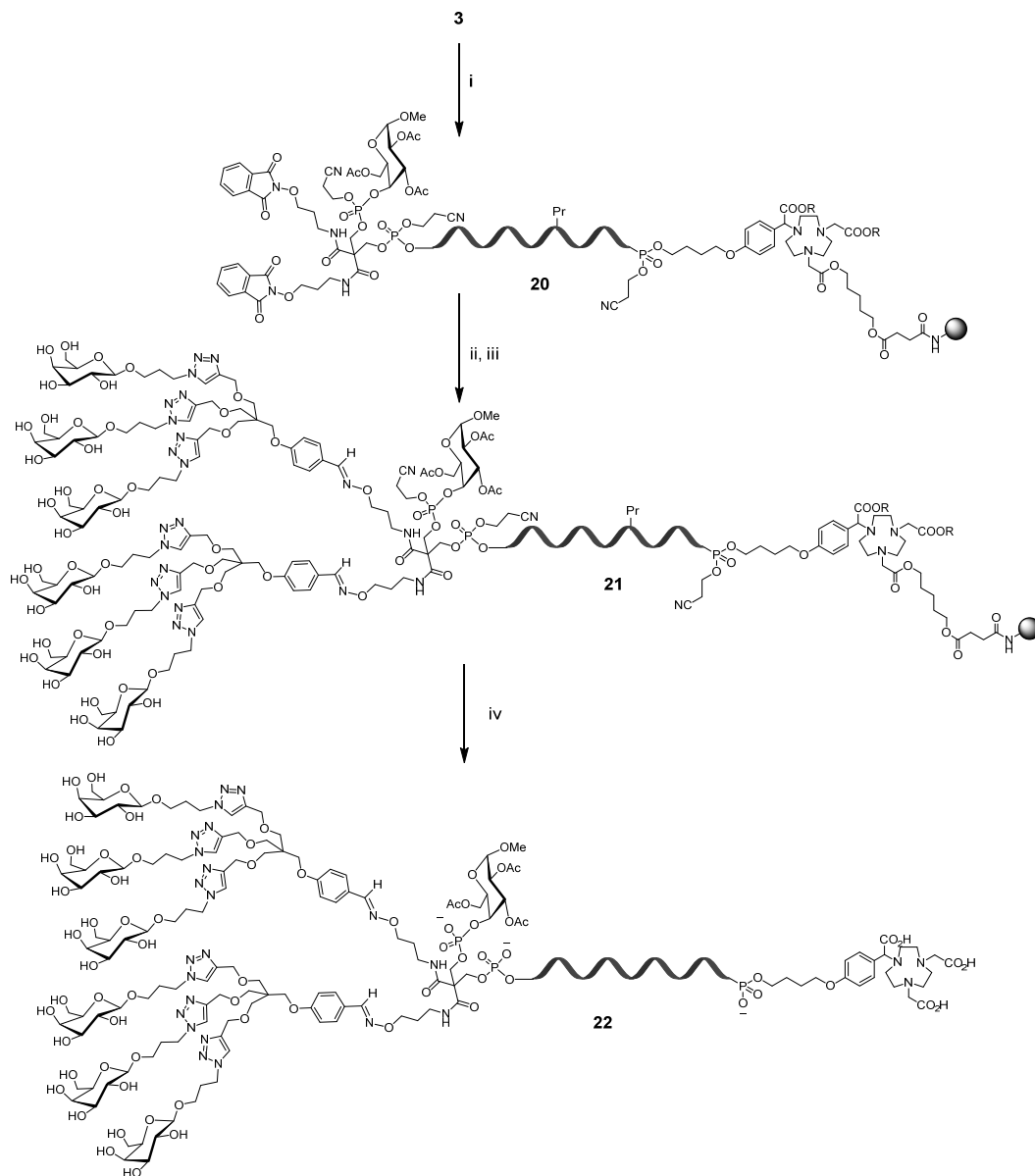
Scheme 4. Reaction and conditions: i) sequential phosphoramidite coupling with **11** and **9** on automated ON synthesizer, ii) hydrazinium acetate, AcOH, pyridine, iii) 0.17 mol L^{-1} of **12** in MeCN, overnight at r.t., iv) (1) 0.1 mol L^{-1} aq NaOH, 3h at 55ºC (2) conc. aq NH$_3$, overnight at 55ºC.

Table 1. MS (ESI-TOF) data the conjugates

entry	ON conjugate	observed average molecular mass[a]	calculated average molecular mass
1	**22**	10719.5	10719.0
2	**19**	9146.8	9148.6
3	**16**	8097.1	8097.4

[a]Calculated from the most intensive isotope combination at $[(M-11H+K)/10]^{-10}$
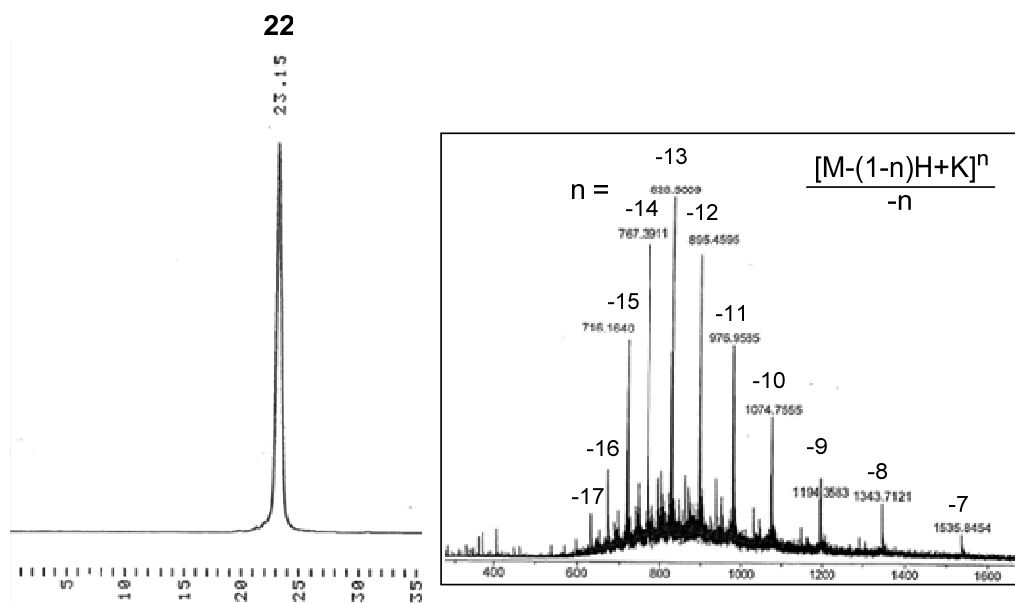
Figure 13. RP HPLC chromatogram and MS (ESI-TOF) spectrum of the homogenized hepta-galactose-ON conjugate. RP HPLC conditions: A gradient from 0% to 35% MeCN in 50 mmol L^{-1} aqueous NH_4OAc over 35 min (flow rate 1 mL min^{-1}, detection at 260 nm) on a Thermo ODS Hypersil column (150 × 4.6 mm, 5µm).

3.5 Hyaluronic acid -oligonucleotide conjugates

Hyaluronic acid (Hyaluronan, HA) is the only non-sulfated member of linear glycosaminoglycan polysaccharide family [chondroitin sulfate (CS), heparan sulfates (HS), dermatan sulfate (DS), keratan sulfate (KS)]. HA is composed of *β*-1,3-linked repeating disaccharide unit of 2-acetamido-2-deoxy-D-glucose-*β*-(1,4)-D-glucuronic acid. HA is a major component of extracellular matrix, which is essential for structural organ stability, tissue organization and cell growth. HA of size 6-8 monosaccharides has binding affinity to specific cell surface transmembrane glycoprotein receptor such as CD44 (cluster of differentiation 44).[160] In many cancer types, CD44 is up-regulated in active high-affinity state, which binds and internalize the HA ligand by endocytosis.

However, in normal primary cells, CD44 is endogenously expressed in low level and pre-activation of CD44 receptor is required for binding of HA ligand.

3.5.1 Synthesis of hyaluronic acid building blocks

Syntheses of HA tetramer and hexamer were carried out by convergent glycosylation using TMSOTf as an activator. Appropriately protected glucosamine glycosyl acceptor **28** was synthesized as per previously reported method,[161] starting from commercially available *β*-D-glucosamine hydrochloride **23**. (Scheme **5**) The 2-amino position was protected with the *N*-trichloroacetyl group (*N*-TCA), a well-known participating group for stereoselective formation of the required 1,2–*trans* glyosidic linkage. A difficulty associated with the use of 2-deoxy-2-trichloroacetamido glycosyl donor is the formation of stable trichlorooxazoline side products.[162,163] In addition, deprotection of multiple *N*-TCA groups from oligosaccharide via global hydrolysis conditions can also be challenging. Alternatively used method, radical reduction with Zn/AcOH or tributylstannane/AIBN may produce undesirable mono- and dichloroacetamido intermediates.[164,165,166] We decided to use conc. ammonia treatment for *N*-TCA deprotection step. Tetraacetylated *N*-TCA glucosamine **24** was treated with hydrazinium acetate for selective removal of acetate group at the anomeric position to afford hemiacetal **25**. *tert*-Butydimethylsilyl group was employed at the anomeric center as a temporary protecting group **26**. 4,6-*O*-Benzylidene protected glycosyl acceptor **28** was obtained by removal of acetyl groups with methoxide ion catalyzed transesterification in MeOH, followed by acid-catalyzed transacetalization with benzaldehyde dimethyl acetal. To obtain glucuronate donor **39,** previously reported methods were used, [167] as outlined in Scheme **6**. Commercially available peracetylated glucose **29** was converted to 1-phenylthio tetraacetate glucose **30** by glycosylation reaction with thiophenol, using BF$_3$:Et$_2$O as an activator.
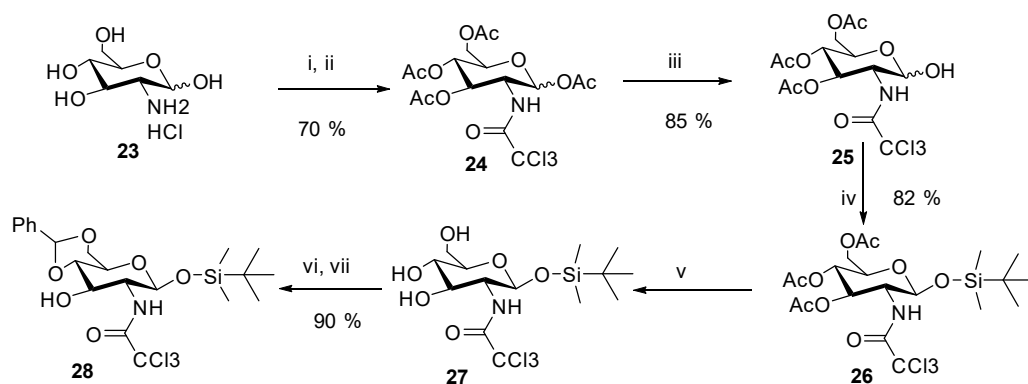
Scheme 5. Reaction conditions: i) Trichloroacetyl chloride, NaHCO$_3$, H$_2$O, rt, 16h; ii) Ac$_2$O, Pyridine, 0°C to rt, overnight; iii) H$_2$NNH$_2$ AcOH, DMF, rt, 3h; iv) TBSCl, Imidazole, DMF, rt, 4h; v) 0.1 M NaOMe, MeOH, rt, 3h; vi) PhCH(OMe)$_2$, p-TSA, CH$_3$CN, rt, 1 h.
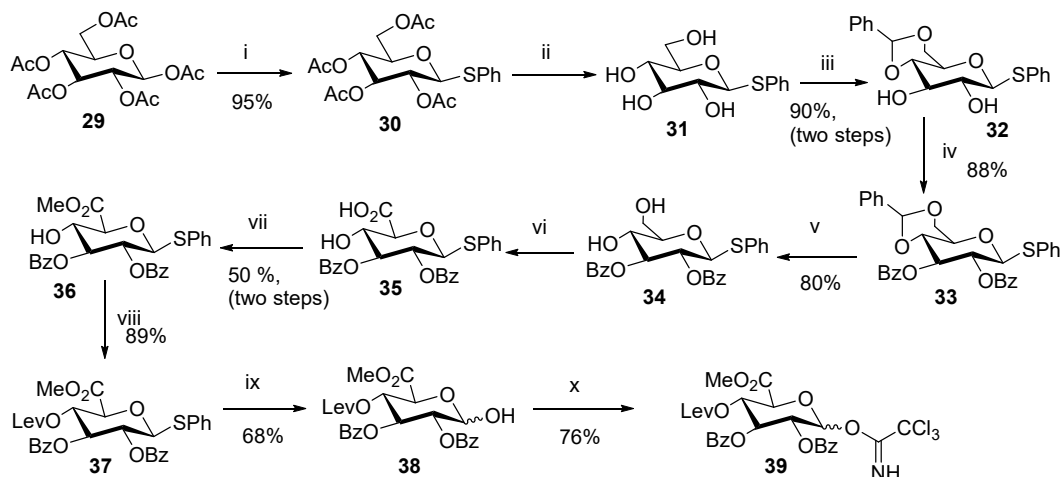
Scheme 6. Reaction conditions: i) PhSH, BF$_3$·Et$_2$O, CH$_2$Cl$_2$, rt, 5h; ii) 0.1 M NaOMe, MeOH, rt, 3h; iii) PhCH(OMe)$_2$, *p*-TSA, CH$_3$CN, rt, 1h; iv) PhCOCl, DMAP, pyridine, 0°C to rt, 1h; v) *p*-TSA, CH$_2$Cl$_2$, MeOH, rt; vi) TEMPO, BAIB, CH$_2$Cl$_2$, H$_2$O, rt, 45 min; vii) MeI, K$_2$CO$_3$, DMF, rt; viii) levulinic acid, DCC, DMAP, CH$_2$Cl$_2$, rt; ix) NIS, Tf$_2$O, CH$_2$Cl$_2$, H$_2$O, rt; x) CCl$_3$CN, DBU, CH$_2$Cl$_2$, 0°C to rt, 2.5 h.

Acetyl groups were removed by transesterification with sodium methoxide in methanol, and resultant tetraol **31** was converted to 4,6-*O*- benzylidene protected glucose **32**. The remaining C-2 and C-3 hydroxy groups were benzoylated and the 4,6-*O*-benzylidene protection was removed under acidic condition to obtain **34**. The 6-OH was oxidized regioselectively by free radical mediated TEMPO/BAIB approach to afford the corresponding glucuronic acid **35**. After esterification of the carboxy function, 4-OH was protected by levulinyl group and finally trichloroacetimidate glucuronate donor **39** was obtained by hydrolysis of 1-phenylthio glucuronate methyl ester followed by DBU catalyzed acetimidate formation.
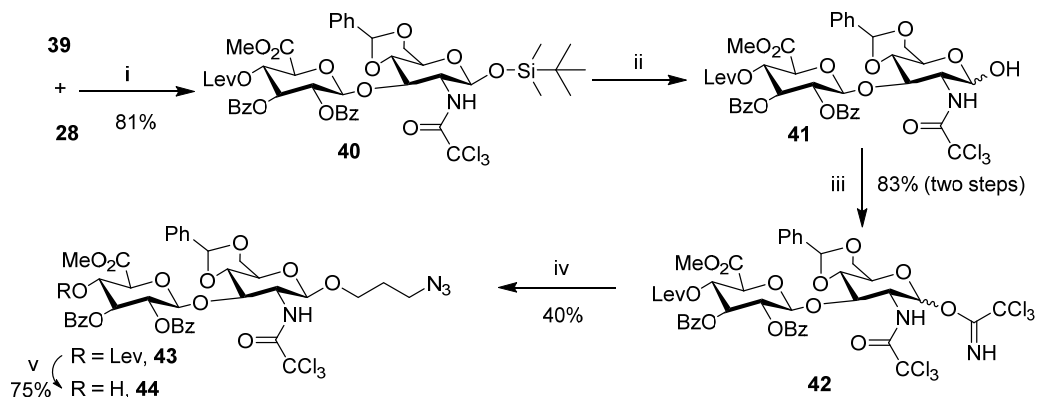
Scheme 7. Reaction conditions: i) TMSOTf, CH$_2$Cl$_2$, 0 °C, 45 min; ii) Et$_3$N 3HF, THF, rt; iii) CCl$_3$CN, DBU, CH$_2$Cl$_2$, 0 °C, 30 min; iv) 3-azidopropanol, TMSOTf, CH$_2$Cl$_2$, 0 °C; v) H$_2$NNH$_2$.H$_2$O: AcOH, pyridine, rt, 15 min.

3.5.2 Synthesis of functionalized hyaluronic acid oligosaccharides

TMSOTf-catalyzed glycosidation between acceptor **28** and donor **39** in CH$_2$Cl$_2$ afforded the β-glycoside **40** (Scheme **7**). Desilylation of **40** and subsequent treatment of the hemiacetal with trichloroacetonitrile in the presence of catalytic amount of DBU gave disaccharide trichloroacetimidate donor **42**. Anomeric functionalization with propyl azide was achieved by TMSOTf catalyzed condensation of disaccharide donor **42** with 1,3-azidopropanol in CH$_2$Cl$_2$. 4'-Levulinoyl protection of **43** was removed by hydrazine hydrate treatment to afford azide functionalized glycosyl disaccharide acceptor **44**. The coupling reaction of disaccharide glycosyl donor **42** with disaccharide glycosyl acceptor **44** as described above, afforded the HA tetrasaccharide derivative **45** (Scheme **8**). Acidolytic removal of the benzylidene groups of compound **45** gave partially protected azido propyl functionalized HA tetramer **47**. Similarly, hexasaccharide was obtained from glycosylation reaction with **42** and **46** and acidolytic removal of benzylidene protections gave partially protected azide functionalized hexasacchride derivative **48,** ready to conjugation.
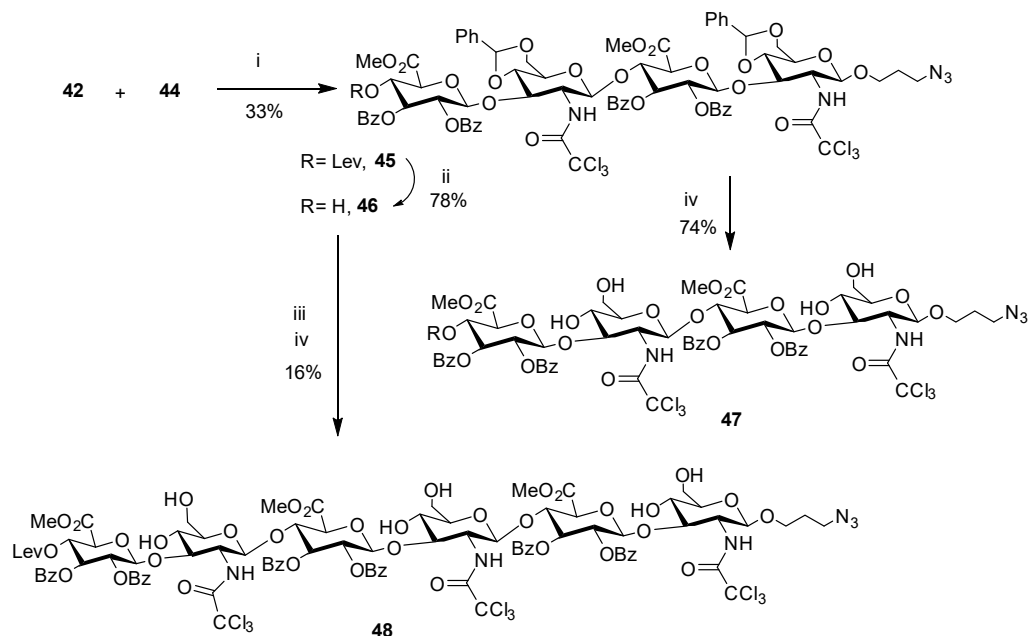
Scheme 8. Reaction conditions: i) TMSOTf, CH$_2$Cl$_2$, 0 ºC, 45 min; ii) H$_2$NNH$_2$.H$_2$O: AcOH, Pyridine, rt; iii) **42**, TMSOTf, CH$_2$Cl$_2$, 0 ºC, iv) *p*-TSA, CH$_2$Cl$_2$: MeOH, rt.

3.5.3 Synthesis of 5'-hyaluronan 3'-NOTA oligonucleotide-conjugates

Anti-miR-15b and T6 were assembled on NOTA modified CPG support (**2**) as described earlier (Section **3.3**). Commercially available 2-(bicyclo[6.1.0]non-4-yn-9-yl)ethyl 2-cyanoethyl *N,N*-diisopropylphosphoramidite (BCN phosphoramidite) was then coupled at the 5'-end of the ONs (Scheme **9**). ONs were released from NOTA-CPG support by

treatments with, aqueous alkali followed by concentrated ammonia.[142] BCN-anti-miR-15b-NOTA and BCN-T6 conjugates were purified by RP HPLC (Figure **14**) and characterized by ESI-MS. (Table **2**). BCN-anti-miR-15b-NOTA (**50**, 0.1 μmol) and BCN-T6 sequences (**49**, 0.1 μmol) could be virtually quantitatively conjugated with azide modified hyaluronic acid hexasaccharide (**48**, 0.2 μmol) and tetrasacharide (**47**, 0.2 μmol) via copper-free strain promoted azide alkyne cycloaddition (SPAAC) in CH$_3$CN:H$_2$O (1:9, v/v, 100 μL), overnight at 55°C.
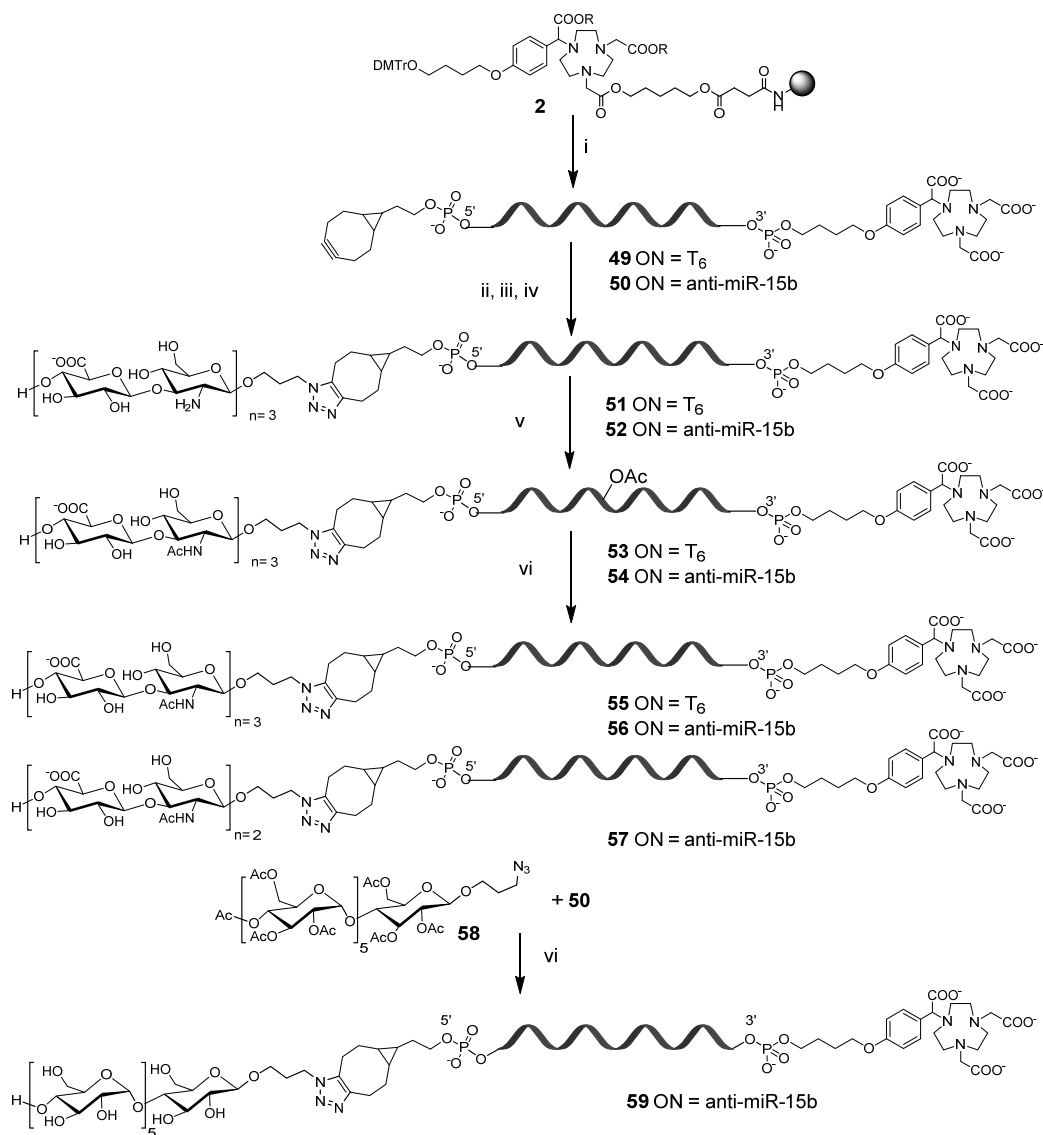
Scheme 9. Reaction conditions: i) Automated ON synthesis by phosphoramidite coupling chemistry., ii) **48**, MeCN-H$_2$O (1:9, *v/v*), overnight at r.t., iii) 0.1 mol L^{-1} aq NaOH, 3h at 55°C, iv) conc. aq NH$_3$, 5 days at 55°C, v) Ac$_2$O, Et$_3$N, H$_2$O, CH$_3$CN, 6h at r.t., vi) conc. aq NH$_3$, overnight at 55°C.

Removal of remaining protecting groups of the HA conjugates was achieved by two steps: esters were first hydrolyzed in aq. NaOH and then concentrated ammonia was used to complete the removal of the trichloroacetyl groups from the glucosamine units (5 days at 55°C). Progress of the global deprotections was monitored by RP-HPLC (Figure **14)** and ESI-MS. Acetylation of glucosamine units was carried out in aqueous medium with acetic anhydride and triethyl amine mixture. During acetylation step, nucleobases were also acetylated, and hence concentrated ammonia treatment was, once again, carried out to afford desired *N*-acetylated HA-ON conjugates. Homogeneity and identity of the ON conjugates were monitored by RP-HPLC (Figure **14**), and ESI-MS (Table **2**). Using a similar protocol, synthesis of HA hexamer-T6-NOTA **55** conjugates and HA tetramer-antimiR-15b-NOTA **57** were achieved. In addition, as a reference linear sugar-ON conjugate, azide modified peracetylated maltohexose **58** was conjugated with BCN-anti-miR-15b-NOTA **50**, for this case deprotection needed only ammonolysis at 55 °C to obtain conjugate **59**.
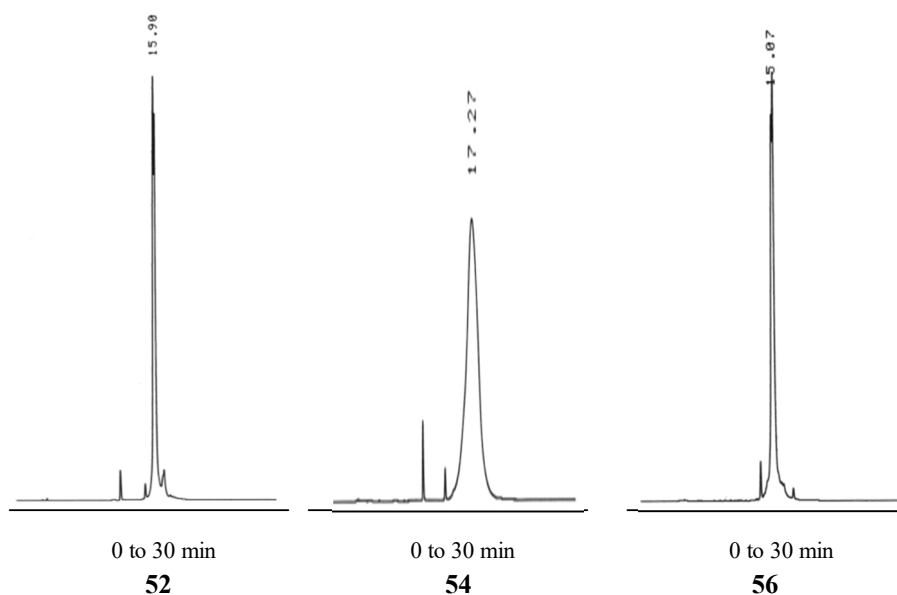
Figure 14. RP HPLC chromatograms of post conjugation modifications. RP HPLC conditions: A gradient from 0% to 35% MeCN in 50 mmol L^{-1} aqueous NH_4OAc over 25 min (flow rate 1 mL min^{-1}, detection at 260 nm) on a Thermo ODS Hypersil column (150 × 4.6 mm, 5μm).

Table 2

entry	conjugate	Calculated molecular mass	Observed molecular mass[a]
1	**55**	3755.9	3755.4
2	**56**	9306.6	9306.5
3	**57**	8927.3	8927.8
4	**59**	9141.5	9142.2

[a]Observed monoisotopic masses are calculated from $[M-nH]^{n-}$ and from the corresponding potassium and sodium adducts.

3.6 Bisphosphonate-oligonucleotide conjugates

BPs are well-known bone seeking agents. They are analogs of the naturally occurring pyrophosphates (P-O-P), in which the oxygen is replaced by a methylene group, forming a P-C-P structure. The methylene group is usually substituted (R^1 and R^2, Figure **15**). The P-C-P backbone and R^2 group (preferably a hydroxyl group) have high affinity to bone mineral, hydroxyapatite. The R^1 chain determines the potency of bisphosphonates to inhibit osteoclast-mediated bone resorption. Recently, bisphosphonates have been covalently linked to cytotoxic agents via a phosphate group.[168,169] These high affinity properties of bisphosphonates can be applied in targeting of therapeutic ONs to bones tissues.

60: $R_1 = -N\diagup\diagdown N$ $R_2 = OH$

61: $R_1 = -CH_2NH_2$ $R_2 = OH$

62: $R_1 = -(CH_2)_2NH_2$ $R_2 = OH$
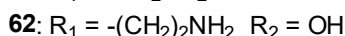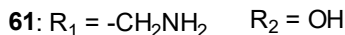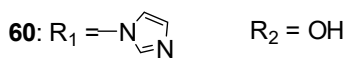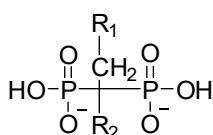
Figure 15. Structures of bisphosphonate derivatives.

3.6.1 Synthesis of alendronate azide

Alendronic acid/salt **62** is highly polar in nature, but still barely soluble in water or any polar solvents. Triethyl amine salts of alendronic acid was treated in water with imidazole-1-sulfonyl azide hydrogen chloride to result in a diazo transfer reaction (Scheme **10**). Progress of the reaction was monitored by ESI-MS. The product could be enriched from the starting material by repeated washings and precipitations in DMF, MeOH and CH_3CN and used then for the conjugation (contained still ca. 40% of starting material).
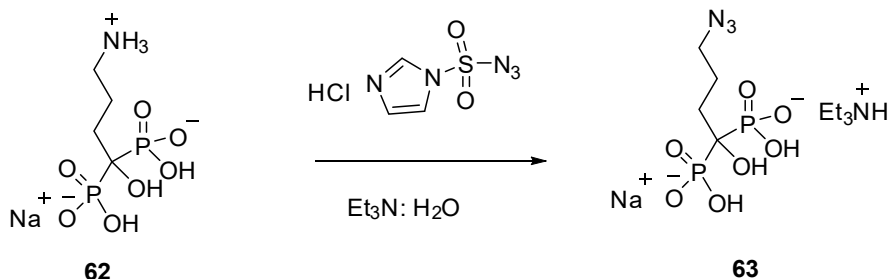
Scheme 10: Synthesis of alendronate azide **63**, via diazo transfer reaction.

3.6.2 Synthesis of 5'-alendronate 3'-NOTA oligonucleotide-conjugate

An anti-miR-21 and T6 sequences were assembled on NOTA support as described earlier (Section **3.3**). BCN phosphoramidite (0.1 molL^{-1}) was introduced to the 5'-terminus of the support-bound anti-miR-21 and T6 sequences in the last coupling cycle. The ON conjugates were released from the support and deprotected by two-step cleavage protocol (Section **3.3**). The product was purified by RP-HPLC. Crude alendronate azide (0.5 µmol) was coupled to 5'-BCN-3'-NOTA-anti-miR-21 (0.2 µmol) by SPAAC conjugation in H$_2$O (100 µL) overnight at 55ºC. The product was purified by RP-HPLC, yielded 0.17 µmol (87%) of the desired conjugate and the authenticity was verified by MS (ESI-TOF) (Table **3**).
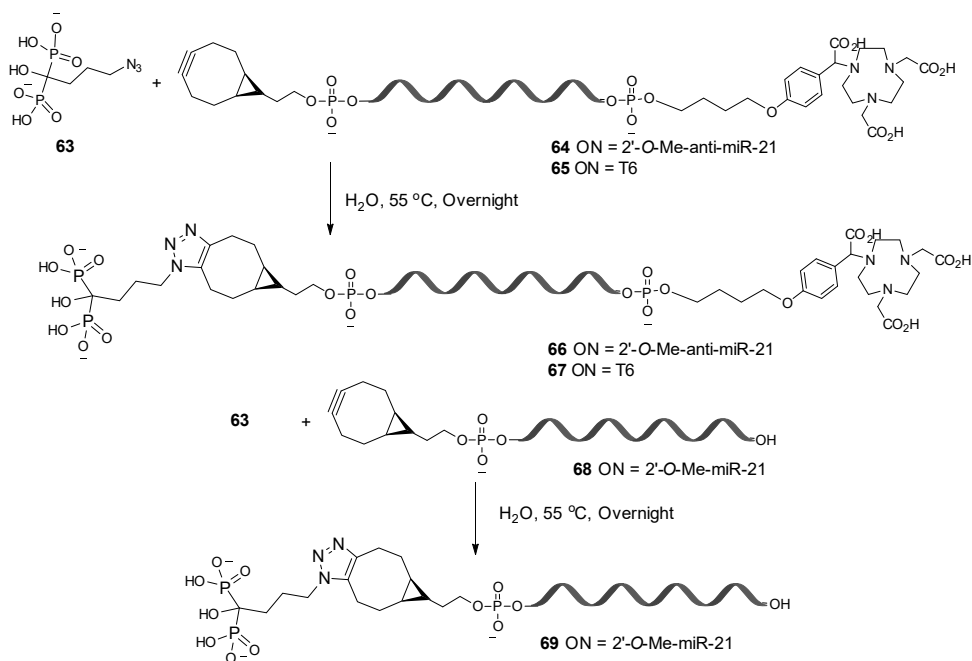
Scheme 11: SPAAC conjugation of alendronate azide.
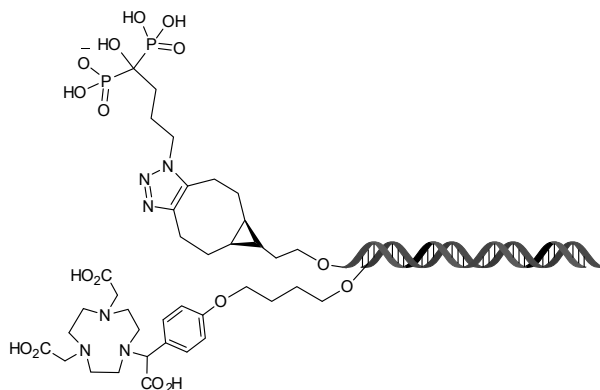
Scheme 12: Duplex formation of **69** and **7**.

In another approach, the alendronate and NOTA groups were introduced to separate ON strands (Scheme **12**). Complementary sequence of anti-miR21-NOTA **7**, *i.e.* miR-21 was assembled on standard 2'-*O*-Me support, bearing cyclooctyne modification at the 5'-terminus and this sequence was released by ammonolytic conditions. Furthermore, SPAAC conjugation of alendronate azide **63** with 5'BCN-miR21 **68**, gave efficiently alendronate-miR-21 conjugate **69**. Finally, these conjugates were purified by RP-HPLC and their authenticity was verified by MS (ESI-TOF) (Table **3**).

Table 3. MS (ESI-TOF) data of the alendronate-ON conjugates

entry	ON conjugate	observed average molecular mass[a]	calculated average molecular mass
1	**67**	2793.9	2793.6
2	**66**	8309.6	8309.2
3	**69**	7813.2	7812.1
4	**7**	7808.0	7808.3

[a]Calculated from the most intensive isotope combination at $[(M-11H+K)/10]^{-10}$

3.7 Solid-supported porphyrins

Applicability of the solid supported porphyrins *viz.* 2-(1-Hexyloxyethyl)-2-devinyl pyropheophorbide-a (Photochlor, HPPH)[170] and meso-tris(pyridin-4-yl)-(4-carboxyphenyl) porphyrin (PyCPP)[171] was demonstrated for the synthesis of various potential bioconjugates. HPPH is the commercially available effective photosensitizer that is currently in phase II clinical trials.[172] Porphyrin shows high affinity to G-quadruplexes,[173] offering additional binding motives for targeting of ONs. Conjugate **76** has a potential G-quadruplex-targeting ON sequence, complementary to single strand region of c-Myc, a cancer causing gene that induces transcription of growth-stimulating genes in many types of human cancer.[174] Synthesis of dendritic galactose cluster conjugates of porphyrin **77-80** was also demonstrated. Galectins are galactose–binding lectins, overexpressed on breast cancer cells[175] and melanomas.[176] Dendritic galactose clusters of porphyrin may, hence, play vital roles as cancer cell specific targeting of photosensitizers in photodynamic therapy (PDT).[177]

3.7.1 Synthesis of solid-supported porphyrins

For the synthesis of solid supported porphyrins (HPPH and PyCPP) (1*R*, 2*S*, 3*R*, 4*R*)-2,3,4-trihydroxy-1-aminocyclopentane was utilized as a branching unit (Scheme **13**). The amino group of compound **70** was trifluoroacetylated, the primary hydroxyl group (6-OH) 4, 4′-dimethoxytritylated and the amino group was then re-exposed by a hydrazine hydrate treatment. These three steps could be carried out in one pot to provide compound **71** in 70 % overall yield. HPPH and PyCPP were coupled quantitatively to **71**, via PyBOP-induced amide bond formation. Treatment of compound **72** and **73** with

succinic anhydride gave mixtures of mono- and disuccinate derivatives, which were coupled to LCAA-CPG support using PyBOP-promoted activation. Loadings of PyCPP and HPPH on the CPG support, determined by the DMTr-cation assay, were 20 μmolg^{-1} and 23 μmol g^{-1} respectively. Finally, supports were subjected to treatment with acetic anhydride for capping of unreacted amino and hydroxyl groups on supports **74** and **75**.
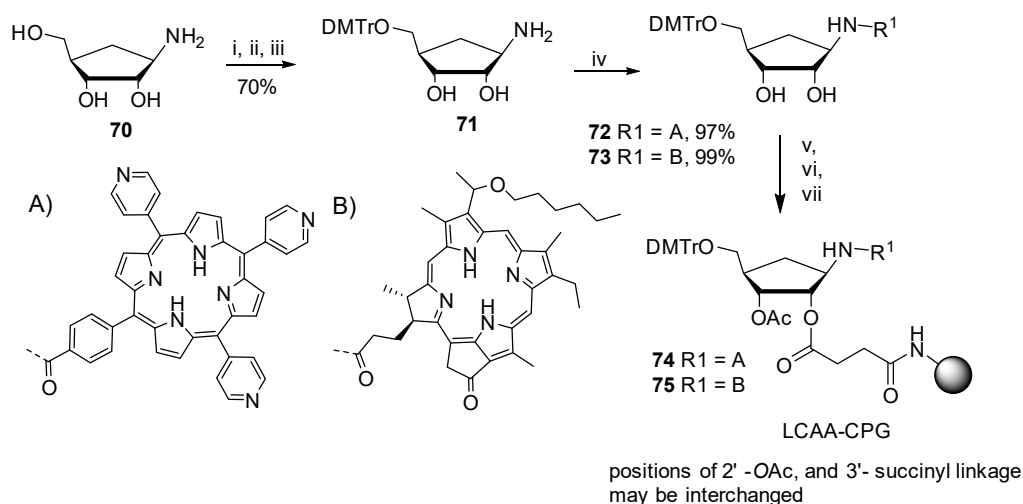
Scheme 13: Reagents and conditions: (i) MeOCOCF$_3$, MeOH, Et$_3$N; (ii) DMTrCl, pyridine; iii) NH$_2$NH$_2$·H$_2$O, dioxane, iv) *meso*-tris(4-*N*-pyridyl)(4-carboxyphenyl)porphyrin or HPPH, PyBOP, DIEA, DMSO-DMF (1:3, *v/v*); (v) Ac$_2$O, DMAP, pyridine; (vi) KOH, H$_2$O, DMF; (vii) succinic anhydride, DMAP, pyridine; (vi) LCAA-CPG, DIEA, PyBOP, DMF; (vii) Ac$_2$O, 2,6-lutidine, *N*-methylimidazol, THF.

3.7.2 Phosphoramidite couplings using supports

In order to prepare dendritic glyco-conjugates, commercially available phosphoramidite, trebler unit **76** was used for the synthesis of conjugate **80-83** (figure **16**). Cyanoethyl (methyl 2,3,4-tri-*O*-acetyl-α-D-galactopyranoside-6-*O*-yl)-*N,N*-diisopropylphosphoramidite **9** was coupled to branched cores. Conjugation of porphyrins with ONs and dendritic galactose clusters (**77−83**) were accomplished by using supports **74** and **75** (0.5 *μ*mol aliquots) on an automated DNA/RNA-synthesizer. Phosphoramidite coupling chemistry was used. Finally, the conjugate was released from the support by treatment with concentrated ammonia (2 h at 55 °C) and purified by RP HPLC. Crude RP HPLC profiles of conjugates (**82** and **83**) are shown in figure **17** and isolated yields were determined on the basis of porphyrin absorption in aqueous solutions. Authenticity of conjugates (**77−83**) was verified by MS (ESI-TOF) (Table **4**).

3.7.3 Synthesis of hyaluronic acid-PyCPP-conjugate

2-(Bicyclo[6.1.0]non-4-yn-9-yl)ethyl 2-cyanoethyl *N,N*-diisopropylphosphoramidite
was coupled to support **74** and the cyclooctyne-modified porphyrin **84** released by
concentrated ammonia. Azide functionalized HA hexamer **48** was subjected to SPAAC
conjugation in solution with strained cyclooctyne functionalized porphyrins, after
released from support by treatment with conc. ammonia. After the SPAAC-conjugation,
the protecting group manipulation of the HA moiety was carried out as described above
for ONs (Scheme **9**). Finally, the desired HA conjugate **85** was obtained by RP-HPLC
purification in 20% overall isolated yield. Identity of the conjugate was verified by MS
(ESI-TOF).
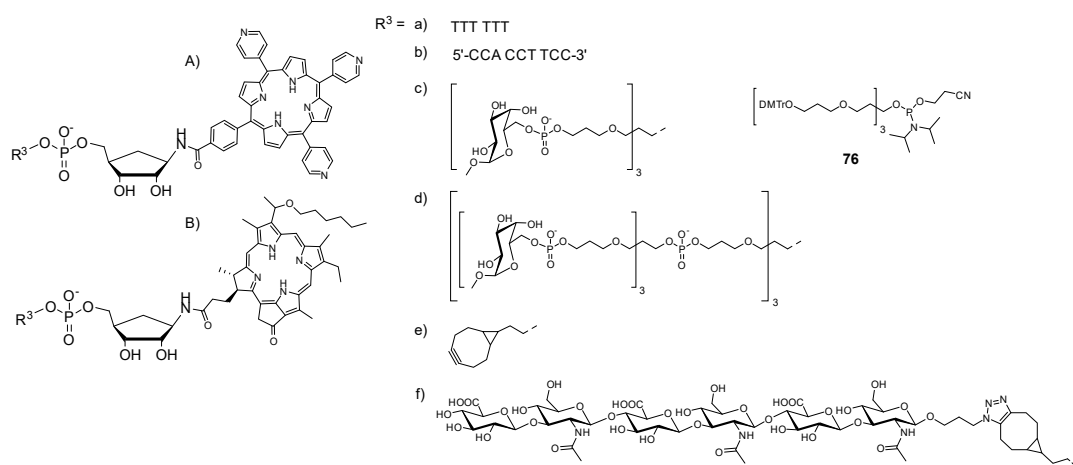
Table 4.

compound	R^1	R^3	Calculated molecular mass	Observed molecular mass[b]	isolated yield
77	A	a	2616.1	2615.3	58%
78	B	a	2591.2	2590.7	31%
79	A	b	3447.6	3446.8	40%
80	A	c	1930.6	1930.6	51%
81	B	c	1905.7	1905.7	36%
82	A	d	4585.6	4584.2	25%
83	B	d	4560.7	4559.3	23%
84	A	e	1016.4	1016.4	n.d.[a]
85	A	f	2256.2	2255.7	20%

[a](isolated yield not determined: n.d.). [b]The observed molecular masses have been calculated from the most intensive isotope combination at $[M-H]^{-1}$ (**84**), $[(M-2H)/2]^{-2}$ (**77-81** and **85**) and $[(M-3H)/3]^{-3}$ (**82** and **83**).
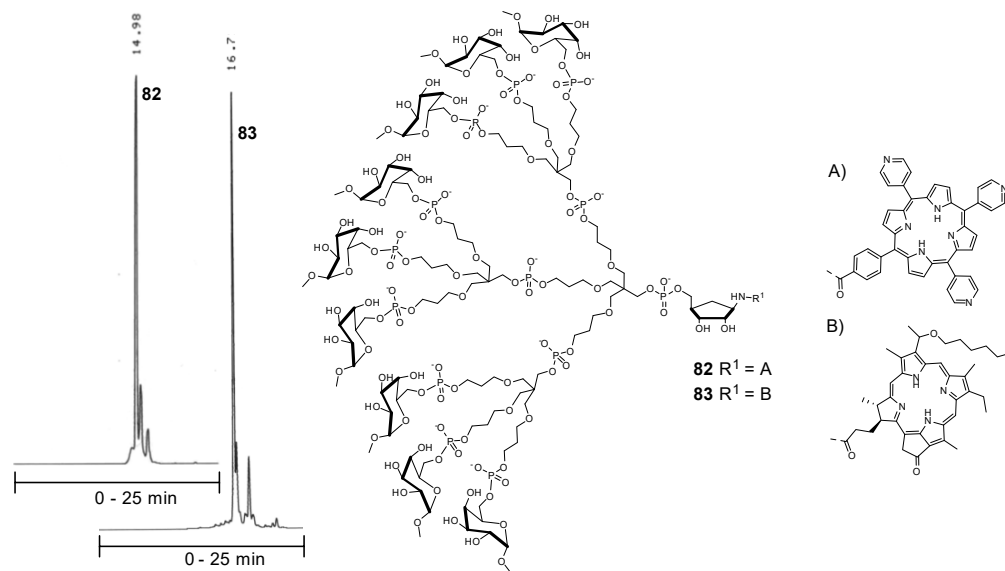
Figure 17. Example of RP HPLC profiles of crude product mixtures (**82** and **83**). RP HPLC conditions: An analytical column (C18, 250 × 4.6 mm, 5 µm), a gradient elution from 20 to 100% MeCN in H$_2$O over 25 min, flow 1.0 mL min^{-1}, detection at λ = 400 nm.

3.8 PET imaging, bio-distribution, and pharmacokinetics

3.8.1 PET studies of galactose conjugates

3.8.1.1 ^{68}Ga-radiolabeling of Gal-oligonucleotide conjugates

For PET labeling, ^{68}Ga is obtained in the form of [^{68}Ga]Cl$_3$ from a ^{68}Ge/^{68}Ga generator. Synthesized Gal-ON conjugates (**22**, **19** and **16**), containing NOTA chelate were subjected to form ^{68}Ga complex. The radiochemical purity of [^{68}Ga]-chelated Gal-ON conjugates were determined by a RP radio-HPLC (Fig. **18**). The radiochemical purity of Gal-ON conjugates was obtained as follows **22** (95%), **19** (97%) and **16** (95%).
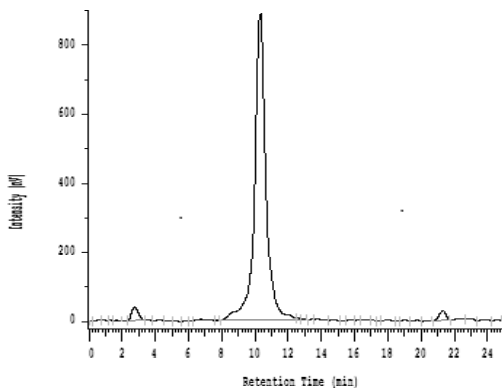
Figure 18. Radio-HPLC chromatograms of hepta Gal- anti-miR-15b -^{68}Ga-NOTA, **22**.

3.8.1.2   PET imaging of galactose cluster oligonucleotide conjugates

PET images on figure **19** represented the bio-distributions of radiolabeled (^{68}Ga) NOTA-galactose-ON conjugates (**22**, **19** and **16**) in healthy rats. Ex vivo data on figure **20** and Table **5**, showed the radioactivity accumulations in liver, kidneys and urine in healthy rats. Figure **21** represented activity *vs.* time curve for liver, kidneys and urinary bladder. Seven galactose cluster ON conjugate **22**, and three galactose cluster ON conjugate **19** exhibited enhanced accumulation in liver. About, 8 fold enhancement in liver activity was observed with seven galactose cluster ON conjugate (Fig. **20**), whereas 5-fold enhancement with three galactose cluster ON conjugates **19** as compared to non-glycosylated ON conjugate **6**. One galactose-ON conjugate **16** and non-glycosylated ON conjugate **6** showed similar liver activity. For conjugate **22**, activity *vs.* time curve on figure **21** showed over 60 min steady activity level in liver. In case of conjugate **19**, liver activity was slightly lower. One galactose **16** and non-glycosylated **6** ON conjugates exhibited low activity level in liver. Ex-vivo experiments on Table **5** depicted that, highest activity in kidney was observed for non-glycosylated ON conjugate, followed by one galactose ON conjugate. Surprisingly, seven galactose cluster ON conjugate **22** showed low activity in kidneys, but high activity in urine. In principle, low kidney uptake should lead to low excretion into urine. However, this may be explained by metabolic cleavage of **22** that takes place in liver and release the PET tracer into urine.
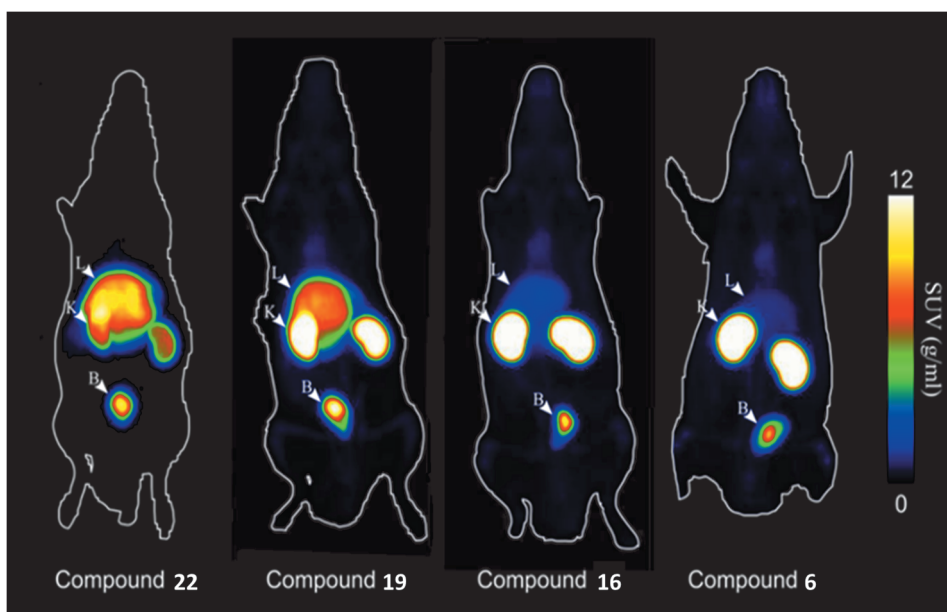
Figure 19. Maximum intensity projections of PET images. Liver (L) showed the highest radioactivity concentration with hepta-Gal-ON conjugate **22** kidneys (K) showed the highest radioactivity concentration with (none Gal) ON-conjugate **6** and the highest radioactivity concentration in the urinary bladder (B) was observed with conjugate **22**. (PET images are mean presentations of all time frames of 60-min acquisition)
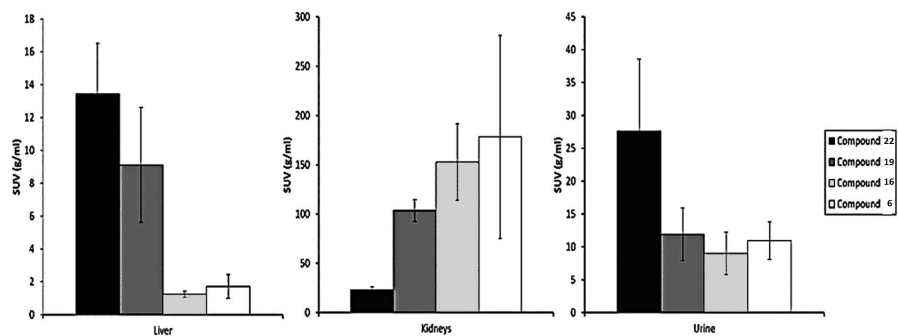
Figure 20. Ex vivo measured radioactivity accumulation data in rat liver, kidneys and urine
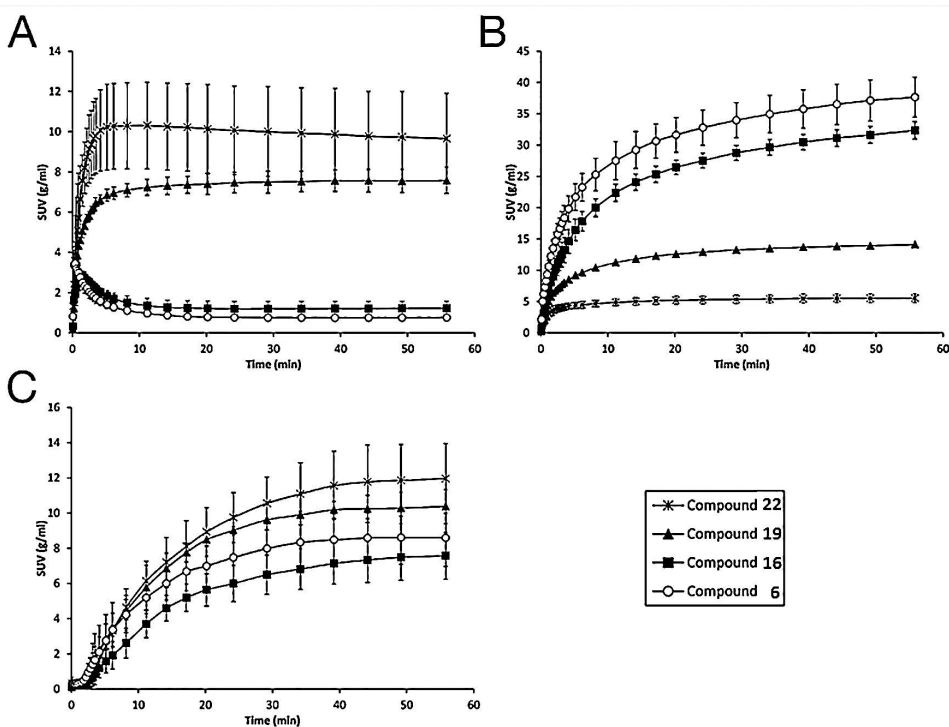
Figure 21. Time radioactivity curves of liver (A), kidneys (B) and urinary bladder (C)

Table 5. Ex vivo biodistribution of intravenously injected ^{68}Ga labeled compounds in healthy rats

	Compound **22** (n=4)	Compound **19** (n=2)	Compound **16** (n=4)	Compound **6** (n=4)
Adrenal gland	0.10 ± 0.024	0.40 ± 0.30	0.12 ± 0.025	0.25 ± 0.069
Blood	0.076 ± 0.031	0.090 ± 0.053	0.13 ± 0.052	0.34 ± 0.19
Bone	0.16 ± 0.055	0.47 ± 0.25	0.27 ± 0.11	0.40 ± 0.18
Bone marrow	0.43 ± 0.069	2.0 ± 1.1	0.46 ± 0.19	0.67 ± 0.054
Brain	0.0044 ± 0.0013	0.0070 ± 0.0048	0.0057 ± 0.0018	0.018 ± 0.0035
Brown adipose tissue	0.077 ± 0.019	0.11 ± 0.061	0.099 ± 0.053	0.21 ± 0.046
Heart muscle	0.076 ± 0.019	0.11 ± 0.038	0.083 ± 0.032	0.18 ± 0.059
Intestine	1.1 ± 0.76	0.24 ± 0.031	0.15 ± 0.031	0.22 ± 0.034
Intestine (cleaned)	0.42 ± 0.18	0.44 ± 0.26	0.19 ± 0.065	0.38 ± 0.11
Kidney	23 ± 3.2	103 ± 11	150 ± 39	180 ± 103
Liver	13 ± 3.1	9.1 ± 3.5	1.2 ± 0.19	1.7 ± 0.71
Lung	0.13 ± 0.04	0.53 ± 0.25	0.16 ± 0.058	0.37 ± 0.089
Muscle	0.028 ± 0.013	0.032 ± 0.011	0.032 ± 0.014	0.070 ± 0.015
Pancreas	0.16 ± 0.026	0.24 ± 0.095	0.15 ± 0.074	0.33 ± 0.071
Plasma	0.13 ± 0.045	0.26 ± 0.17	0.20 ± 0.073	0.62 ± 0.32
Salivary gland	0.20 ± 0.055	0.30 ± 0.087	0.19 ± 0.055	0.43 ± 0.094
Skin	0.11 ± 0.038	0.19 ± 0.047	0.22 ± 0.092	0.29 ± 0.088
Spleen	0.87 ± 0.46	2.1 ± 0.69	0.55 ± 0.11	0.86 ± 0.57
Urine	28 ± 11	12 ± 4.0	9.0 ± 3.2	11 ± 2.8
White adipose tissue	0.030 ± 0.0069	0.025 ± 0.0086	0.027 ± 0.0075	0.061 ± 0.015

Results are expressed as standardized uptake values (mean ± SD)

3.8.2 PET studies of hyaluronic acid conjugates

3.8.2.1 ^{68}Ga-radiolabeling of hyaluronic acid-oligonucleotide conjugates

Radiolabeling with ^{68}Ga for the ON conjugates were carried out as described earlier (Section **3.8.1.1**). Radio-HPLC analysis, demonstrated the radiochemical purities of the conjugates. The observed radiochemical purities as follows: 96 ± 0.21 % (**55**), 94 ± 1.5 % (**56**), 92 % (**57**), 89 % (**59**), 99 % (**6**), 95 ± 1.7 % (**8**) and 98 ± 0.049 % (NOTA alone). Representative radio-HPLC chromatogram is shown in figure **22**. The specific radioactivity was 4.7 ± 2.1 MBq/nmol at the end of syntheses.
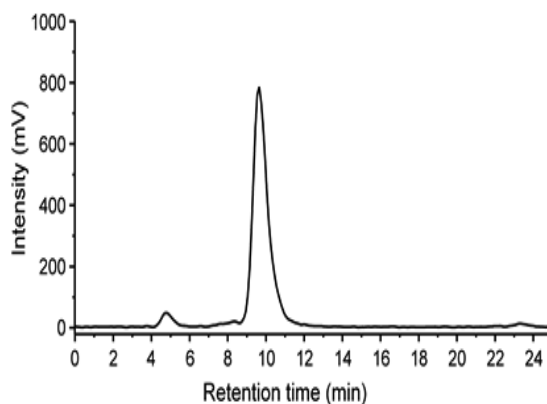
Figure 22. An example (^{68}Ga-NOTA-HA-anti-miR-15b, **56**) of radio-HPLC chromatograms.

3.8.2.2 Whole-body bio-distribution kinetics of hyaluronic acid conjugates in healthy rats

Figure **23** represented the *in vivo* PET images of ^{68}Ga labeled HA-ON conjugates. Time-activity curves of the distribution kinetics are represented in figure **24**. Bio-distribution data obtained by ex vivo studies are showed in figure **25**. High radioactivity accumulation was observed in urinary bladder, kidneys, liver, intestine, spleen and bone marrow. In general, the bio-distribution of the conjugates was found to be varied with ON sequences as well as sugar units. It was observed that, the kidney, bone marrow, salivary gland and liver uptakes of anti-miR-15b conjugates (**56-59** and **6**) were considerably higher (kidney: $P \leq 0.021$, bone marrow: $P \leq 0.0044$, salivary gland: $P \leq 0.00048$, liver: $P \leq 0.049$) as compared to T_6 conjugates (**55** and **8**). Among the conjugates of anti-miR-15b sequences (**56-59** and **8**), carbohydrate moieties exhibited variation in bio-distribution. HA-hexamer-anti-miR15b conjugate **56** showed highest bone marrow uptake, maltohexaose-anti-miR-15b conjugates **59** showed highest uptake in salivary gland. The intestine uptake of HA-hexamer-T6 conjugate **55** was seen higher compared to **56-59, 6** and **8**. Conjugate of anti-miR-15b **6** was the highest in blood uptake. Although, HA-hexamer-T6 conjugate **55** showed lowest kidney uptake, higher activity in urine excretion was observed as compared to all other conjugates ($P \leq 0.031$). In addition, the lung uptake for conjugate of HA-hexamer-T6 **55** was considerably lower as compared to all other conjugates ($P \leq 0.010$), and NOTA-^{68}Ga complex only.
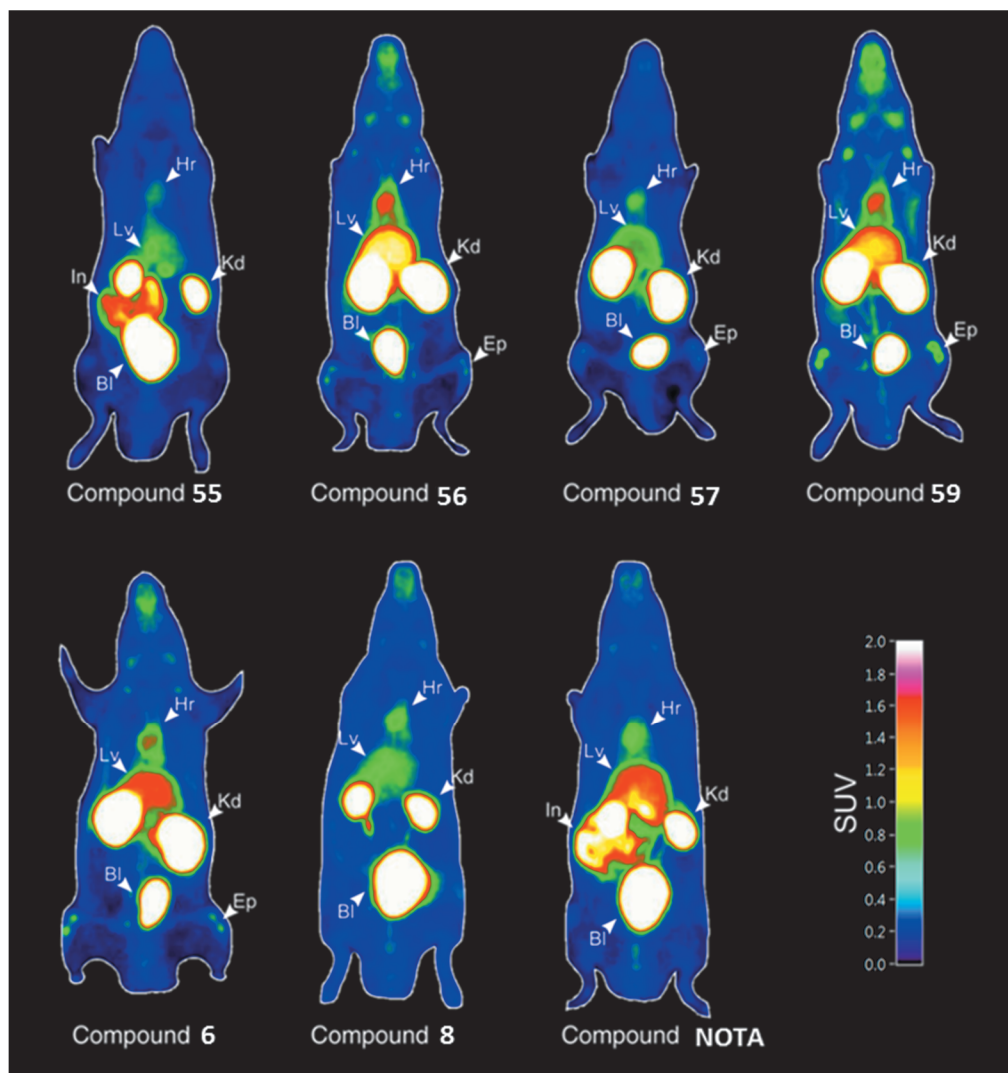
Figure 23. Representative whole-body coronal PET images of rats intravenously injected with ^{68}Ga-conjugates **55-59**, **6**, **8** and **NOTA** alone. Images are summation from 0 to 60 min after injection. Radioactivity accumulates in heart (Hr), liver (Lv), kidneys (Kd) and urinary bladder (Bl). The intestine (In) accumulation is observed with **55**.
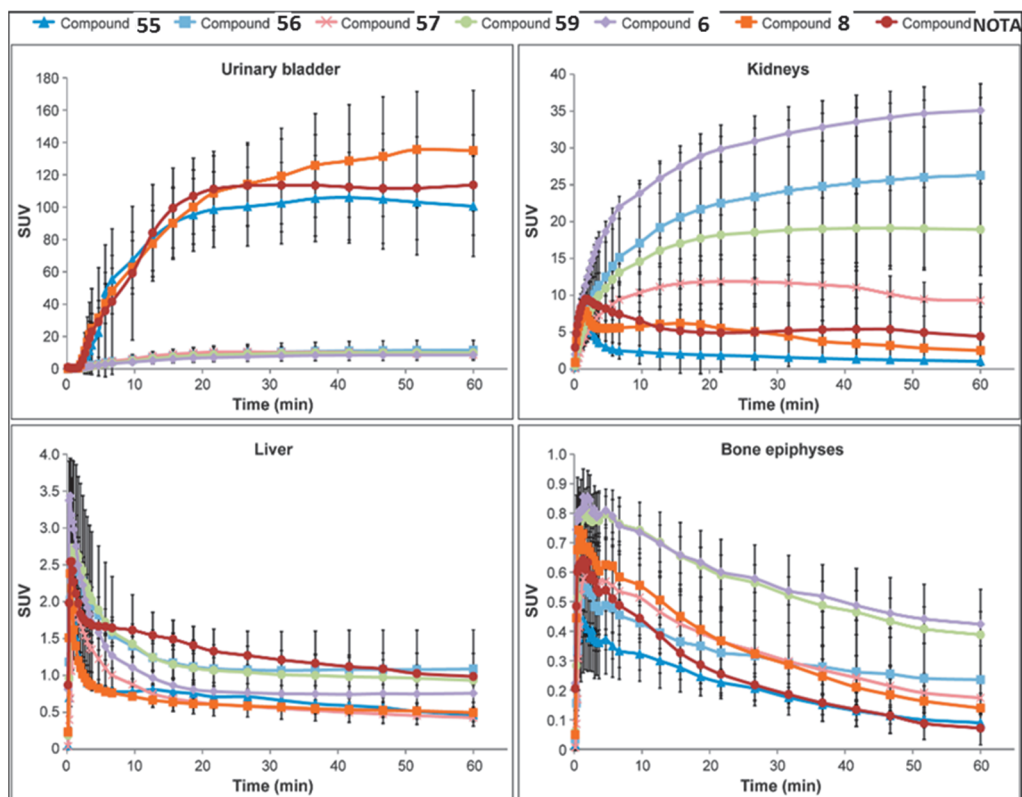
Figure 24. Time-activity curves of the distribution kinetics.

3.8.2.3   Rats with myocardial infarction (MI)

Feasibility of targeting miR-15b by HA ON conjugates **55** and **56** in MI rats has also been demonstrated (Fig. **26**). *Ex vivo* bio-distribution of **55** and **56** are represented in Table **6**. Figure **26**A-C illustrated the autoradiograph, hematoxylin-eosin and CD44 immunohistochemically staining of the heart left ventricle cross section in a rat with MI. Uptake of HA hexamer-T6-^{68}Ga-NOTA **55** conjugate was significantly increased in the infarcted myocardium as compared with the remote non-infarcted areas and myocardium of sham-operated rats (Figure **26**D). The infarction-to-remote ratio of conjugates of HA hexamer-T6-^{68}Ga-NOTA **55** and HA hexamer-anti-miR-15b-^{68}Ga-NOTA **56** were 4.2 ± 0.75 (P = 0.008) and 1.1 ± 0.4 (P = 0.016), respectively (Figure **26**D). *Ex vivo* gamma counting further confirmed the improved uptake of HA hexamer-T6-^{68}Ga-NOTA **55** in the infarcted left ventricle (SUV 0.183 ± 0.003) compared to sham-operated control (0.100 ± 0.009, P = 0.006; Table **6**). Immunohistochemistry showed CD44 positive cells within the infarcted area (Figure **26**C)
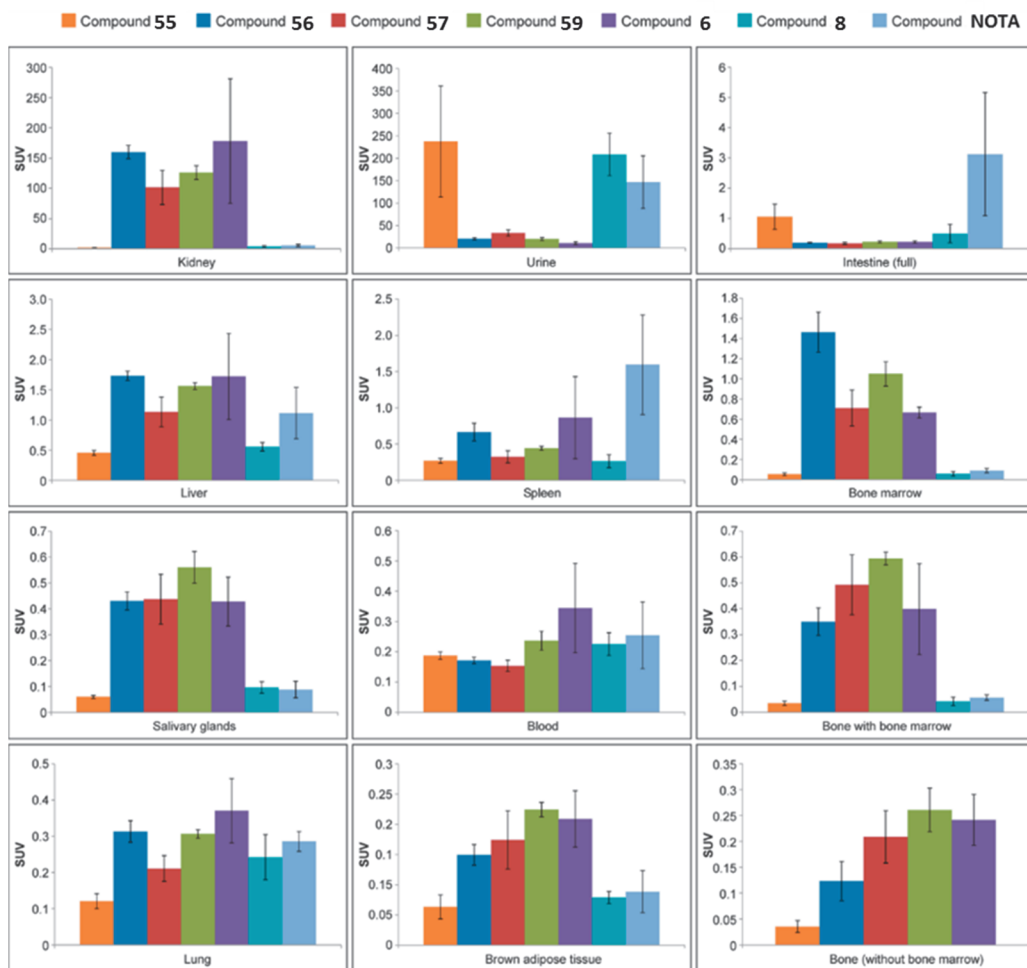
Figure 25. Radioactivity concentration at 60 min after intravenous injection of ^{68}Ga-conjugates **55-59, 8, 6** and **NOTA** as measured *ex vivo* by gamma counting of excised tissues of healthy rats. Results are expressed as standardized uptake value (SUV, mean ± SD).
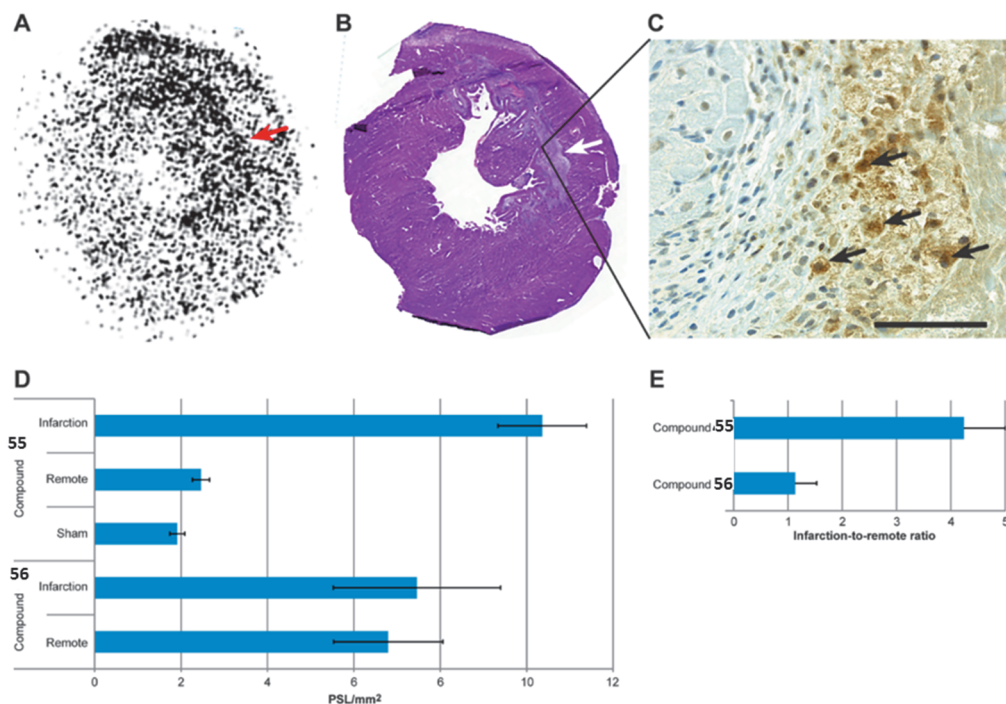
Figure 26. **55** (^{68}Ga-NOTA-HA-T$_6$) and **56** (^{68}Ga-NOTA-HA-hexasaccharide-anti-miR-15b) in rat myocardial infarction. A) Autoradiograph showing focally increased uptake of ^{68}Ga-NOTA-HA-T$_6$ in the anterolateral wall (arrow) of the left ventricle at 7 days after coronary occlusion and B) the same section stained with hematoxylin-eosin that shows an infarcted area in the anterolateral wall (arrow). C) High magnification photomicrograph of immunohistochemical staining shows CD44 positive cells (arrows) in the infarcted area (scale bar 50 μm). Radioactivity concentration expressed as D) photostimulated luminescence per square millimeter (PSL/mm2) and E) infarction-to-remote ratio in myocardial autoradiographs shows higher **55** (^{68}Ga-NOTA-HA-T$_6$) uptake in the infarcted than in the remote non-infarcted area or in the myocardium of sham-operated rats.

Table 6. *Ex vivo* bio-distribution of **55** and **56** at 70 min after intravenous injection in rats studied at 7 days after myocardial infarction or in sham-operation, and in healthy controls

	Compound **55**			Compound **56**	
Tissue	MI (n = 2)	Sham (n = 2)	Healthy (n = 4)	MI (n = 4)	Healthy (n = 4)
Adrenal gland	0.10 ± 0.027	0.079 ± 0.018	0.071 ± 0.011	0.18 ± 0.013	0.17 ± 0.0063
BAT	0.086 ± 0.0018	0.058 ± 0.0072	0.063 ± 0.020	0.20 ± 0.040	0.15 ± 0.017
Blood	0.23 ± 0.023	0.19 ± 0.0027	0.19 ± 0.012	0.30 ± 0.053	0.17 ± 0.011
Blood cells	0.18 ± 0.042	0.17 ± 0.012	0.14 ± 0.012	0.24 ± 0.058	0.090 ± 0.031
Bone	0.055 ± 0.0075	0.051 ± 0.0012	0.035 ± 0.0082	0.56 ± 0.075	0.35 ± 0.053
Bone marrow	0.043 ± 0.037	0.069 ± 0.0075	0.053 ± 0.014	1.2 ± 0.30	1.5 ± 0.20
Bone[wbm]	0.043 ± 0.0035	0.032 ± 0.0014	0.032 ± 0.011	0.40 ± 0.14	0.12 ± 0.038
Brain	0.013 ± 0.0024	0.014 ± 0.0047	0.0092 ± 0.00099	0.014 ± 0.0079	0.011 ± 0.0074
Heart left ventricle	0.18 ± 0.0031	0.10 ± 0.0088	0.040 ± 0.0068	0.25 ± 0.015	0.16 ± 0.011
Intestine (empty)	0.47 ± 0.12	0.32 ± 0.13	0.46 ± 0.22	0.30 ± 0.065	0.37 ± 0.051
Intestine (full)	1.5 ± 1.2	0.42 ± 0.47	1.1 ± 0.42	0.35 ± 0.18	0.20 ± 0.011
Kidney	3.0 ± 0.26	2.9 ± 0.77	1.9 ± 0.23	82 ± 2.4	160 ± 11
Liver	0.41 ± 0.0041	0.41 ± 0.078	0.46 ± 0.040	1.9 ± 0.26	1.7 ± 0.077
Lung	0.19 ± 0.0028	0.17 ± 0.0075	0.12 ± 0.020	0.34 ± 0.067	0.31 ± 0.030
Pancreas	0.080 ± 0.063	0.071 ± 0.0039	0.063 ± 0.018	0.35 ± 0.070	0.38 ± 0.051
Plasma	0.40 ± 0.070	0.36 ± 0.0078	0.31 ± 0.027	0.53 ± 0.12	0.37 ± 0.032
Salivary glands	0.083 ± 0.0062	0.071 ± 0.0035	0.060 ± 0.0059	0.48 ± 0.083	0.43 ± 0.035
Skeletal muscle	0.037 ± 0.0052	0.031 ± 0.0012	0.033 ± 0.011	0.085 ± 0.013	0.056 ± 0.0060
Skin	0.20 ± 0.0024	0.14 ± 0.0012	0.11 ± 0.0082	0.32 ± 0.028	0.34 ± 0.028
Spleen	0.29 ± 0.070	0.26 ± 0.069	0.27 ± 0.032	0.49 ± 0.085	0.66 ± 0.12
Urine	480 ± 130	260 ± 29	240 ± 120	32 ± 3.4	21 ± 2.3
WAT	0.048 ± 0.014	0.030 ± 0.0050	0.035 ± 0.031	0.099 ± 0.024	0.047 ± 0.013

MI: rat with myocardial infarction; Sham: sham-operated rat; BAT: brown adipose tissue; WAT: white adipose tissue; Bone[wbm]: bone without bone marrow. Results are expressed as standardized uptake values (mean ± SD with two significant figures).

3.8.3 PET studies of bisphosphonate conjugates

3.8.3.1   ^{68}Ga-labling of bisphosphonate-oligonucleotide conjugates

Surprisingly, initial attempts of ^{68}Ga labeling for the conjugate **66** and **67** were unsuccessful (as per obtained radio HPLC purity), most likely due to metal binding properties of alendronate moiety, beside NOTA ligand. Recently, Holub *et al*. reported that, presence of chelating BP moiety may lead to slower formation of Ga[III] complex with NOTA owing to the strong out-of-cage binding. [178] Therefore, double stranded ON ^{68}Ga labeling approach has been utilized, in which NOTA conjugate of anti-miR-21 **7** was first subjected to ^{68}Ga-chelation and later alendronate attached to complementary strand *i.e*. miR-21 sequence, allowed to form ^{68}Ga–labeled ON duplex **69** and **7** (figure **27A**). Thermal stability of the double helix was determined, by UV-melting profile analysis, $T_m = 88$ºC, **7**[[69/71]Ga] and **69**, 0.2 M NaOAc and 0.05 M NaCl as a mimics for ^{68}Ga-labelling conditions (Fig. **27A**). Radio-HPLC chromatograms of **7**[^{68}Ga] are depicted in figure **27B**.
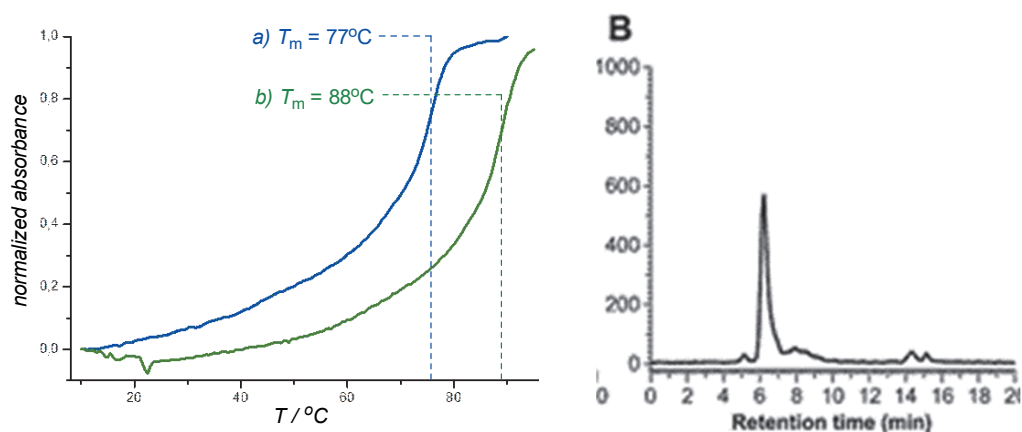
Figure 27. A) UV-melting profiles of **7/69**–double helix. Conditions: *a)* 2 µM of **69** in 10 mM sodium cacodylate and 0.1 M NaCl (pH 7.0), *b)* 2 µM of **7**[[69/71]Ga] and **69**, 0.2 M NaOAc and 0.05 M NaCl (the ^{68}Ga-labelling conditions mimicked). B) Radio–HPLC chromatograms of **7**[^{68}Ga] + **69**.

3.8.3.2   Whole-body bio-distribution kinetics of bisphosphonate conjugates in healthy rats

Targeting of bone tissues with ^{68}Ga-labeled ON duplex bearing BP moiety was demonstrated with *in vivo* PET imaging followed by bio-distribution kinetics in healthy rats. ^{68}Ga-labeled ON duplex **69/7** showed increased uptake in knees (Fig. **28**). Comprehensive ex-vivo measurements exhibited, 40% increased bone accumulation of ^{68}Ga-labeled ON duplex **69/7**, bone marrow radioactivity accumulation was increased for **7** [^{68}Ga] alone. Single stranded **7**[^{68}Ga] exhibited higher uptake in kidneys, liver,

spleen, salivary glands, pancreas, lungs, heart and skin, as compared to uptakes of ^{68}Ga-labeled ON duplex **69/7** (Fig. **29**). Moreover, radioactivity concentration in plasma was decreased and activity in urine was increased for ^{68}Ga-labeled ON duplex **69/7** (Fig. **30**). The stability of ON duplex **69/7** during circulation was verified by adding excess, 2 or 4 equivalents of non-labeled complementary strand bearing BP moiety. Use of excess of **69**, in order to make sure intact hybridization, did not exhibited difference in distribution kinetics as seen in detailed statistical analysis Table **7**.
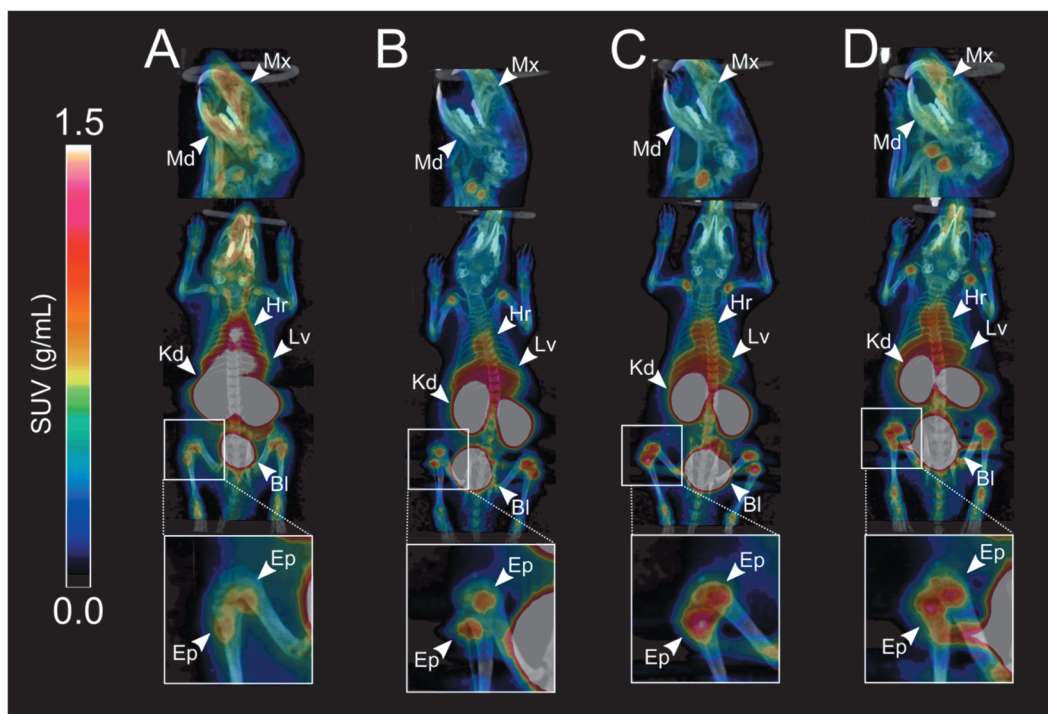
Figure 28. PET/CT images of healthy rats intravenously injected with ^{68}Ga-ONs. Images are summation from 0-60 min post-injection and presented in the same color scale. A) **7**[^{68}Ga] alone, B) **7**[^{68}Ga] + **69** one equivalent C) **7**[^{68}Ga] + **69** two equivalents and D) **7**[^{68}Ga] + **69** four equivalents. SUV = standardized uptake value; Mx = maxilla bone; Md = mandible bone; Hr = heart; Lv = liver; Kd = kidney; Bl = urinary bladder; Ep = epiphysis bone.
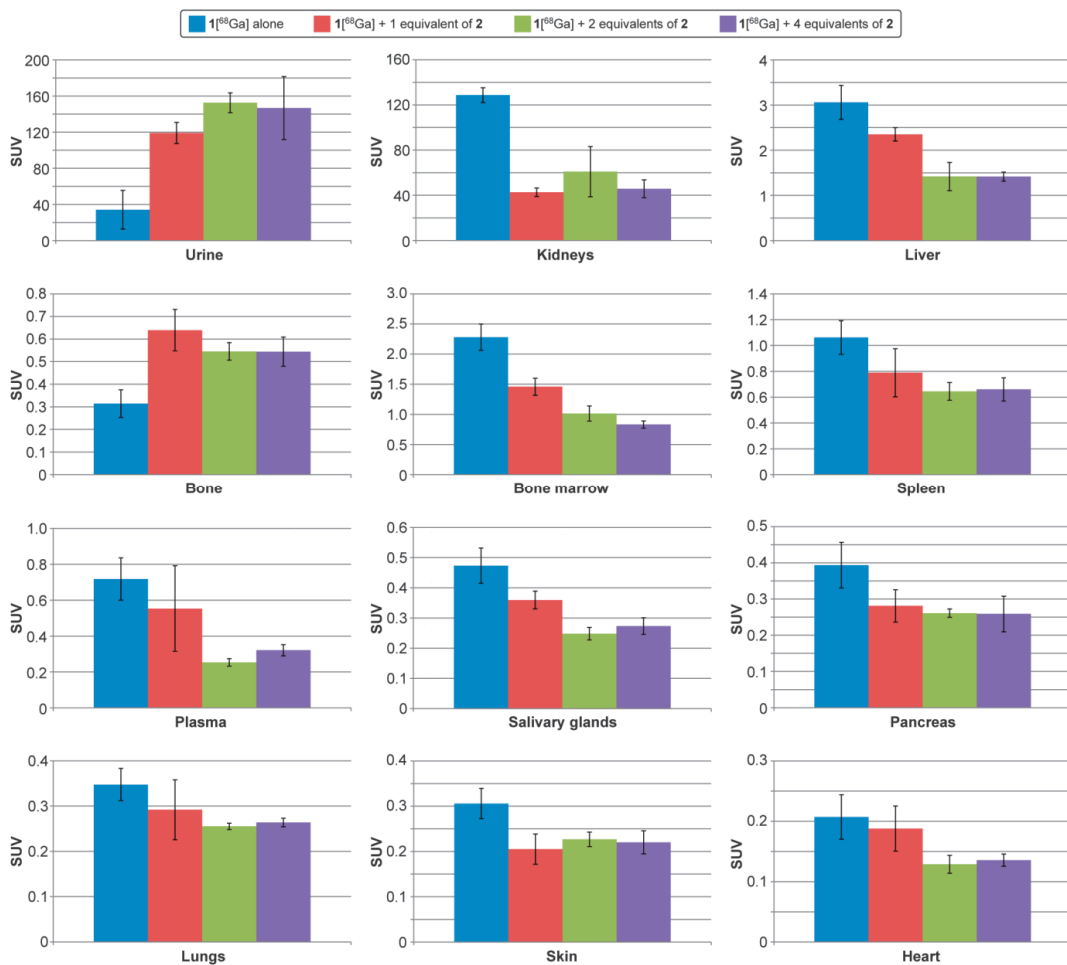
Figure 29. Radioactivity concentration at 60 min after intravenous injection of ^{68}Ga-labelled ONs as measured *ex vivo* by gamma counting of excised tissues of healthy rats. SUV, standardized uptake value. Error bars denote standard deviation (n = 4).

Figure 30. Radioactivity concentration as a function of time (time-activity curves) of the distribution kinetics of ^{68}Ga-labeled ONs: SUV, standardized uptake value. Error bars denote standard deviation (n = 4).

Table 7. *Ex vivo* bio-distribution of ^{68}Ga-labelled ONs in healthy rats at 60 min after intravenous injection.

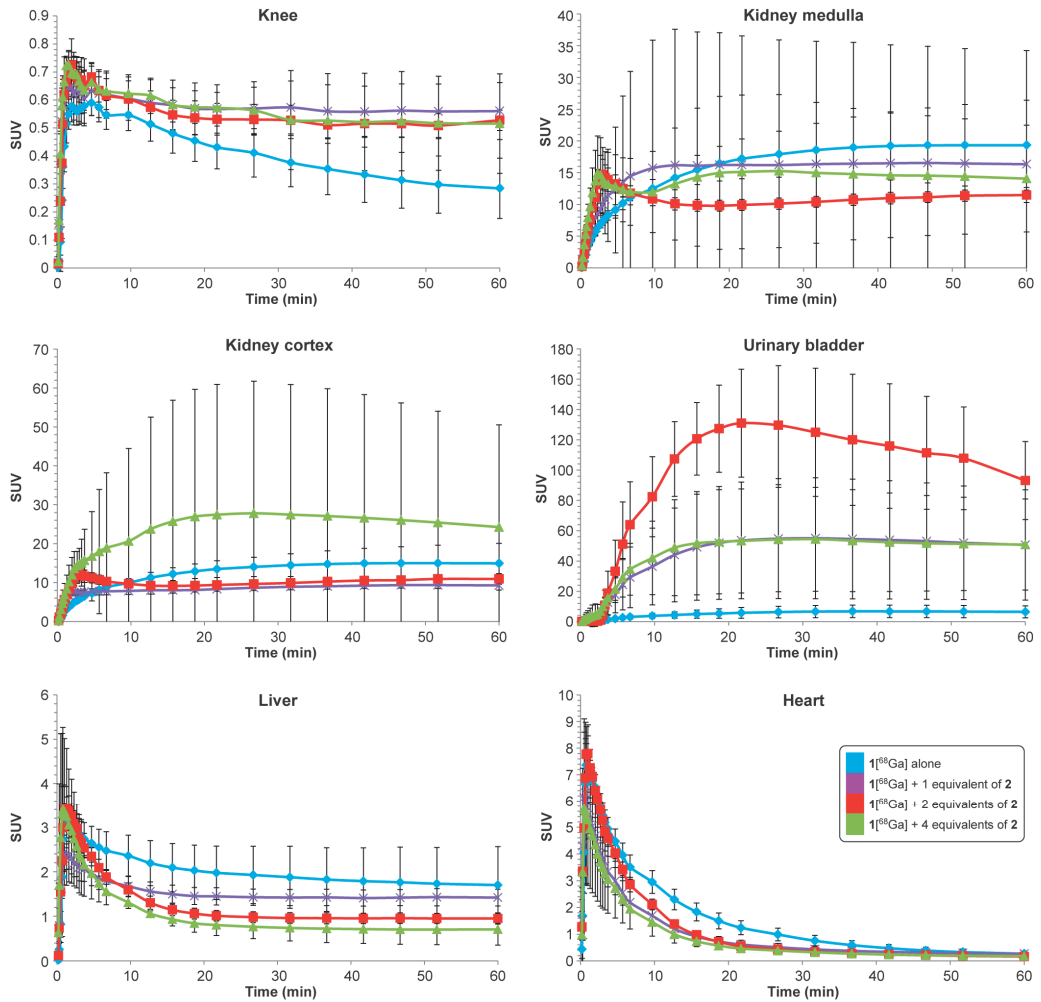| Tissue	A	B	C	D	P value A vs. B	P value A vs. C	P value A vs. D	P value B vs. C	P value B vs. D	P value C vs. D
Adrenal gland	0.22 ± 0.14	0.23 ± 0.038	0.15 ± 0.018	0.17 ± 0.038	0.95	0.37	0.47	0.012	0.063	0.55
BAT	0.13 ± 0.083	0.15 ± 0.039	0.12 ± 0.0030	0.11 ± 0.019	0.31	0.027	0.097	0.12	0.098	0.46
Blood	0.32 ± 0.097	0.34 ± 0.13	0.14 ± 0.0061	0.18 ± 0.022	0.80	0.012	0.035	0.023	0.051	0.017
Blood cells	0.18 ± 0.13	0.23 ± 0.072	0.11 ± 0.013	0.13 ± 0.017	0.55	0.33	0.53	0.018	0.045	0.057
Bone marrow	2.3 ± 0.22	1.5 ± 0.14	1.0 ± 0.13	0.83 ± 0.059	0.0007 2	0.000 055	0.0000 14	0.003 2	0.000 18	0.039
Bone*	0.31 ± 0.061	0.64 ± 0.092	0.55 ± 0.039	0.54 ± 0.065	0.0011	0.000 70	0.0021	0.11	0.14	0.98
Brain	0.018 ± 0.0045	0.015 ± 0.0047	0.010 ± 0.0056	0.0087 ±0.000 84	0.35	0.070	0.0057	0.26	0.039	0.56
Heart	0.21 ± 0.037	0.19 ± 0.037	0.13 ± 0.015	0.14 ± 0.010	0.49	0.007 6	0.0096	0.026	0.035	0.48
Intestine (empty)	0.33 ± 0.026	0.30 ± 0.057	0.24 ± 0.041	0.26 ± 0.046	0.43	0.011	0.059	0.12	0.37	0.41
Intestine (full)	0.22 ± 0.035	0.20 ± 0.050	0.19 ± 0.069	0.16 ± 0.023	0.55	0.47	0.025	0.81	0.17	0.41
Kidney	130 ± 6.5	43 ± 3.7	61 ± 22	46 ± 7.9	0.0000 0045	0.001 1	0.0000 036	0.16	0.52	0.24
Liver	3.1 ± 0.38	2.4 ± 0.15	1.4 ± 0.31	1.4 ± 0.10	0.013	0.000 53	0.0001 5	0.001 7	0.000 046	0.98
Lung	0.35 ± 0.036	0.29 ± 0.066	0.26 ± 0.070	0.26 ± 0.095	0.19	0.002 3	0.0040	0.31	0.43	0.20
Pancreas	0.39 ± 0.063	0.28 ± 0.045	0.26 ± 0.012	0.26 ± 0.049	0.027	0.006 0	0.015	0.41	0.53	0.94
Plasma	0.72 ± 0.12	0.55 ± 0.24	0.25 ± 0.021	0.32 ± 0.031	0.26	0.000 24	0.0006 3	0.046	0.11	0.011
Salivary glands	0.47 ± 0.058	0.36 ± 0.029	0.25 ± 0.021	0.27 ± 0.027	0.013	0.000 33	0.0008 0	0.000 77	0.005 0	0.19
Skeletal muscle	0.061 ± 0.028	0.057 ± 0.015	0.046 ± 0.0033	0.048 ± 0.0031	0.81	0.34	0.39	0.21	0.27	0.53
Skin	0.31 ± 0.034	0.21 ± 0.034	0.23 ± 0.016	0.22 ± 0.025	0.0054	0.005 4	0.0066	0.29	0.50	0.67
Spleen	1.1 ± 0.13	0.79 ± 0.19	0.64 ± 0.069	0.66 ± 0.090	0.053	0.001 3	0.0023	0.20	0.26	0.79
Urine	34 ± 22	120 ± 12	150 ± 11	150 ± 35	0.0004 4	0.000 064	0.0015	0.29	0.19	0.76
WAT	0.043 ± 0.0024	0.047 ± 0.0083	0.042 ± 0.011	0.037 ± 0.0070	0.35	0.87	0.19	0.46	0.12	0.50

Results are expressed as standardized uptake values (mean ± SD, n = 4) and P values of Student's t test, with 2 significant figures. **A** = **1**[^{68}Ga] alone; **B** = **1**[^{68}Ga] + 1 equivalent of **2**; **C** = **1**[^{68}Ga] + 2 equivalents of **2**; **D** = **1**[^{68}Ga] + 4 equivalents of **2**; BAT, brown adipose tissue; WAT, white adipose tissue, * without bone marrow.

3.8.4 ^{64}Cu labeling and in vitro receptor affinity of hyaluronic acid-PyCPP conjugate

^{64}Cu in the form of [^{64}Cu]CuCl$_2$ was produced via the ^{64}Ni(p,n)64Cu nuclear reaction, as previously described.[179] An efficient ^{64}Cu labeling of HA-PyCPP conjugate **85** was demonstrated (Fig. **31**) in NH$_4^+$AcO$^-$ buffer at 60 °C for 20−30 min, without use of any stabilizing agents (e.g., ascorbic acid, ethanol). Vortex mixing in 1-octanol/water: logP (15[^{64}Cu] =−1.73±0.11) gave the lipophilicity of the ^{64}Cu labeling of HA-PyCPP conjugate. HA hexamer is the natural ligand for CD44 receptors, expressed on cancer cells including MDA-MB-231 and MCF-7 breast cancer.[180] In vitro receptor affinity studies (Table **8**) showed low radio localization in these tumor cells. It was observed that about only 10% radioactivity was seemed to be bound or internalized after 30 min. incubation with MDA-MB-231 cells.
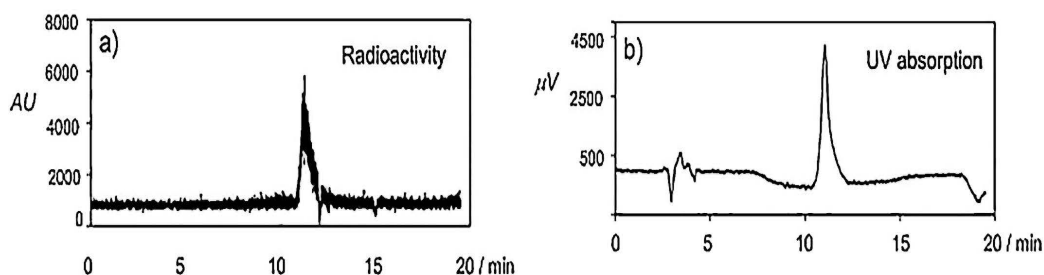
Figure 31. Conditions: (i) ^{64}CuCl$_2$, aq. 0.5 mol L^{-1} NH$_4$OAc. (pH 5.5), 30 min at 60 °C. RP HPLC chromatograms (a) radio- and (b) UV-detector, λ = 400 nm, respectively.

Table 8: Cell binding evaluation of ^{64}Cu-labeled PyCPP–HA conjugate (85[^{64}Cu]) with MDA-MB-231 and MCF-7 tumor cell lines.

Competitor (nM)	MDA-MB-231			MCF-7
	30 min (n = 3)	60 min (n = 2)	120 min (n = 2)	60 min (n = 2)
0	10.4 ± 0.3	9.3 ± 0.9	10.4 ± 0.5	10.5 ± 0.6
2	9.9 ± 1.0	8.7 ± 0.3	9.9 ± 0.3	9.6 ± 0.7
20	9.6 ± 0.8	8.6 ± 0.2	8.7 ± 0.3	9.5 ± 0.3
200	8.0 ± 0.6	7.0 ± 0.1	6.6 ± 0.2	7.9 ± 1.0

Receptor binding properties of **15**[^{64}Cu] was determined from *in vitro* incubation experiments with two tumor cell lines in the presence of increasing concentration of unlabeled PyCPP-HA conjugate (**15**) as the competitor. Values are expressed as ratio (%) of cell-bound radioactivity to the applied total radioactivity (mean ± SD).

4. SUMMARY

Galactose-ON conjugates comprising 5'-terminus modification with seven, three or one Gal units have been attached to the 3'-NOTA modified anti-miR-15b sequence via on-support oximation approach. NOTA-CPG support was used for assembly of ON sequence by standard phosphoramidite chemistry. Liver hepatocytes targeting of the galactose–anti-miR-15b cluster conjugates (**22**, **19** and **16**) was demonstrated by an *in vivo* PET imaging in healthy rats. Synthesized conjugates has been efficiently radiolabeled with ^{68}Ga and their whole body bio-distribution kinetics was studied by PET techniques. The galactose unit is the natural ligand for asialoglycoprotein (ASGPR) receptors, overexpressed on liver hepatocytes. Significance of glycocluster effect was successfully demonstrated,[68]Ga labeled conjugates bearing seven galactose-ON conjugate **22** showed remarkably higher activity, approximately 8 fold increase in liver activity as compared to one or none galactose-ON conjugate. Whereas tri Gal-ON cluster also showed 5 fold increment in liver radioactivity compared to one or none Gal-ON conjugate. Consistent with enhanced liver accumulation, the heptavalent Gal-ON cluster conjugate **22** showed low radioactivity in kidney. Urine activity was, however, increased as compared to other Gal-ON conjugates. In summary, significant increment was observed in the liver uptake of the Gal-ON conjugates (**22** > **19** > **16** ~ **6**), most likely due to glycocluster effect for targeting of ASGPR in liver. Importantly, this study provided a rational quantitative data for liver targeting of ON drugs, which has been monitored by PET technique, possibly guide for development of ON therapeutics. It is also worth noting that a substantial proportion of the ON was taken into the liver, although an unmodified phosphodiester backbone was used.

Hyaluronic acid oligosaccharides has been efficiently conjugated to 5'-terminus of the ON conjugates, *e.g*. HA-hexamer-T6 **55**, HA-hexamer-anti-miR-15b **56**, and HA-tetramer-anti-miR-15b **57**. Synthesis of HA hexamer has been achieved from appropriately protected HA disaccharides units via trichloroacetimidate activated glycosylation method, and TMSOTf as a glycosylation activator. A copper free click, strain promoted azide alkyne cycloaddition (SPAAC) conjugation approach has been demonstrated with partially protected azide functionalized HA oligomers with 5'-strained cyclooctyne modified anti-miR-15b sequence, bearing 3'-NOTA ligand. The critical deprotections of oligosaccharides including removal of trichloroacetyl amide functions was carried out by concentrated ammonia treatment. Synthesized HA-ONs conjugate have been subjected to efficient radiolabeling with [68]Ga. The PET imaging in healthy rats exhibited whole body bio-distribution kinetics, radioactivity distribution was varied with ON parts (anti-miR-15b and T6) along with sugar groups (e.g. HA hexamer, HA tetramer, Maltohexaose, and without sugar unit).

In general, higher radioactivity was observed in kidney, bone marrow, salivary gland, and liver for anti-miR-15b conjugates, as compared to conjugates of T6. Among these ^{68}Ga labeled conjugates, HA-hexamer-T6 **55** and HA-hexamer-anti-miR-15b **56** were demonstrated in rat disease model, myocardial infarction (CD44 positive cells). It was found that, HA hexamer mediated uptake of the conjugates **55** and **56** into CD44 cells, in the infarcted myocardium as compared with the remote non-infarcted areas and myocardium of sham-operated rats. The conjugate HA-hexamer-T6 **55** showed infarction-to remote ratio 4.2 ± 0.75 (P = 0.008). Surprisingly, the conjugate HA-hexamer-anti-miR-15b **56** showed only 1.1 ± 0.4 (P = 0.016). In general, HA conjugates of T6 sequence verified the HA-CD44 interactions/binding. This study requires further detailed evaluation of ON structure, *i.e.* backbone modifications, length and sequence.

Bone targeting PET labeled bisphosphonate-ON conjugates has been employed in this study. Alendronate azide derivative was prepared via copper free, diazo-transfer reaction. Similar to previous conjugation approach, synthesized azide derivative of alendronate was subjected to SPAAC conjugation with cyclooctyne modified anti-miR-21 sequence. However, the presence of both moieties, 5'-alendronate and 3'-NOTA on a single stranded ON chain, turned out to be challenging for ^{68}Ga radiolabeling. Hence, double stranded ONs strategy, in which a complementary sequence, bearing 5'-alendronate modified miR-21, was hybridized with anti-miR-21 containing 3'-NOTA ligand. Interestingly, duplex of conjugate **69** with **7** exhibited, approximately ca. 40% (SUV) increased radioactivity accumulations in knee monitored by PET/CT imaging and measured *ex vivo* experiments in rats.

Solid supported porphyrins were utilized for synthesis of potential bioconjugates such as, porphyrin conjugates with ONs, and glycodendrimers. In this study, porphyrins (HPPH and PyCPP), applicable photosensitizers were efficiently coupled on (LCAA-CPG) support and synthesis of porphyrin conjugates with various oligomeric biomolecules was demonstrated using standard automated phosphoramidite coupling chemistry. In addition, ^{64}Cu radiolabeling of porphyrin conjugates, HA−porphyrin **85** was also verified and also their affinity was demonstrated in CD44-expressing cancer cells.

5.   EXPERIMENTAL

5.1   General

The syntheses of building blocks and ON conjugates are described in the original publications. Synthesized novel compounds were characterized by ^{1}H NMR, ^{13}C NMR, (400 and 500 MHz) and ESI-MS methods when applicable. The ON sequences were prepared on an Applied Biosystems 392 DNA synthesizer as per standard oligo's assembly protocol. Oligo conjugates were analyzed by RP-HPLC, a Thermo ODS Hypersil C18 (150 × 4.6 mm, 5 μm) analytical column and a Phenomenex Oligo-RP C18 (250 × 10 mm, 5 μm) semi-preparative column, gradient elution from 0% to 40% MeCN in aqueous 0.1 mol L^{-1} Et$_3$NH$^+$ AcO$^-$. The flow rates 1.0 mL min^{-1} for analytical column and 3.0 mL min^{-1} for semi-preparative column were used at detection wavelength 260 nm.

5.2   PET labeling

The ^{68}Ga labeling protocols for ON conjugates are also described in the original publications. ^{68}Ga was achieved as a [^{68}Ga]Cl$_3$ from the ^{68}Ge/^{68}Ga generator (Eckert & Ziegler, Valencia, California, USA). The radiochemical purity of ^{68}Ga-labeled ON conjugates were determined by a reversed phase high performance liquid chromatography coupled with an online radioactivity detector (radio-HPLC) on a μBondapak C18 column (3.9 × 150 mm, 125 Å, 10 μm; Waters, Ireland).

5.3   Distribution kinetics

Whole-body distribution kinetics was assessed over a 60 min dynamic PET imaging (High Resolution Research Tomograph, Siemens Medical Systems, Knoxville, TN, USA). The uptake was reported as a standardized uptake value (SUV), calculated as the radioactivity concentration of the ROI normalized with the injected radioactivity dose and animal weight., The radioactivity concentration of various tissue samples was measured ex vivo by gamma counter (1480 Wizard 3″, PerkinElmer/Wallac, Turku, Finland), instantly afterward PET imaging.

6. REFERENCES

1. Cech, T. R., Zaug, A. J., Grabowski, P. J. Cell 1981, 27, 487-496.

2. Guerrier-Takada, C., Gardiner, K., Marsh, T., Pace, N., Altman, S. Cell 1983, 35, 849-857.

3. Groβhans, H., Filipowicz, W. Nature 2008, 451, 414-416.

4. Mattick, J. S. PLoS Genet. 2009, 5, e1000459.

5. Serganov, A., Dinshaw, P. J. Nat. Rev. Genetics 2007, 8, 776-790.

6. Esteller, M. Nature Rev. Genet. 2011, 12, 861-874.

7. Elbashir, S. M., Harborth J., Lendeckel, W., Yalcin, A., Weber, K., Tuschl, T. Nature 2001, 411, 494–498.

8. Hannon, G. J., Rossi, J. J. Nature 2004, 431, 371–378.

9. Kim, V. N. Genes Dev. 2006, 20, 1993–1997.

10. Zamecnik, P. C., Stephenson, M. L. Proc. Natl. AcAD. Sci. U.S.A. 1978, 75, 1, 280–284.

11. Uhlmann, E.; Peyman, A. Chem. Rev. 1990, 90, 543–584.

12. Kole, R., Krainer, A. R., Altman, S. Nature Rev. Drug Discov. 2012, 11, 125–140.

13. Juliano, R. L., Ming, X., Nakagawa, O. Acc. Chem. Res. 2012, 45, 1067–1076.

14. Uhlmann, E., Peyman, A. Chem. Rev. 1990, 90, 543-584.

15. Crook, S. T., Vickers, T., Lima, W. F., Wu, H. Antisense Drug Technology: Principles, Strategies, and Applications, 2nd ed.CRC Press, Boca Raton, 2007, 3-46.

16. Bennett, C. F., Swayze, E. E., Annu. Rev. Pharmacol. Toxicol. 2010, 50, 259-293.

17. Crook, S. T. Drug Discov Today Ther Strateg. 2013, 10, e110-e117.

18. Cerritelli, S. M., Crouch, R. J. FEBS J. 2009, 276, 1494-1505.

19. Ozsolak, F. & Milos, P. M. Nature Rev. Genet. 2011, 12, 87–98.

20. Fire, A., Xu, S., Montgomery, M. K., Kostas, S. A., Driver, S. E., Mello, C. C. Nature 1998, 391, 806–811.

21. de Fougerolles, A., Vornlocher, H. P., Maraganore, J., Lieberman, J. Nature Rev. Drug Discov. 2007, 6, 443-453.

22. Thum, T., Gross, C., Fiedler, J., Fischer, T., Kissler, S., Bussen, M., Galuppo, P., Just, S., Rottbauer, W., Frantz, S., Castoldi, M., Soutschek, J., Koteliansky, V., Rosenwald, A., Basson, M. A., Licht, J. D., Pena, J. T. Rouhanifard, S. H., Muckenthaler, M. U., Tuschl, T., Martin, G. R., Bauersachs, J., Engelhardt, S. Nature 2008, 456, 980–984.

23. Haramati, S., Chapnik, E., Sztainberg, Y., Eilam, R., Zwang, R., Gershoni, N., McGlinn, E., Heiser, P.W., Wills, A. M., Wirguin, I., Rubin, L.L., Misawa, H., Tabin, C. J., Brown, R. Jr., Chen, A., Hornstein, E. Proc Natl Acad Sci USA 2010, 107, 3111–13116.

24. Garzon, R., Marcucci, G., Croce, C. M. Nat Rev Drug Discov 2010, 9, 775–789.

25. Lanford, R. E., Hildebrandt-Eriksen, E. S., Petri, A., Persson, R., Lindow, M., Munk, M. E. Kauppinen S, Ørum H. Science 2010, 327, 198–201.

26. Arenz, C. Angew. Chem. Int. Ed. 2006, 45, 5048.

27. Schratt, G. Nat. Rev. Neurosci. 2009, 10, 842-849.

28. Eckstein, F. Nucleic Acid Ther. 2014, 24, 374-387.

29. Behlke, M. A. Oligonucleotides, 2008, 18, 305-320.

30. Hall, A. H. S., Wan, J., Shaughnessy, E. E., Shaw, B. R., Alexander, K. A. Nucleic Acids Res. 2004, 32, 5991-6000.

31. Nielsen, P. E. Chem. Biodiversity 2010, 7, 786-804.

32. Summerton, J. Biochim. Biophys. Acta 1999, 1489, 141-158.

33. Summerton, J., Weller, D. Antisense Nucleic Acid Drug Dev. 1997, 7, 187-195.

34. Damidov, V. V., Potaman, V. N., Frank-Kamenetskii, M. D. Egholm, M., Buchard, O., Sönnichsen, S. H., Nielsen, P. E. Biochem. Pharmacol.1994, 48, 1310-1313.

35. Rettig, G. R., Behlke, M. A. Mol. Ther. 2012, 20, 483-512.

36. Manoharan, M. Biochim. Biophys. Acta 1999, 1489, 117-130.

37. Gore, K. R., Nawale, G. N., Harikrishna, S., Chittoor, V. G., Pandey, S. K., Hö-bartner, C., Patankar, S., Pradeepkumar, P. I. J. Org. Chem. 2012, 77, 3233, 3245.

38. Leydier, C., Bellon, L., Barascut, J. L., Morvan, F., Rayner, B., Imbach, J. L. Antisense Res. Dev. 1995, 5, 167-174.

39. Kalota, A., Karabon, L., Swider, C. R., Viazovkina, E., Elzagheid, M., Damha, M. J., Gewirtz, A. M. Nucleic Acids Res. 2006, 34, 451-461.

40. Wahlestedt, C., Salmi, P., Good, L., Kela, J., Johnsson, T., Hökfelt, T., Broberger, C., Porreca, F., Lai, J., Ren, K. Proc. Natl. Acad. Sci. USA 2000, 97, 5633-5638.

41. Verbeure, B., Lescrinier, E., Wang, J., Herdewijn, P., Nucleic Acids Res. 2001, 29, 4941-4947.

42. Sabatino, D., Damha, M. J. J. Am. Chem. Soc. 2007, 129, 8259-8270.

43. Cerritelli, S. M., Crouch, R. J. FEBS J. 2009, 276, 1494-1505.

44. Majlessi, M., Nelson, N. C., Becker, M. M. Nucleic Acids Res.1998, 26, 2224-2229.

45. Kawasaki, A. M., Casper, M. D., Freier, S. M., Lesnik, E. A., Zounes, M. C., Cummins, L. L., Gonzalez, C., Cook, P. D. J. Med. Chem. 1993, 36, 831-841.

46. Damha, M., Wilds, C., Noronha, A., Brukner, I., Borkow, G., Arion, D., Parniak, M. J. Am. Chem. Soc. 1998, 120, 12976-12977.

47. Koshkin, A., Singh, S., Nielsen, P., Rajwanshi, V., Kumar, R., Meldgaard, M., Olsen, C. E., Wengel, J. Tetrahedron 1998, 54, 3607-3630.

48. Obika, S., Nanbu, D., Hari, Y., Andoh, J., Morio, K., Doi, T., Imanishi, T. Tetrahedron Lett. 1998, 39, 5401- 5404.

49. Campbell, M. A., Wengel, J. Chem. Soc. Rev. 2011, 40, 5680-5689.

50. Seth, P. P., Vasquez, G., Allerson, C. A., Berdeja, A., Gaus, H., Kinberger, G. A., Prakash,T. P., Migawa, M. T., Bhat, B., Swayze, E. E. J. Org. Chem. 2010, 75, 1569-1581.

51. Srivastava, P.; Barman, J.; Pathmasiri, W.; Plashkevych, O.; Wenska, M.; Chattopadhyaya, J. J. Am. Chem. Soc. 2007, 129, 8362-8379.

52. Prakash, T.P., Siwkowski, A., Allerson, C.R., Migawa, M.T., Lee, S., Gaus, H.J., Black, C., Seth, P.P., Swayze, E.E., and Bhat, B. J. Med. Chem. 2010, 53, 1636-1650.

53. Marquez, V.E., Siddiqui, M.A., Ezzitouni, A., Russ, P., Wang, J., Wagner, R.W., Matteucci, M.D. J. Med. Chem. 1996, 39, 3739-3747.

54. Renneberg, D., Bouliong, E., Reber, U., Schü̈mperli, D., Leumann, C.J. Nucleic Acids Res. 2002, 30, 2751¬-2757

55. Wang, J., Verbeure, B., Luyten, I., Lescrinier, E., Froeyen, M., Hendrix, C. Rosemeyer, H., Seela, F., Van Aerschot, A., Herdewijn, P. J. Am. Chem. Soc. 2000, 122, 8595-8602.

56. Fisher, M., Abramov, M., Van Aerschot, A., Rozenski, J., Dixit, V., Juliano, R.L., Herdewijn, P. Eur. J. Pharmacol. 2009, 606, 38-44.

57. Yu, R. Z., Grundy, J. S., Geary, R. S. Expert Opin. Drug Metab. Toxicol. 2013, 9, 169-182.

58. Geary, R. S., Norris, D., Yu, R., Bennett, C. F. Adv. Drug Deliv. Rev. 2015, 87, 46–51.

59. R.S. Geary, Expert Opin Drug Metab Toxicol. 2009, 5, 381–391.

60. Manoharan, M. Antisense Nucleic Acid Drug Dev. 2002, 12, 103-128.

61. Juliano, R. L., Carver, K. Adv. Drug Deliv. Rev. 2015, 87, 35–45.

62. Lee, H., Lytton-Jean, A. K. R., Chen, Y., Love, K. T., Park, A. I., Karagiannis, E. D., Sehgal, A., Querbes, W., Zurenko, C. S., Jayaraman, M., Peng, C. G., Charisse, K., Borodovsky, A., M. Manoharan, M., Donahoe, J. S., Truelove, J. Nahrendorf, M., Langer, R., Anderson, D. G. Nat. Nanotechnol. 2012, 7, 389–393.

63. Vigderman, L., Zubarev, E. R. Adv. Drug Deliv. Rev. 2013, 65 663–676.

64. Tseng, Y. C., Mozumdar, S., Huang, L. Adv. Drug Delivery Rev. 2009, 61, 721–731.

65. Tamura, A.; Nagasaki, Y. Nanomedicine (London, U.K.) 2010, 5, 1089–1102.

66. Ming, X. Expert Opin. Drug Deliv. 2011, 8, 435–449.

67. Ming, X., Laing, B. Adv. Drug Deliv. Rev. 2015, 87, 81–89.

68. Marlin, F., Simon, P., Saison-Behmoaras, T., Giovannangeli, C. ChemBioChem 2010, 11, 1493-1500.

69. Alam, M. R., Dixit, V., Kang, H., Li, Z. B., Chen, X., Trejo, J., Fisher, M., Juliano, R. L. Nucleic Acids Res. 2008, 36, 2764–2776.

70. Czauderna, F., Fechtner, M. Dames, S., Aygun, H., Klippel, A., Pronk, G. J., Giese, K., Kaufmann, J. Nucleic Acids Res. 2003, 31, 2705–2716.

71. Winkler, J. Ther. Deliv. 2013, 4, 791–809.

72. Jeong, J. H., Mok, H., Oh, Y.-K., Park, T. G., Bioconjugate Chem. 2009, 20, 5-14.

73. Soutschek, J., Akinc, A., Bramlage, B., Charisse, K., Constien, R., Donoghue, M., Elbashir, S., Geick, A., Hadwiger, P., Harborth, J., John, M., Kesavan, V., Lavine, G., Pandey, R. K., Racie, T., Rajeev, K. G., Röhl, I., Toudjarska, I., Wang, G., Wuschko, S., Bumcrot, D., Koteliansky, V., Limmer, S., Manoharan, M., Vornlocher, H.-P. Nature, 2004, 432, 173-178.

74. Lorenz, C., Hadwiger, P., John, M., Vornlocher, H.-P., Unverzagt, C. Bioorg. Med. Chem. Lett. 2004, 14, 4975-4977.

75. Wolfrum, C., Shi, S., Jayaprakash, K. N., Jayaraman, M., Wang, G., Pandey, R. K., Rajeev, K. G., Nakayama, T., Charrise, K., Ndungo, E. M., Zimmermann, T., Koteliansky, V., Manoharan, M., Stoffel, M. Nat.Biotechnol. 2007, 25, 1149-1157.

76. DiFiglia, M., Sena-Esteves, M., Chase, K., Sapp, E., Pfister, E., Sass, M., Yoder, J., Reeves, P., Pandey,

R. K., Rajeev, K. G., Manoharan, M., Sah, D. W. Y., Zamore, P. D., Aronin, N. Proc. Natl. Acad. Sci. U. S. A., 2007, 104, 17204–17209.

77. Chen, Q., Butler, D., Querbes, W., Pandey, R. K., Ge, P., Maier, M. A., Zhang, L., Rajeev, K. G., Nechev, L., Kotelianski, V., Manoharan, M., Sah, D. W. Y. J. Controlled Release, 2010, 144, 227-232.

78. Krutzfeldt, J., Rajewsky, N., Braich, R., Rajeev, K. G., Tuschl, T., Manoharan, M., Stoffel, M. Nature, 2005, 438, 685-689.

79. Ma, L., Reinhardt, F., Pan, E., Soutschek, J., Bhat, B., Marcusson, E. G., Teruya-Feldstein, J., Bell, G.W., Weinberg, R. A. Nat. Biotechnol., 2010, 28, 341-347.

80. Godeau, G., Staedel, C., Barthelemy, P. J. Med. Chem. 2008, 51, 4374–4376.

81. Gryaznov, S. M. Chem. Biodiversity, 2010, 7, 477.

82. Nishina, K., Unno, T., Uno, Y., Kubodera, T., Kanouchi, T., Mizusawa, H., Yokota, T. Mol. Ther. 2008, 16, 734-740.

83. Uno, Y., Piao, W., Miyata, K., Nishina, K., Mizusawa, H, Yokota, T. Hum. Gene Ther. 2011, 22, 711-719.

84. Sato, Y., Murase, K., Kato, J., Kobune, M., Sato, T., Kawano, Y., Takimoto, R., Takada, K., Miyanishi, K., Matsunaga, T., Takayama, T., Niitsu, Y. Nat. Biotechnol. 2008, 26, 431–442.

85. Nakagawa, O., Ming, X., Huang, L., Juliano, R. L. J. Am. Chem. Soc. 2010, 132, 8848–   8849.

86. Thomas, M., Kularatne, S. A., Qi, L., Kleindl, P., Leamon, C. P., Hansen, M. J., Low, P. S. Ann N Y Acad Sci. 2009, 1175, 32–39.

87. Dohmen, C., Frohlich, T., Lachelt, U., Rohl, I., Vornlocher, H. P., Hadwiger, P., Wagner, E., Mol. Ther. Nucleic Acids, 2012, 1 e7.

88. Willibald, J., Harder, J., Sparrer, K., Conzelmann, K. K., T. Carell, T. J. Am. Chem. Soc. 2012, 134, 12330–12333.

89. Brunner, K., Harder, J., Halbach, T., Willibald, J., Spada, F., Gnerlich, F., Sparrer, K., Beil, A., Mçckl, L., Bruchle, C., Conzelmann, K., Carell, T. Angew. Chem. Int. Ed. 2015, 54, 1946 –1949.

90. Boisguerin, P., Deshayes, S., Gait, M. J., O'Donovan, L., Godfrey, C., Betts, C. A., Wood, M., J. A., Lebleu, B. Adv. Drug Deliv. Rev. 2015, 87, 52–67.

91. Pooga, M., Soomets, U., Hallbrink, M., Valkana, A., Saar, K., Rezaei, K., Kahl, U., Hao, J-X., Xu, X-J., Wiesenfeld-Hallin, Z., Hokfelt, T., Bartfai, T., Langel, U. Nat. Biotechnol. 1998, 16, 857.

92. Pichavant, C., Aartsma-Rus, A., Clemens, P. R., Davies, K. E., Dickson, G., Takeda, S., Wilton, S. D.,Wolff, J. A., Wooddell, C. I., Xiao, X., Tremblay, J. P. Mol. Ther. 2011, 19, 830-840.

93. Wu, B., Moulton, H. M., Iversen, P. L., Jiang, J., Li, J., Li, J., Spurney, C. F., Sali, A., Guerron, A. D., Nagaraju, K., Doran, T., Lu, P., Xiao, X., Lu, Q. L. Proc. Natl. Acad. Sci. U.S.A, 2008, 105, 14814-14819.

94. Yin, H., Moulton, H. M., Betts, C., Seow, Y., Boutilier, J., Iverson, P. L., Wood, M. J. A. Hum. Mol. Gen. 2009, 18, 4405.

95. Yin, H., Saleh, A. F., Betts, C., Camelliti, P., Seow, Y., Ashraf, S., Arzumanov, A., Hammond, S., Merritt, T., Gait, M. J., Wood, M. J. A. Mol. Ther. 2011, 19, 1295-1303.

96. Alam, M. R., Ming, X., Fisher, M., Lackey, J. G., Rajeev, K. G., Manoharan, M., Juliano, R. L. Bioconjug. Chem. 2011, 22, 1673–1681.

97. Ming, X., Alam, M. R., Fisher, M., Yan, Y., Chen, X., Juliano, R. L. Nucleic Acids Res. 2010, 38, 6567–6576.

98. Keefe, A. D., Pai, S., Ellington, A. Nature Rev. Drug Discov. 2010, 9, 537-550.

99. Tan, W., Wang, H., Chen, Y., Zhang, X., Zhu, H., Yang, C., Yang, R., Liu, C. Trends Biotechnol. 2011, 29 634–640.

100. J.O. McNamara II, E.R. Andrechek, Y. Wang, K.D. Viles, R.E. Rempel, E. Gilboa, B.A. Sullenger, P.H. Giangrande, Nat. Biotechnol. 24 (2006) 1005–1015.

101. Dassie, J. P., Liu, X. Y., Thomas, G. S., Whitaker, R. M., Thiel, K. W., Stockdale, K. R., Meyerholz, D. K., McCaffrey, A. P., McNamara II, J. O., Giangrande, P. H. Nat. Biotechnol. 2009, 27, 839–849.

102. Neff, C. P., Zhou, J., Remling, L., Kuruvilla, J., Zhang, J., Li, H. Smith, D. D., Swiderski, P., Rossi, J. J., Akkina, R. Sci Transl Med. 2011, 3, 66ra6.

103. Gantier, M. P., Williams, B. R. G. Nat. Biotechnol. 2009, 27, 911–912.

104. Kortylewski, M., Swiderski, P., Herrmann, A., Wang, L., Kowolik, C., Kujawski, M., Lee, H., Scuto, A., Liu, Y., Yang, C., Deng, J., Soifer, H. S., Raubitschek, A., Forman, S., Rossi, J. J., Pardoll, D.M., Jove, R., Yu. H., Nat. Biotechnol. 2009, 27, 925–932.

105. Gabius, H.-J., Siebert, H.-C., André, S., Jiménez-Barbero, J., Rüdiger, H. ChemBioChem 2004, 5, 740–764.

106. Ernst, B., Magnani, J. L. Nat. Rev. Drug Discovery 2009, 8, 661– 677.

107. Lundquist, J. J., Toone, E. J. Chem. Rev. 2002, 102, 555-578.

108. Lee, Y. C., Lee, R. T. Carbohydrates in Chemistry and Biology, edited by Ernst B, Hart GW, Sinaý P, Weinheim, Germany: Wiley-VCH Verlag GmbH, 2000, 4, 549-561.

109. D'Souza, A. A., Devrajan, P. V. J. Control. Release 2015, 203, 126-139.

110. Lönnberg, H. Bioconjugate Chem. 2009, 20, 1065-1094.

111. Nair, J. K., Willoughby, J. L. S., Chan, A., Charisse, K., Alam, Md. R., Wang, Q., Hoekstra, M., Kandasamy, P., Kel'in A. V., Milstein, S., Taneja, N., O'Shea, J., Shaikh, S., Zhang, L., van der Sluis, R. J., Jung, M. E., Akinc, A., Hutabarat, R., Kuchimanchi, S., Fitzgerald, K., Zimmermann, T., van Berkel, T. J. C., Maier, M. A., Rajeev, K. G., Manoharan, M. J. Am. Chem. Soc. 2014, 136, 16958–16961.

112. Hangeland, J. J., Flesher, J. E., Deomand, S. F., Lee, Y. C., TS'O, P. O. P., Frost, J. J. Antisense Nucleic Acid Drug Dev. 1997, 7, 141-149.

113. Duff, R. J. Deamond, S. F., Roby, C., Zhou, Y., TS'O, P. O. P. Methods Enzymol. 1999, 313, 297-321.

114. Biessen, E. A. L., Vietsch, H., Rump, T., Fluiter, K., Bijsterbosch, M. K., van Berkel, T. J. C. Biochem. J., 1999, 340, 783-792.

115. Biessen, E. A. L., Vietsch, H., Rump, T., Fluiter, K., Bijsterbosch, M. K., van Berkel, T. J. C. Methods Enzymol. 2000, 314, 324-342.

116. Zhu, L., Ye, Z., Cheng, K., Miller, D. D., Mahato, R. I. Bioconjugate Chem. 2008 19, 290-298.

117. Zhu, L., Mahato, R. I. Bioconjugate Chem. 2010 21, 2119-2127.

118. Hamzavi, R., Dolle, F., Tavitian, B., Dahl, O., Nielsen, P. E. Bioconjugate Chem. 2003 14, 5, 941-954.

119. . Biessen, E. A. L., Sliedregt-Bol, K., Hoen, P. A. Chr. T., Prince, P., Van der Bilt, E., Valentijn, A. R. P. M., Meeuwenoord, N. J., Princen, H., Bijsterbosch, M. K., Van der Marel, G. A., Van Boom, J. H., Van Berkel, T. J. C. Bioconjugate Chem. 2002, 13, 295-302.

120. Rajeev, K. G., Zimmermann, T., Manoharan, M., Maier, M., Kuchimanchi, S., Charisse, K. Patent WO 2013075035 A1, 2013.

121. Sehgal, A., Barros, S., Ivanciu, L., Cooley, B., Qin, J., Racie, T., Hettinger, J., Carioto, M., Jiang, Y., Brodsky, J., Prabhala, H., Zhang, X., Attarwala, H., Hutabarat, R., Foster, D., Milstein, S., Charisse, K., Kuchimanchi, S., Maier, M. A., Nechev, L., Kandasamy, P., Kel'in, A. V., Nair, J. P., Rajeev, K. G., Manoharan, M., Meyers, R., Sorensen, B., Simon, A. R., Dargaud, Y., Negrier, C., Camire, R. M., Akinc, A. Nat. Med. 2015, 21, 5, 492-497.

122. Prakash, T. P., Graham, M. J., Yu, J., Carty, R., Low, A. Chappell, A., Schmidt, K., Zhao, C., Aghajan, M., Murray, H.F., Riney, S., Booten, S.L., Murray, S.F., Gaus, H., Crosby, J., Lima, W.F., Guo, S., Monia, B.P., Swayze, E.E., Seth P.P. Nucleic Acids Res., 2014, 42, 8796-8807.

123. Østergaard, M. E.; Yu, J.; Kinberger, G. A.; Wan, W. B.; Migawa, M. T.; Vasquez, G.; Schmidt, K.; Gaus, H. J.; Murray, H. M.; Low, A.; Swayze, E. E.; Prakash, T. P.; Seth, P. P. Bioconjugate Chem. 2015, 26, 1451-1455.

124. Prakash, T. P., Yu, J., Migawa, M. T., Kinberger, G. A., Brad Wan, W., Østergaard, M. E., Carty, R. L., Vasquez, G., Low, A., Chappell, A., Schmidt, K., Aghajan, M., Crosby, J., Murray, H. M., Booten, S. L., Hsiao, J., Soriano, A., Machemer, T., Cauntay, P., Burel, S. A., Murray, S. F., Gaus, H., Graham, M. J., Swayze, E. E., Seth, P. P. J. Med.Chem. 2016, 59, 2718-2733.

125. Rozema, D. B., Lewis, D. L., Wakefield, D. H., Wang, S. C., Klein, J. J., Roesch, P. L., Bertin, S. L., Reppen, T. W., Chu, Q., Blokhin, A. V., Hagstrom, J. E., Wolff, J. A. Proc. Natl. Acad. Sci. USA, 2007, 104, 12982–12987.

126. Ugarte-Uribe, B., Pérez-Rentero, S., Lucas, R., Aviñó, A., Reina, J. J., Alkorta, I., Eritja, R., Morales, J. C. Bioconjugate Chem. 2010, 21, 1280-1287.

127. Reyes-Darias, J. A., Francisco J. Sanchez-Luque, F. J., Morales, J. C., Perez-Rentero, S., Eritja, R., Berzal-Herranz, A. ChemBioChem 2015, 16, 584 – 591.

128. Das, I., Desire, J., Manvar, D., Baussanne, I., Pandey, V. N., Décout, J-L. J. Med. Chem. 2012, 55, 6021−6032.

129. Virta, P., Katajisto, J., Niittymäki, T., Lönnberg, H. Tetrahedron 2003, 59, 5137-5174.

130. Singh, Y., Spinelli, N., Defrancq, E. Curr. Org. Chem. 2008, 12, 263-290.

131. Singh, Y., Murat, P., Defrancq, E. Chem. Soc. Rev. 2010, 39, 2054-2070.

132. Spinelli, N., Defrancq, E., Morvan, F. Chem. Soc. Rev., 2013, 42, 4557-4573.

133. Saito, G., Swanson, J. A., Lee, K-D., Adv. Drug Deliv. Rev. 2003, 55, 199-215.

134. El-Sagheer, A. H., Brown, T. Chem. Soc. Rev., 2010, 39, 1388-1405.

135. Agard, N. J., Prescher, J. A., Bertozzi, C. R. J. Am. Chem. Soc. 2004, 126, 15046–15047.

136. El-Sagheer, A. H., Brown, T. Chem. Soc. Rev., 2010, 39, 1388–1405.

137. Singh, I., Heaney, F. Chem. Commun., 2011, 47, 2706–2708.

138. Marchan, V., Ortega, S., Pulido, D., Pedroso, E., Grandas, A. Nucleic Acids Res, 2006, 34, e24.

139. Wang, C., C.-Y., Seo, T. S.,Li, Z., Ruparel, H., Ju, J. Bioconjugate Chem. 2003, 14, 697−701.

140. Jeffery, D. A., Bogyo, M. Curr. Opin. Biotechnol. 2003, 14, 87-95.

141. Lesley, J., Hascall, V. C., Tammi, M., Hyman, R. J. Biol Chem. 2000, 275, 26967-26975.

142. Hirabayash, H., Fujisaki, J. Clin. Pharmacokinet. 2003, 42, 1319-1330.

143. Reinholz, G. G., Getz, B., Sanders, E. S., Karpeisky, M. Y., Padyukova, N. S., Mikhailov, S. N., Ingle, J. N., Spelsberg, T. C. Breast Cancer Res. Treat. 2002, 71, 257-268.

144. Cole, L. E., Vargo-Gogola, T., Roeder, R. K. Adv Drug Deliver Rev. 2016, 99, 12-27.

145. Clézardin, P., Ebetino, F. H., Fournier, P. G. J. Cancer. Res. 2005, 65, 4971-4974.

146. Rex, E., Ebner, S., Attali, B., Shabat, D. Bioorg. Med. Chem. Lett. 2008, 18, 816-820.

147. Shi, J., Liu, T. W. B., Chen, J., Green, D., Jaffray, D., Wilson, B. C., Wang, F., Zheng, G. Theranostics, 2011, 1, 363-370.

148. Singh, S., Aggarwal, A., Bhupathiraju, N. V. S. D. K., Arianna, G., Tiwari, K., and Drain, C. M. Chem. Rev. 2015, 115, 10261-10306.

149. Mukai, H., Wada, Y., Watanabe, Y. Ann Nucl Med, 2013, 27, 625–639.

150. Guo, C-J., Pan, Q., Li, D-G., Sun, H., Liu, B-W. J. Hepatol. 2009, 50, 766-778.

151. An, F., Gong, B., Wang, H., Yu, D., Zhao, G., Lin, L., Tang, W., Yu, H., Bao, S., Xie, Q. Apoptosis, 2012, 17, 702-716.

152. Hullinger, T. G., Montgomery, R. L., Seto, A. G., Dickinson, B. A., Semus, H. M., Lynch, J. M., Dalby, C. M., Robinson, K., Stack, C., Latimer, P. A., Hare, J. M., Olson, E. N., van Rooij, E. Circ. Res 2011, 109, 1-11.

153. Li, Z., Rana, T. M. Nat. Rev. Drug Discovery, 2014, 13, 622−638.

154. Roivainen, A., Tolvanen, T., Salomäki, S., Lendvai, G., Velikyan, I., Numminen, P., Välilä, M., Sipilä, H., Bergström, M., Härkönen, P., Lönnberg, H., Långström, B. J Nucl Med, 2004, 45, 347–355.

155. Kiviniemi, A., Mäkelä, J., Mäkilä, J., Saanijoki, T., Liljenbäck, H., Poijärvi-Virta, Lönnberg, H., Laitala-Leinonen, T., Roivainen, A., Virta, P. Bioconjugate Chem. 2012, 23, 1981–1988.

156. Salo, H., Virta, P., Hakala, H., Prakash, T. P., Kawasaki, A. M., Manoharan, M., Lönnberg, H. Bioconjugate Chem. 1999, 10, 815-823.

157. Katajisto, J., Virta, P., Lönnberg, H. Bioconjugate Chem. 2004, 15, 890-896.

158. Joosten, J. A. F., Loimaranta, V., Appeldoorn, C. C. M., Haataja, S., El Maate, F. A., Liskamp, R. M., Finne, J., Pieters, R. J. J. Med. Chem. 2004, 47, 6499-6508.

159. Ugarte-Uribe, B., Pérez-Rentero, S., Lukas, R., Aviñó, A., Reina, J. J., Alkorta, I., Eritja, R., Morales, J. C. Bioconjugate Chem. 2010, 21, 1280-1287.

160. Lesley, J., Hascall, V. C., Tammi, M., Hyman, R. J. Biol. Chem. 2000, 275, 26967-26975.

161. Palmacci, E. R., Seeberger, P. H. Tetrahedron, 2004, 60, 7755−7766.

162. Chassagne, P.; Raibaut, L.; Guerreiro, C.; Mulard, L. A. Tetrahedron 2013, 69, 10337-10350.

163. Lu, X. W.; Kamat, M. N.; Huang, L. J.; Huang, X. F. J. Org. Chem. 2009, 74, 7608-7617.

164. Vibert, A.; Lopin-Bon, C.; Jacquinet, J. C. Tetrahedron Lett. 2010, 51, 1867-1869.

165. Gold, H.; Munneke, S.; Dinkelaar, J.; Overkleeft, H. S.; Aerts, J. M. F. G.; Codee, J. D. C.; van der Marel, G. A.; Carbohydr. Res. 2011, 346, 1467-1478.

166. Guillemineau, M.; Auzanneau, F.-I. J. Org. Chem. 2012, 77, 8864-8878.

167. Bindschadler, P., Noti, C., Castagnetti, E., Seeberger, P. H. Helv. Chim. Acta, 2006, 89, 2591−2610.

168. Reinholz, G. G., Getz, B., Sanders, E. S., Karpeisky, M. Y., Padyukova, N. S., Mikhailov, S. N., Ingle, J. N., Spelsberg, T. C. Breast Cancer Res. Treat. 2002, 71, 257.

169. Ora, M., Lönnberg, T., Florea-Wang, D., Zinnen, S., Karpeisky, A., Lönnberg, H. J. Org. Chem. 2008, 73, 4123.

170. Zheng, X., Morgan, J., Pandey, S. K., Chen, Y., Tracy, E., Baumann, H., Missert, J. R., Batt, C., Jackson, J., Bellnier, D. A., Henderson, B. W. J. Med. Chem. 52, 4306-4318.

171. Li, H., Fedorova, O. S., Trumble, W. R., Fletcher, T. R., Czuchajowski, L. Bioconjugate Chem. 1997, 8, 49-56.

172. Zheng, X., Morgan, J., Pandey, S. K., Chen, Y., Tracy, E., Baumann, H., Missert, J. R., Batt, C., Jackson, J., Bellnier, et al. J. Med. Chem. 2009, 52, 4306−4318.

173. Han, F. X., Wheelhouse, R. T., Hurley, L. H. J. Am. Chem. Soc. 1999, 21, 3561-3570.

174. Sun, D., Hurley, L .H. J. Med. Chem. 2009, 52, 2863-2874.

175. Irie, A., Yamauchi, A., Kontani, K., Kihara, M., Liu, D., Shirato, Y., Seki, M., Nishi, N., Nakamura, T., Yokomise, H., et al. Cancer Res. 2005, 11, 2962−2968.

176. Kageshita, T., Kashio, Y., Yamauchi, A., Seki, M., Abedin, M. J., Nishi, N., Shoji, T., Nakamura, T., Ono, T. M., Hirashima, M. Int. J. Cancer, 2002, 99, 809−816.

177. Bellnier, D. A., Greco, W. R., Nava, H., Loewen, G. M., Oseroff, A. R., Dougherty, T. J. Cancer Chemother. Pharmacol. 2006, 57, 40-45.

178. Holub, J., Meckel, M., Kubíček, V., Rösch, F., Hermann, P. Contrast Media Mol. Imaging, 2014, 10, 122-134.

179. Yim, C. B., Mikkola, K., Fagerholm, V., Elomaa, V. V., Ishizu, T., Rajander, J., Schlesinger, J., Roivainen, A., Nuutila, P., Solin, O. Nucl. Med. Biol. 2013, 40, 1006−1012.

180. Almeida, P., Shahbazi, M.-A., Mäkilä, E., Kaasalainen, M., Salonen, J., Hirvonen, J., Santos, H. A. Nanoscale, 2014, 6, 10377−10387.